TECHNICAL REPORT

Man-Portable Vector EMI Sensor for Full UXO Characterization

ESTCP Project MR-201005

March 2012

Nicolas Lhomme
Sky Research, Inc.

This document has been cleared for public release

REPORT DOCUMENTATION PAGE	*Form Approved OMB No. 0704-0188*

The public reporting burden for this collection of information is estimated to average 1 hour per response, including the time for reviewing instructions, searching existing data sources, gathering and maintaining the data needed, and completing and reviewing the collection of information. Send comments regarding this burden estimate or any other aspect of this collection of information, including suggestions for reducing the burden, to the Department of Defense, Executive Services and Communications Directorate (0704-0188). Respondents should be aware that notwithstanding any other provision of law, no person shall be subject to any penalty for failing to comply with a collection of information if it does not display a currently valid OMB control number.

PLEASE DO NOT RETURN YOUR FORM TO THE ABOVE ORGANIZATION.

1. REPORT DATE *(DD-MM-YYYY)*	2. REPORT TYPE	3. DATES COVERED *(From - To)*
15-03-2012	Final Technical Report	May 2011-March 2012

4. TITLE AND SUBTITLE
Demonstration of MPV Sensor at former Camp Beale, California:
ESTCP MR-201005 Man Portable Vector EMI Sensor for Full UXO Characterization

5a. CONTRACT NUMBER
W912HQ-10-C-0030

5b. GRANT NUMBER

5c. PROGRAM ELEMENT NUMBER

6. AUTHOR(S)
Dr. Nicolas Lhomme, Sky Research, Inc.

5d. PROJECT NUMBER

5e. TASK NUMBER

5f. WORK UNIT NUMBER

7. PERFORMING ORGANIZATION NAME(S) AND ADDRESS(ES)
Sky Research, Inc.
445 Dead Indian Memorial Road
Ashland, OR 9520

8. PERFORMING ORGANIZATION REPORT NUMBER

9. SPONSORING/MONITORING AGENCY NAME(S) AND ADDRESS(ES)
Environmental Security Technology Certification Program
901 North Stuart Street, Suite 303
Arlington, VA 22203-1821

10. SPONSOR/MONITOR'S ACRONYM(S)

11. SPONSOR/MONITOR'S REPORT NUMBER(S)

12. DISTRIBUTION/AVAILABILITY STATEMENT
Approved for public release; distribution is unlimited

13. SUPPLEMENTARY NOTES

14. ABSTRACT
The Man-Portable Vector electromagnetic induction sensor is a new-generation instrument designed to extend classification of unexploded ordnance (UXO) to sites where vegetation or terrain limit access to vehicle-based advanced geophysical platforms. The MPV participated in the ESTCP live-site demonstration at former Camp Beale, California in June 2011, where data were collected in cued interrogation mode over 911 anomalies at a site with variable forest density and sloped terrain. Data were distributed to ESTCP partners for analysis and processed as part of this study. Demonstration objectives were attained. All buried targets of interest were detected and recommended for excavation through geophysical inversion and statistical classification. The prioritized dig list achieved over 80% reduction in unnecessary clutter excavation. Sensor positioning solely relied on the MPV-dedicated, prototype beacon positioning system. The method proved to be reliable and accurate within classification requirements (1-2 cm accuracy). The MPV technology will be involved in further ESTCP demonstrations in 2012.

15. SUBJECT TERMS
Man Portable Vector Sensor, Electromagnetic Induction Sensor, UXO, Camp Beale, Live-Site Demonstration, Classification, Geophysical Inversion

16. SECURITY CLASSIFICATION OF:			17. LIMITATION OF ABSTRACT	18. NUMBER OF PAGES	19a. NAME OF RESPONSIBLE PERSON
a. REPORT	b. ABSTRACT	c. THIS PAGE			Dr. Herb Nelson
UU	UU	Uu	UU	79	19b. TELEPHONE NUMBER *(Include area code)* 703-696-8726

Table of contents

List of Figures

List of Tables

Acronyms

BUD	Berkeley UXO Discriminator
CFR	Code of Federal Regulations
cm	Centimeter
CO	Colorado
CRREL	Cold Regions Research and Engineering Laboratory (ERDC)
DAQ	Data Acquisition System
DGM	Digital Geophysical Mapping
EMI	Electromagnetic Induction
ERDC	Engineering Research and Development Center
ESTCP	Environmental Security Technology Certification Program
GPS	Global Positioning Systems
HASP	Health and Safety Plan
IDA	Institute for Defense Analyses
IVS	Instrument Verification Strip
m	Meter
mm	Millimeter
MPV	Man Portable Vector
ms	millisecond
MR	Munitions Response
NH	New Hampshire
NSMS	Normalized Surface Magnetic Source
OR	Oregon
PI	Principal Investigator
POC	Points of Contact
RTK	Real-time Kinematic
s	Second
SERDP	Strategic Environmental Research and Development Program
SKY	Sky Research, Inc.
SNR	Signal to Noise Ratio
SOP	Standard Operating Procedure
SVM	Support Vector Machine
TEMTADS	Time Domain Electromagnetic Towed Array Detection System
UXO	Unexploded Ordnance
YPG	Yuma Proving Ground

ACKNOWLEDGMENT

The MPV demonstration at former Camp Beale, California was funded by the Environmental Security Technology Certification Program project MR-201005. Initial sensor development and testing was supported by *Strategic Environmental Research and Development Program* project MM-1443. The field deployment involved Dr. Benjamin Barrowes (CRREL-ERDC), David George (G&G Sciences), Jon Jacobson and the P.I. (both from Sky Research). The P.I. was the main performer for all other tasks. Joy Rogalla and Erik Russell assisted with project coordination. Dr. Laurens Beran and Dr. Leonard Pasion participated in discussions on classification and soil mitigation strategies. Dr. Gregory Schultz reviewed the final report.

EXECUTIVE SUMMARY

This document reports on the classification study that was performed with the Man-Portable Vector (MPV) sensor at former Camp Beale, California in the summer of 2011. The study covers the data collection survey, data processing and classification, and performance analysis.

The MPV technology is designed to extend classification of unexploded ordnance (UXO) to sites where vegetation or terrain limits access to vehicle-based advanced geophysical platforms. The former Camp Beale site presents such conditions and was therefore selected to test portable UXO detectors. The second-generation MPV prototype is an electromagnetic induction (EMI) sensor that consolidates on the same portable unit a 50-centimeter diameter transmitter, an array of three-dimensional receivers and a field-programmable control display. The display provides immediate visual data feedback and thus enables quality assurance and adaptive surveys. The MPV can be deployed with multiple positioning systems. Besides standard GPS technology, centimeter-level accuracy can also be obtained with a specific portable local positioning system that is based on locating the MPV transmitter, which acts as a beacon when turned on. The method is not affected by natural obstacles, as opposed to GPS and roving lasers; a survey can therefore be performed in forested and rugged environments. The MPV can be utilized for detection through dynamic survey and for target classification through static, cued interrogation survey in which the highest quality data are acquired near a target. The first demonstration of the current MPV technology took place at Yuma Proving Ground, Arizona UXO Standardized Test Site in October 2010. Objectives were met and exceeded. In particular, our study achieved over 90% correct classification of all targets within 1 meter depth. Beacon positioning accuracy was confirmed. Sensor hardware proved to be maneuverable and generally resilient. Therefore the system was deemed to be fit for live-site surveys.

ESTCP organized the first live-site demonstration for portable systems at former Camp Beale, California in June 2011. The MPV was deployed with 2-3 field operators to acquire cued interrogation data over 912 anomalies. A calibration study was performed on the first day to measure the sensor response over known targets. A sensor verification procedure was done at the beginning of each survey day. Initial survey indicated the presence of significant noise from magnetic soil, and suggested frequent offsets between flagged target locations and MPV peak anomaly. Standard field survey procedures were adapted to mitigate both effects. As a result, survey productivity was slightly diminished with an average of 90 targets per day. The collected data were pre-processed, packaged and sent to several groups for advanced processing and classification. Our classification approach is detailed in this report. All groups were successful at efficiently identifying all UXO and avoiding excavation of over 80% of the clutter, which exceeded demonstration objectives. The demonstration was a success.

The YPG and Beale studies are the first stage in a series of live site demonstrations that are aimed at establishing the performance, limitations, optimum usage and costs of the MPV technology. The initial demonstrations were successful and suggested a strong potential for shallow UXO detection and classification. Today there are no commercially available systems with such capabilities. The MPV and beacon technology is scheduled to be deployed and tested at several sites through year 2012 as part of the ESTCP ongoing live-site demonstration program.

1.0 INTRODUCTION

This is the fifth study in the series of Environmental Security Technology Certification Program (ESTCP) demonstrations of classification technologies for Munitions Response (MR). This demonstration is designed to investigate the evolving classification methodology at a site that is partially wooded with a mix of munitions types.

The primary objective of this project is to demonstrate field use of a man portable discrimination system, the Man Portable Vector (MPV) sensor. The MPV electromagnetic induction (EMI) sensor was designed to extend advanced discrimination capabilities to sites with challenging surveying conditions and, thus allow for advanced discrimination to be applied at most human trafficable land locations at moderate cost. The system is deployed in conjunction with a portable local positioning system free from "line-of-sight" requirements to facilitate survey in treed areas, where traditional location systems like global positioning system (GPS) and laser (e.g., dense forests and steep terrain) can fail.

1.1 BACKGROUND

The Fiscal Year (FY) 2006 Defense Appropriation contains funding for the “Development of Advanced, Sophisticated Discrimination Technologies for UXO Cleanup” in the ESTCP. As the Defense Science Board observed in 2003, “The […] problem is that instruments that can detect the buried unexploded ordnance (UXO) also detect numerous scrap metal objects and other artifacts, which leads to an enormous amount of expensive digging. Typically 100 holes may be dug before a real UXO is unearthed! The Task Force assessment is that much of this wasteful digging can be eliminated by the use of more advanced technology instruments that exploit modern digital processing and advanced multi-mode sensors to achieve an improved level of discrimination of scrap from UXO.”

ESTCP responded by conducting a Discrimination Pilot Study and funding development of a new generation of geophysical sensors. Results for the first three discrimination studies (at Camp Sibert, Alabama, San Luis Obispo, California, and Camp Butner, North Carolina) were encouraging. In particular, new sensors combined with advanced classification methods allowed the demonstrators to correctly identify a significant fraction of the anomalies as arising from non-hazardous items that could be safely left in the ground. Such performance was facilitated by favorable survey conditions, vegetation, and modest topographical variations that permitted deployment of vehicular and cart-based geophysical platforms.

The results from these studies are encouraging; however, there are many Department of Defense (DoD) sites where terrain and vegetation limit the use of large wheel-based sensor systems. Terrain and vegetation conditions (e.g., dense forests and steep terrain) at many sites also preclude use of traditional sensor positioning systems like global positioning system (GPS) and laser ranging. These systems can fail at sites when terrain and vegetation interfere and line-of-sight surveying is not possible.

1.2 OBJECTIVE OF THE DEMONSTRATION

The goal of this ESTCP demonstration at former Camp Beale is to evaluate the MPV technology for UXO characterization at a site where difficult topography and vegetation preclude deployment of wheel-based advanced geophysical platforms and traditional "line-of-sight" positioning methods (e.g. GPS, laser). Sensor performance is measured as the capability to

correctly classify munitions of different size buried at various depths against clutter. Secondary metrics such as reliability, productivity, effectiveness of field procedures and ease of use of the technology are also assessed.

In terms of benefits, successful deployment of the MPV extends advanced discrimination capabilities to sites with challenging surveying conditions and thus allow for advanced discrimination to be applied at most human trafficable land locations at moderate cost.

Figure 1: Survey with MPV and beacon in open field (Beale Combined area).

1.3 REGULATORY DRIVERS

The Defense Science Board Task Force on UXO noted in its FY03 report that 75% of the total cost of a current clearance is spent on digging scrap. A reduction in the number of scrap items dug per UXO item from 100 to 10 could reduce total clearance costs by as much as two-thirds. Thus, discrimination efforts focus on technologies that can reliably differentiate UXO from items that can be safely left undisturbed.

Discrimination only becomes a realistic option when the cost of identifying items that may be left in the ground is less than the cost of digging them. Because discrimination requires detection as a precursor step, the investment in additional data collection and analysis must result in enough fewer items dug to pay back the investment. Even with perfect detection performance and high Signal-to-Noise Ratio (SNR) values, successfully sorting the detections into UXO and non-hazardous items is a difficult problem but, because of its potential payoff, one that is the focus of significant current research. This demonstration represents an effort to transition a promising discrimination technology into widespread use at UXO-contaminated sites across the country.

2.0 TECHNOLOGY

The MPV technology is based on a man-portable EMI sensor with a transmitter coil and a set of vector receivers. The system was tested at Yuma Proving Ground (YPG) and is the second generation prototype MPV.

2.1 MPV TECHNOLOGY DESCRIPTION

2.1.1 Electromagnetic sensor

The MPV is a man-portable, wide-band, time-domain, EMI sensor composed of a single transmitter coil and an array of five receiver units that measure all three components of the EM field (Figure 2). The sensor was specifically designed to (1) be man portable and therefore easy to deploy, maneuver and adapt to a survey environment, and (2) acquire data that is suitable for discriminating unexploded ordnance (UXO) from non-UXO targets. The MPV sensor head for this demonstration comprises a 50-centimenter (cm) diameter circular loop transmitter coiled around a disk that intermittently illuminates the subsurface, and five multi-component receiver units (cubes) that measure the three orthogonal components of the transient secondary EM field decay with three air-induction 8-cm square coils. One receiver cube is co-axial with the transmitters while four receivers are placed off-axis around the transmitter loops in a cross pattern. Gasperikova et al (2007) and others have shown that having multi-component receivers placed at multiple locations can help reduce the ambiguity between the size and depth of a buried target by more readily allowing recovery of the components of the polarizability tensor associated with a buried metallic object, an indicator of the target shape.

The MPV is a programmable instrument. The duration of the excitation and time decay recording can be adjusted to any given time to accommodate survey needs. The MPV features distinct operating modes for detection and discrimination with a seamless switch between the two. Detection mode consists of dynamic data collection for digital geophysical mapping (DGM). It is based on fast EMI transmit-receive cycles so that the sensor can continuously move (e.g., 1 millisecond [ms] time decay, similar to Geonics EM-61). Discrimination mode is tailored for optimizing data quality and the ensuing target characterization. In this mode the sensor is static so that signals can be stacked (averaged to reduce noise); longer EMI cycles are applied to capture variations in time decay rates (e.g., 25 milliseconds (ms), similar to Geonics EM-63). This late-time information has been shown to be very useful for distinguishing between intact ordnance and thinner walled shrapnel and cultural debris (Billings et al., 2007). Other currently available systems with multiple time channel measurement capabilities (e.g., Berkeley UXO Discriminator [BUD], Geonics EM63, Time Domain EM Towed Array Detection System [TEMTADS]) are required to be mounted on a cart platform due to the size and weight of the multiple coils of wire required for the transmitters and receivers.

The MPV user interface has real-time monitoring and feedback capabilities on data quality, spatial coverage and other key features (signal intensity, time decay, secondary targets, and presence of magnetic soil). For example, the interface includes a target location tool obtained by displaying the direction and amplitude of the measured EMI field at each receiver unit (the so-called “dancing arrows” in top left corner of Figure 3). All these features assist the field operator in efficient data collection, so that detection and discrimination data can be collected as part of the same survey, thus limiting the need to revisit an anomaly for further characterization

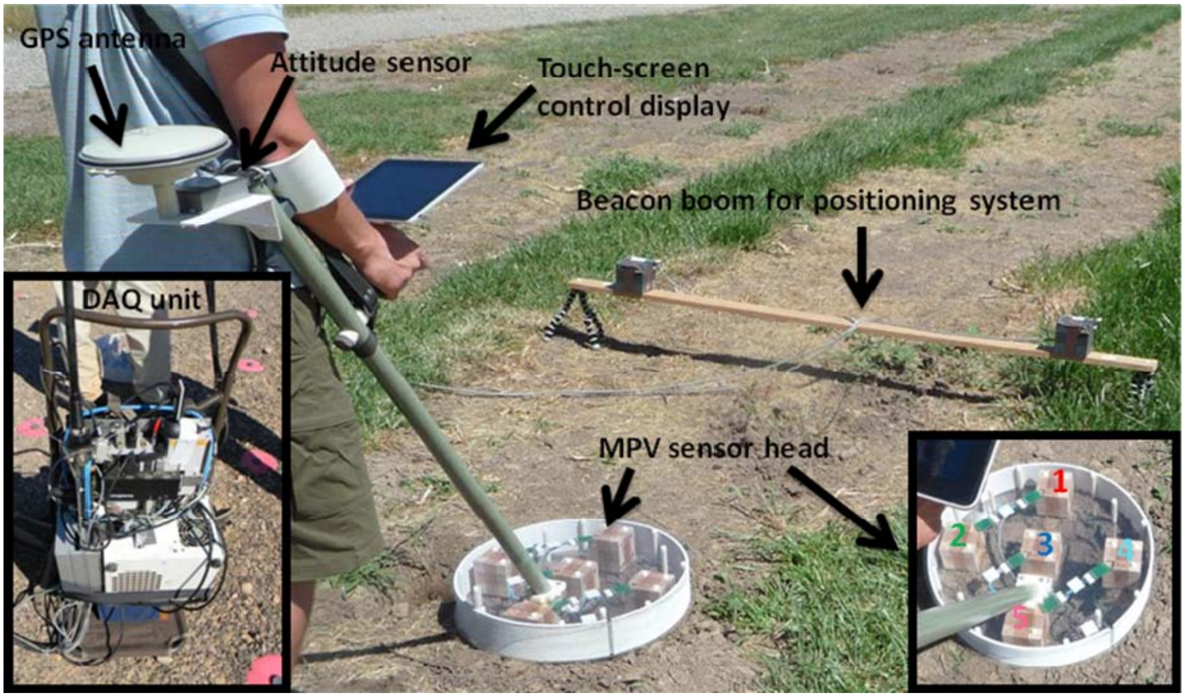

Figure 2: The second generation MPV.
Positioning can be achieved with GPS (for open field survey) or beacon receivers (for survey in forest and/or in steep terrain). Left inset shows data acquisition (DAQ) and power unit mounted on a backpack frame. Right panel shows view of sensor head from above with cube numbers.

2.1.2 Geolocation

Detection and classification have different spatial accuracy requirement; therefore a field survey with the MPV would utilize two complementary positioning systems. Detection mapping has decimeter accuracy requirements and can be performed with a GPS or a spool-mounted cotton thread and optical encoder.

Classification based on inverted geophysical data requires centimeter-level sensor positioning when surveying a target (Bell, 2005). Because of the presence of trees, GPS cannot guarantee such accuracy. Due to these limitations we implemented the MPV-beacon positioning system to obtain local, accurate sensor positioning when surveying a target (Lhomme et al., 2011). The operating principle consists of locating the origin of the primary field generated by the MPV transmitter coil, acting as a beacon, with a pair of EMI receivers rigidly attached to a portable beam, placed horizontally on the ground and supported by a pair of tripods to act as a base station (Figure 2). The azimuth of the MPV and boom are recorded with a digital compass (3-component attitude sensor). Field trials performed with the MPV sensor head showed that position and orientation estimated with this beacon system were accurate to within 1 cm and 1 degree, respectively, out to distances of 3-4 meters (m). This method is at least as accurate as a GPS in open field when considering that it directly predicts the sensor head location while the GPS has to be mounted at least one meter away from sensor head. If the anomaly is marked and geo-referenced then the cued interrogation and predicted target location can be converted to global positions by placing the first sounding at the marked location and using the azimuth measurement to orient the survey. Alternatively, we can search a location where GPS is accurate and relate that location to the rest of the survey.

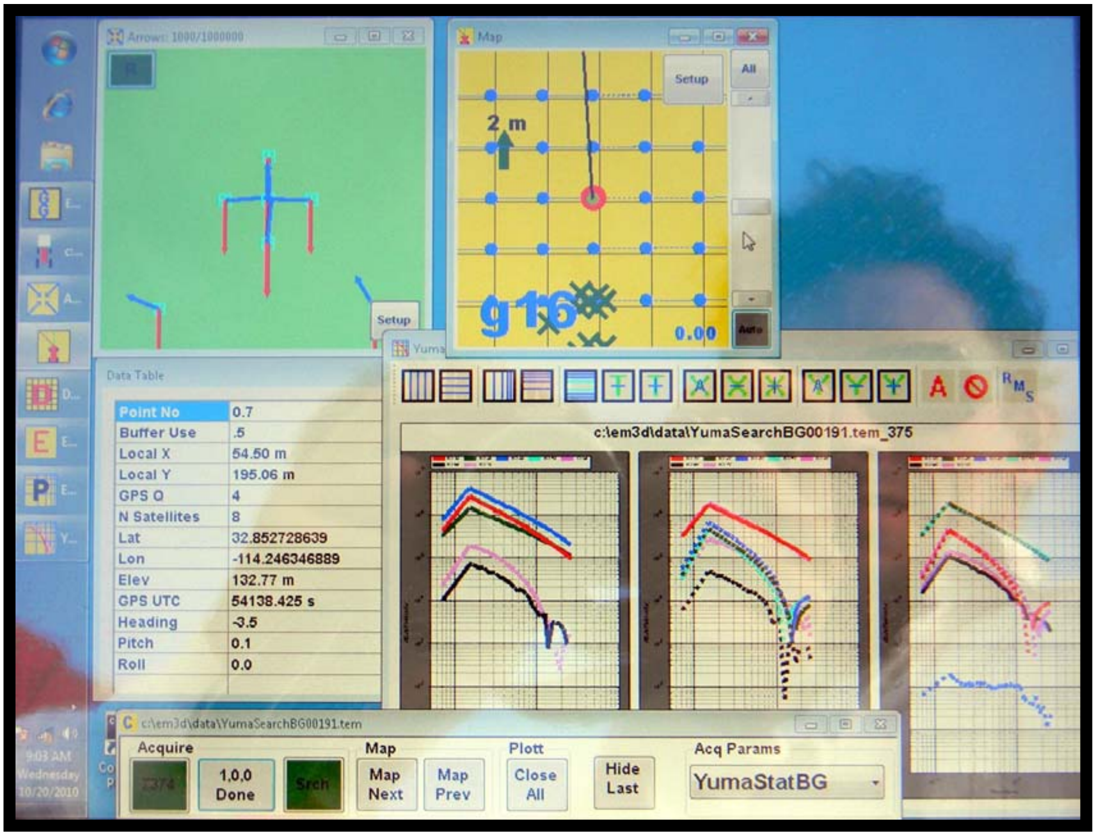

Figure 3: The MPV detection display window in dynamic data collection mode.
The top left panel indicates with arrows the direction of the nearest compact metallic object relative to the MPV receiver cubes and directs the operator to the target (here the MPV sits atop the target). The top middle panel shows a field map with the MPV location (red dot) and azimuth (black line), potential target locations (blue dots), and cued interrogation soundings (green crosses).

2.2 MPV TECHNOLOGY DEVELOPMENT

Development and characterization of the MPV sensor were conducted under the Strategic Environmental Research and Development Program (SERDP) MM-1443 project by Engineering Research and Development Center-Cold Regions Research and Engineering Laboratory (ERDC-CRREL) in Dartmouth, New Hampshire (NH) from 2005-2009 under the leadership of Benjamin Barrowes and Kevin O'Neil. The first MPV prototype was built in 2005-2006 by David George of G&G Sciences, Grand Junction, Colorado (CO). It was tested in 2007 at ERDC in a laboratory setting, where data were collected over a series of test ordnance in a highly controlled, low-noise environment. Interpretation of these data proved that the MPV could meet discrimination expectations under cooperative survey conditions. The ArcSecond laser positioning system was tested in 2007 and proved to deliver accurate location for local survey. The ArcSecond relied on three roaming laser stations and three receiver units placed on top of the MPV head.

The SERDP project was extended in 2008 to continue sensor testing and development of data modeling methods. The first field tests took place at the Sky Research test plot in Ashland, Oregon in the summer. A series of standard UXO were surveyed in various modes, static and dynamic, while location was provided using a template with marked locations and the ArcSecond. Cued interrogation data provided stable discrimination results and confirmed the

potential to extend advanced UXO classification capabilities to man-portable systems with the MPV. The effect of strongly magnetic soil on EMI sensors were also investigated during that survey as part of SERDP MM-1573 (Len Pasion, Sky Research). It was found that the MPV offered possibilities to defeat adverse soil effects owing to its array structure. These field trials also showed that ArcSecond positioning was impractical and not reliable enough for effective field application because of the requirement to keep all three rovers in the field of view, and the long setup and calibration time. This experience led to development and testing of an alternative positioning method based on the beacon principle.

The SERDP project was extended in 2009 to test that beacon concept and prepare modification of the original MPV prototype for further field deployment. The sensor head was redesigned and rebuilt: lighter materials were employed and the circular head diameter was reduced to reduce weight and improve maneuverability, receiver cubes were brought inside the transmitter coil to reduce fragility, and transparent material was employed to allow the operator to see the ground through the unit. Figure 4 shows the first and second generation sensor heads for comparison.

Figure 4: Two generations of MPV prototypes.
A: Original sensor with double transmitter, wood frame and ArcSecond positioning (head weights 23 lbs).
B: Second generation sensor and touch-screen control display (head weights 12 lbs).

The MPV was tested at Yuma Proving Ground (YPG) UXO Standardized Test Site in October 2010. The Calibration Lanes, Blind Grid and a portion of the Desert Extreme were surveyed over the course of two weeks. Data were collected as part of a one-pass survey: a dynamic detection sweep search would be performed until a potential target would be detected; the search would then be interrupted and immediately followed with a cued interrogation survey, during which a series of static soundings would be acquired so as to map the spatial extent of the anomaly; then the search would resume. Cued data were processed following the usual geophysical inversion and model-based feature classification. Stable polarizability transients were generally recovered (Figure 5 for Calibration Lanes). The demonstration was successful with detection rate and probability of correct classification exceeding 90% for targets buried within one meter of the surface.

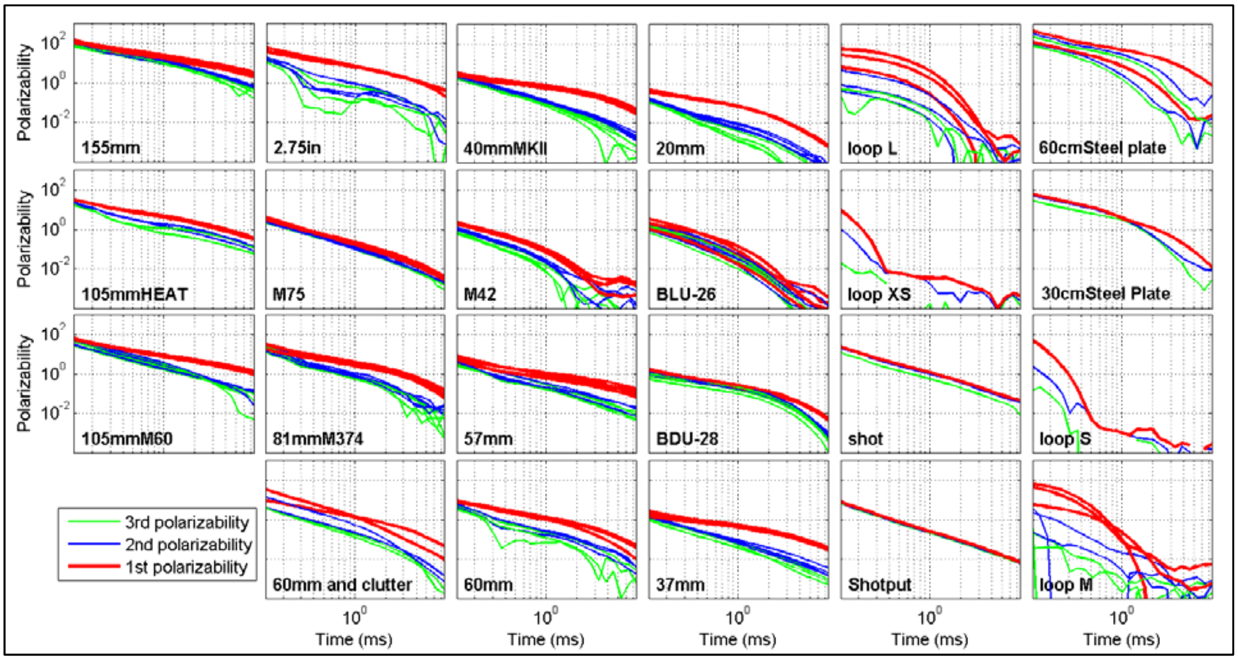

Figure 5: Recovered polarizabilities for MPV survey of standard munitions at YPG Calibration Lanes. Main polarizability (L1) is showed in red; secondary polarizabilities (L2, L3) are showed in blue and green.

2.3 ADVANTAGES AND LIMITATIONS OF THE MPV TECHNOLOGY

The MPV is the only available non-cart-based system that can acquire multi-static, multi-component data on a wide and programmable range of time channels. The MPV offers several key benefits:

- By being man-portable, the MPV can be deployed at sites where terrain and vegetation preclude use of heavier, cart-based systems. The greater portability (no wheels) can greatly improve productivity, especially over rough terrain or for cued interrogation. Maneuverability also offers the ability to tilt the sensor head such that the transmitter illuminates the buried target at multiple angles. Standard horizontal loop transmitters produce a strong vertical field when directly above the target, with horizontal field components being significant when the transmitter is positioned at a lateral offset from the target. At these offset distances, the magnitude of the transmit fields is reduced and lower signal-to-noise ratio data is acquired. By tilting the MPV we can take multiple "looks" of the target so that different combinations of the target's polarization tensor components are excited, resulting in more robust estimates of the target parameters and, therefore, more reliable discrimination (Smith et al., 2005).
- For each measurement, there are 5 receivers simultaneously recording three orthogonal components of the scattered field with near-perfect relative positioning among receivers. The multi-component, multi-axis design relaxes requirements on the number of soundings required to accurately predict depth, orientation, and target parameters, and on the positional accuracy (Grzegorczyk et al., 2009). This number of soundings is dependent on the target type and on field conditions. Processing of low-noise test-stand MPV data with perfect

positioning has shown that a UXO can be identified with as few as 5 soundings (Barrowes et al., 2007b). Analysis of MPV data collected on the SKY UXO test plot in Ashland, Oregon over magnetic soil also show that a 4x4 grid of measurements could be used to robustly recover target parameters.

- The combination of multi-component and multi-time channel measurement capabilities and the geometric arrangement of the receivers offer potential for identifying and neutralizing the effect of magnetic soil, in particular with soil compensation techniques developed in SERDP MM-1414 and 1573. When the MPV is positioned with its sensor head parallel to ground surface, above magnetic soil over even ground (in the absence of a metallic target), signal in the receivers measuring the radial component of the signal (i.e., X component of side receivers and Y component of front receiver) should be equal, and the horizontal components of the co-axial receivers should be zero. The measured decays should have the characteristic decay of viscous remanent magnetic soil (Figure 6). The effect of soil can therefore be modeled and successful discrimination can be achieved even in the presence of magnetic soils (Lhomme et al., 2008; Pasion et al., 2008). The MPV response due to sensor motion and topography over magnetic soil is predicable (Kingdon et al., 2009). Soil characterization can also help exploit data collected when tilting the MPV to obtain "multiple looks" at an anomaly. These data would otherwise be difficult to interpret in presence of a significant background because the intensity of its effect would significantly vary between receivers. The ability to accurately model the MPV signal from compact metallic targets in the presence of magnetic soils is a key contributor to a robust inversion and discrimination capability.

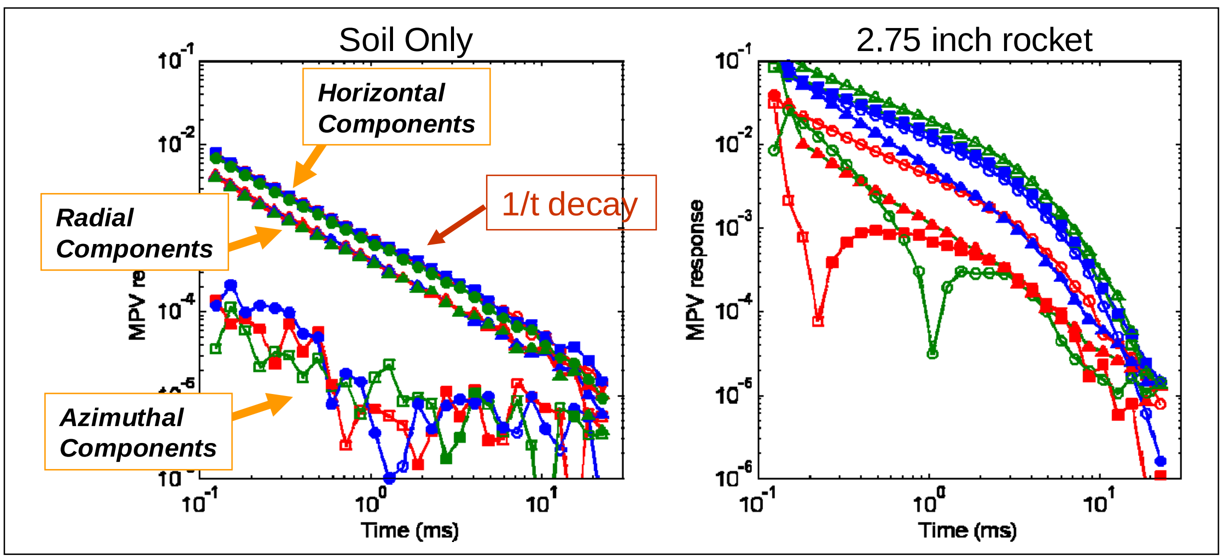

Figure 6: Comparison of MPV response between magnetic soil and a metallic target. Data collected at Sky Research test plot in Ashland, OR, where magnetic soils have shown to have a significant effect on EMI sensors (Pasion et al., 2008). The recorded signal (left panel) shows a time decay that is typical of soils with viscous remanent magnetization.

- The MPV is fully programmable and equipped with a graphical field-user interface that controls acquisition parameters such as transmitter waveform characteristics, the duration of the excitation, the number of measurement cycles to be stacked and the recording time channels. Short acquisition times are sufficient for detection, whereas discrimination

improves with stacking many measurements over a long time window.

- The MPV has highly stable EMI components, which have a response that is directly predictable using standard EMI theory. In field tests conducted throughout all seasons of last year we verified that MPV components had imperceptible measurement drift and were largely insensitive to survey conditions (sun exposure, temperature). In general, instrument drift is removed by performing along-line high-pass filtering of the data, which has the potential of introducing filtering artifacts to the data and can bias target parameter estimates. A second method for identifying and removing instrument drift is to periodically measure the instrument response over a known item - this check is part of standard survey procedures performed in the field. The transmitter current is also monitored and recorded at all times during the survey to detect any variation in the excitation (e.g., due to changes in battery power).
- The MPV is well suited for small target discrimination. Smaller caliber anomalies have localized and rapidly-varying spatial response. An air induction coil measures a voltage by spatially averaging the secondary field of a target over the face of the loop. Therefore, large receivers tend to “smear out” the secondary field. The 8 cm x 8 cm receivers of the MPV are typically smaller than most multi-channel sensors (for example the Geonics EM63 receivers are 50x50 cm, TEMTADS are 25x25 cm) and thus better suited to detecting and sampling the secondary field over small targets.

3.0 PERFORMANCE OBJECTIVES

The MPV field survey at former Camp Beale serves two purposes: (1) to characterize the sensor at a live site and (2) to participate in ESTCP evaluation of classification methods. The MPV was only tested for the data collected in cued interrogation of targets that have been provisionally located using a Geonics EM-61 MkII cart and marked with a flag. We shall refer to these anomalies as flagged or selected targets.

This project comprises both data collection and classification objectives. The first four objectives, as described in Table 1, are mostly intrinsic to the quality of the sensor and of the deployment method. The data were analyzed by the demonstrator and by other ESTCP partners. Given that similar performance was attained by all analysts, scoring here only reflects the results obtained through this study and provides a realistic assessment of the instrument quality for UXO classification.

Table 1: Performance Objectives

Performance Objective	Metric	Data Required	Success Criteria	Result
Data Collection Objectives				
Detection of all munitions of interest	Percent detected of selected anomalies	• Maximum signal amplitude	95% of targets for which depth is less than the minimum of 10 target diameters and 1 m	All targets were detected
Repeatability of instrument verification tests	Amplitude of EM anomaly. Measured target locations	• Daily instrument verification strip	Amplitude within 25%. Location within 0.25 m	Recovered polarizability within 20%. Target location within 0.02 m
Production rate	Number of cued interrogations per day. Time required to prepare data for delivery	• Log of field work and data pre-processing time accurate to 15 minutes	Survey: 100 anomalies per day. Pre-processing time: <3 minutes per target	Average daily survey rate of 90 targets. Pre-processing time of 5 min per target
Minimize number of anomalies to resurvey	Number of anomalies for which data quality can be improved	• List of anomalies selected for resurvey	Less than 5% of anomalies to resurvey	1% of anomalies were resurveyed
Analysis and Classification Objectives				
Maximize correct classification of munitions	Number of false targets eliminated at a specified confidence level and number of true targets kept	• Prioritized dig list with probabilities • Scoring reports by IDA	Correct classification of at least 95% of munitions. Reduction of false alarms by > 40%	100% of munitions were identified. False alarm was reduced by over 80%

Location and depth accuracy	Average error and standard deviation in depth, northing and easting for targets	• Ground-truth within 0.05 m • Estimation from inverted data	$\Delta Z < 0.10$ m ΔN & $\Delta E < 0.05$ m $\sigma Z < 0.10$ m σN & $\sigma E < 0.15$ m	$\Delta Z = 0.05$ m $\Delta N = \Delta E = 0.01$ m $\sigma Z = 0.09$ m $\sigma N = \sigma E = 0.15$ m
Minimize number of anomalies that cannot be analyzed	Number of anomalies that cannot be analyzed	• Demonstrator target parameter • IDA list of anomalies • Ground-truth labels and depth	Reliable target parameters can be estimated for > 95% of selected targets in adequate depth range	Parameters were inferred for all targets

3.1 OBJECTIVE: DETECTION OF ALL MUNITIONS OF INTEREST

Quality data should lead to high probability of detecting the targets that are selected for cued interrogation at the site.

3.1.1 Metric

The metric for this objective was the percentage of anomalies for which one of the cued interrogation soundings exceeded the detection threshold.

3.1.2 Data requirements

Given that the MPV was only deployed in cued interrogation mode, there was no actual detection survey. Instead the amplitude of the recorded signal could be expressed in terms of Signal to Noise Ratio (SNR) value for the data tile that was associated with each target.

3.1.3 Success criteria evaluation and results

The objective of 95% detection was exceeded with a 100% detection rate of TOI and metallic clutter. There was no false alarm; flags with no contact generally coincided with weak instrument response (low SNR).

3.2 OBJECTIVE: REPEATABILITY OF INSTRUMENT VERIFICATION TESTS

Reliability of survey data depends on stability of survey equipment. This objective concerns daily verification on an Instrument Verification Strip (IVS) where metallic targets were buried. Cued interrogation was performed to verify the stability of the data amplitude and the inferred target parameters and verify the sensor background response. Given that the IVS was located in open field we could also directly verify the accuracy of the beacon positioning system relative to the RTK GPS.

3.2.1 Metric

The metrics for this objective were the amplitude and decay of the target polarizability parameters, the inferred target location and the difference between GPS and beacon locations.

3.2.2 Data requirements

The EMI response for target soundings, background measurements and location on the IVS were recorded.

3.2.3 Success criteria evaluation and results

This objective was attained if the target parameters amplitude remained within 25% of the mean value and the location within 0.25 m. The objective was met. We verified that the recovered polarizabilities were remarkably stable, that the inferred location remained within 0.02 m and that the beacon remained accurate with less than 0.02 m difference with GPS. Background noise was stable – the soil response was negligible at the IVS, which was ideal for the specific purpose of verifying sensor stability.

3.3 OBJECTIVE: PRODUCTION RATE

Ultimately discrimination survey and data analysis should be quicker than excavating every potential target. This particular objective only included the sensor-specific tasks of data collection and pre-processing. The latter task involved preparing data for distribution to analysts and included: digitizing field notes, consolidating all soundings for each anomaly, inferring sensor position with the beacon and merging with the EM data, removing background and normalizing by transmitter current.

3.3.1 Metric

The metrics for this objective were the mean daily survey rate and the mean pre-processing time per anomaly.

3.3.2 Data requirements

The number of surveyed anomalies and pre-processing time were recorded every day.

3.3.3 Success criteria evaluation and results

The productivity objective was a mean daily survey rate of 100 anomalies and mean pre-processing time of less than 3 minutes per target. Productivity at Camp Beale was 90 targets per day and 5 minutes pre-processing time per target. The lower productivity rate was due to additional tasks that had to be performed to ensure high data quality.

The original procedure was based on a standard survey pattern of 6 points per target (5 point in a square, plus one tilt, plus one beacon boom shot). This procedure assumed that the peak anomaly was well located to mark the survey center. At Camp Beale we found at an early stage that marked target locations – flags – often seemed to be offset with the MPV peak location, as indicated in the receiver data collected at the flag. To ensure adequate spatial coverage we changed the survey pattern to a 3 x 3 point grid. Having noticed the presence of a significant soil response, we also decided to acquire a soil-background sounding for each flag so that the potential for spatial variations in background signal could be documented. These modifications increased the number of soundings from 7 to 12 and diminished productivity.

Pre-processing time was mostly increased because of the necessity to account for a significant soil response. Following data collection, background soundings had to be checked against a soil model for validation. Beacon data processing had to be revised to implement new verification procedures – our existing process was too simple, having only been tested in flat, horizontal survey environments (test bench and YPG).

3.4 OBJECTIVE: MINIMIZE NUMBER OF ANOMALIES TO RESURVEY

High quality data are necessary to achieve reliable discrimination and minimize the number of anomalies that cannot be analyzed. Insufficient spatial coverage or noisy measurements might require that additional soundings at new locations or with increased stacking time need to be collected to improve the potential of characterizing a selected anomaly. Data quality was reviewed on site to verify that each target had sufficient number of usable soundings for classification. We also verified that MPV and beacon receivers were recording plausible data.

3.4.1 Metric

The metric for this objective was the number of targets that required additional soundings.

3.4.2 Data requirements

The number and identity of targets that required resurvey was recorded.

3.4.3 Success criteria evaluation and results

The objective was a maximum of 5% targets to resurvey. The crew was sent to resurvey only 1% (10 out of 912 targets). Targets were only resurveyed because their peak anomaly was significantly offset from the flag location, resulting in insufficient spatial coverage. None of these anomalies was related to a target of interest (TOI). Note that these resurveys could have been avoided if the MPV had embarked a data gridding display capability.

3.5 OBJECTIVE: MAXIMIZE CORRECT CLASSIFICATION OF MUNITIONS

This is the most important objective of the classification study: all shallow munitions should be recommended for excavation after geophysical inversion. This objective required that sufficient, high-quality data were collected, and that the ensuing data analysis, inversion and statistical classification process recognized the presence of munitions.

3.5.1 Metric

The metric for this objective was the number of targets that were correctly classified.

3.5.2 Data requirements

A ranked anomaly list was submitted to ESTCP for scoring by the Institute for Defense Analyses (IDA).

3.5.3 Success criteria evaluation and results

The objective of identifying at least 95% of the TOI with at least 40% clutter rejection was met. All TOI were found with over 80% clutter rejection.

3.6 OBJECTIVE: LOCATION AND DEPTH ACCURACY

Correct target classification relies on the capability to extract accurate target parameters, including target location and depth. The capability to accurately locate a target of interest is also of importance for safe and efficient site remediation.

3.6.1 Metric

The metric was the accuracy in estimating target depth and geographic location.

3.6.2 Data requirements

Target location and depth for the models selected for the submitted dig list were compared with recorded ground truth measurements. Note that there was some uncertainty in the documented locations, especially in the densely forested areas.

3.6.3 Success criteria evaluation and results

The objective was met. The error between predicted and observed geographical location had a two-dimensional log-normal distribution with mean below 0.01 m; the standard deviation was 0.15 m for all targets and only 0.10 m for TOI. Mean depth error and standard deviation were 0.05 m and 0.15 m for all targets, and 0.03 m and 0.03 m for TOI.

3.7 OBJECTIVE: MINIMIZE NUMBER OF ANOMALIES THAT CANNOT BE ANALYZED

Some anomalies may not be classified either because the data are not sufficiently informative – the sensor physically cannot provide the data to support classification for a given target at a given depth – or because the data processing was inadequate. The former is a measure of instrument performance measured by the aggregate performance of all data analysts. The latter is a measure of the data analysis undertaken in this study relative to that of other analysts.

3.7.1 Metric

The metric for this objective was the number of anomalies that cannot be analyzed by our method, and the intersection of all anomaly lists among all analysts.

3.7.2 Data requirements

Each analyst submitted their anomaly lists. IDA scored all dig lists.

3.7.3 Success criteria evaluation and results

The objective was to be able to confidently analyze at least 95% of the selected anomalies that fall within the MPV’s detection range. Data quality was such that 100% of the anomaly were inverted and fitted with a model. There were cases for which multiple anomalies occurred in the vicinity of a flag. Each anomaly was masked and inverted and the most likely TOI for that given flag was determined at the classification stage. There were also cases with no distinct anomaly at the flag location. The data were nonetheless inverted. In the case of the 36 No-Contact flags, the fitted models corresponded either to small, distant metallic debris or to soil-like targets at large burial depth (0.5-1.2 m). Because such targets may resemble large ordnance such as 81 mm or 105 mm, one of these targets was included in the training data request.

4.0 SITE DESCRIPTION

The site description material is extracted from the Site Inspection Report, which includes full details. Camp Beale is an approximately 60,000 acre site located in Yuba and Nevada Counties, CA. The demonstration was conducted in a 10 acre area that is located within the historical bombing Target 4 and the Proposed Toss Bomb target area. An aerial photo of the demonstration area is shown in Figure 7.

4.1 SITE SELECTION

This site was chosen as the next in a progression of increasingly more complex sites for demonstration of the classification process. The first site in the series, former Camp Sibert in Alabama, had only one target-of-interest and item “size” was an effective discriminator. A hillside range at the former Camp San Luis Obispo in California was selected for the second of these demonstrations because of the wider mix of munitions, including 60-mm, 81-mm, and 4.2-in mortars and 2.36-in rockets. Three additional munitions types were discovered during the course of the demonstration. The third site chosen was the former Camp Butner in North Carolina. This site is known to be contaminated with items as small as 37-mm projectiles, adding yet another layer of complexity into the process. The fourth site, the former Mare Island Naval Shipyard (MINS) in Vallejo, CA, was selected because of an opportunity in the Navy’s remediation schedule at MINS to conduct the study in the midst of their ongoing munitions response project and prior to the upcoming removal action in 2012.

This site was selected for demonstration because it is partially wooded and is thought to contain a wide mixture of munitions. These two features increase the site’s complexity and both characteristics are likely to be encountered on production sites. The tree cover poses a navigation challenge by increasing the difficulty of obtaining accurate GPS readings. Future sites including this one will provide additional opportunities to demonstrate the capabilities and limitations of the classification process on a variety of site conditions.

4.2 SITE HISTORY

Prior to Department of Defense (DOD) usage in 1940, the property was a settling point for miners, who had moved on to other regions when the area was depleted of gold. However, the miners that remained used the land for agriculture and cattle grazing. Currently, the former Camp Beale project area consists of multiple land use property areas. The east region is predominantly undeveloped and used for cattle grazing. The central section is designated as the Spenceville Wildlife and Recreation Area. Both the southeast and southwest regions of the former Camp Beale are moderately populated with rural residential areas. Many of the surrounding areas are used for ranching activities and remain undeveloped. Detailed information regarding occupation of this area by Native Americans and early settlers can be found within the ASRs.

The former Camp Beale property area was acquired by the U.S. Government prior to 1940 and consisted of 85,654 acres. It was originally established as a training post for the 13th Armored Division, which departed in December 1943 and eventually ended up as part of the 3rd Army in Europe. Two other Divisions (the 81st and 96th infantries) also trained at Camp Beale. The camp was used for various other military activities such as a personnel replacement depot, an overseas replacement depot, an induction center, a prisoner of war encampment, and a West

Coast separation center. Camp Beale provided a complete training environment for divisional training, which included ranges for all of the division weapons, plus areas for joint training with Army Air Corps units from such bases as Sacramento and Santa Rosa.

In 1943, Camp Beale was selected as the site for the West Coast Chemical Warfare School (CWS). By1944, the threat of chemical warfare with the Japanese had diminished, and in June 1944, the school was moved to Rocky Mountain Arsenal. In 1945, Camp Beale was designated as a point for classification, rehabilitation, and repacking of the CWS materiel (returning from the Pacific Theater) until its closure in 1947. In May 1947, the Camp Beale reservation was declared surplus by the War Department (effective 31 May 1947) when it was placed on the surplus list. By 29 September 1947, the War Assets Administration had assumed custody with certain regions being reserved for use by the National Guard. It was during this time that a large number of the buildings were sold. In early 1948, the Air Force acquired this land (designated it as Beale AFB) through transfer and used it to train bombardier-navigators in radar techniques. The land was segregated into 6 bombing targets (approximately 1,200 acres each). By 1956, the Navy began using two of the target areas until 1957, when there was no more need for the bombing areas and ranges. At that time, a large portion of the site (approximately 65,000 acres) was declared excess.

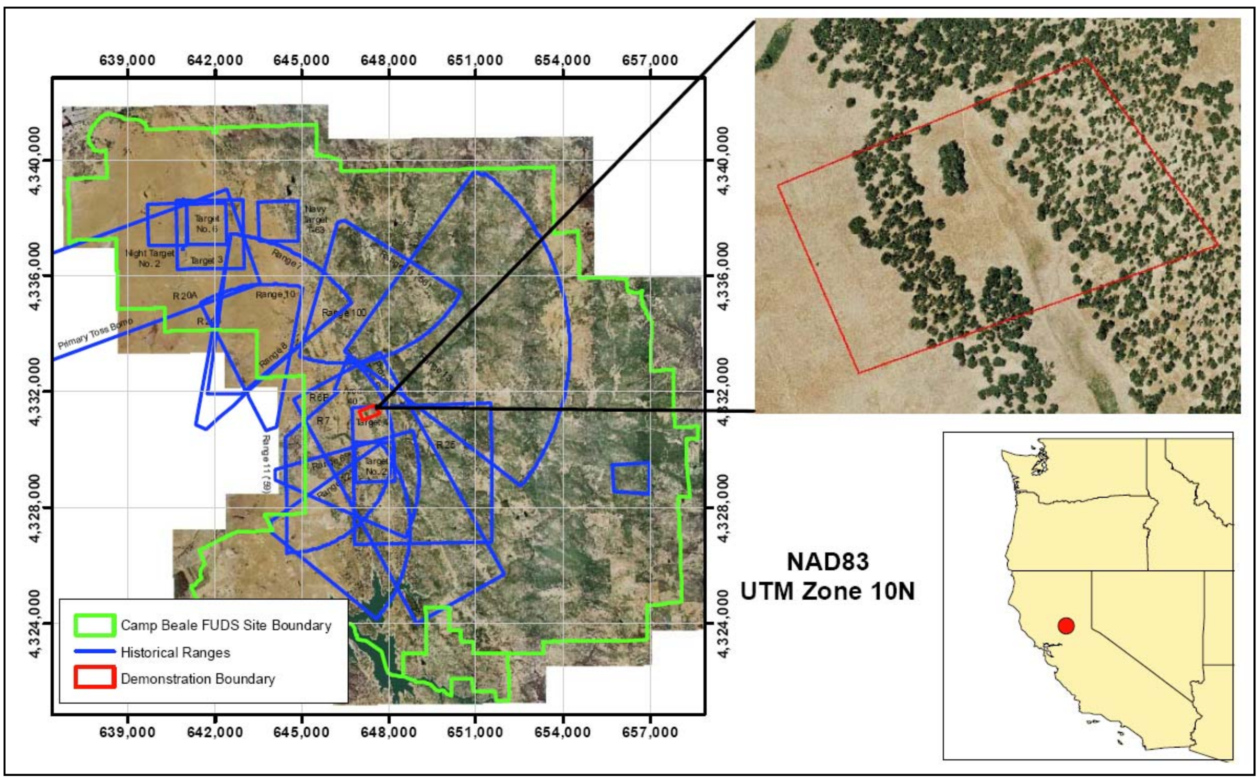

Figure 7: Aerial photograph of the former Camp Beale FUDS with historic ranges overlain. The original 50 acre site boundary is shown in the blow-up.

4.3 MUNITIONS CONTAMINATION

The suspected munitions in this demonstration area include, but are not limited to:

- 37 mm projectiles
- 60mm mortars

- 81 mm mortars
- 105 mm projectiles

At the particular site of this demonstration, evidence of 81mm mortars and 105mm projectiles was found during the Site Inspection intrusive investigation in 2005. It is also suspected that 60mm mortars may be present. In addition, 37mm projectiles have been found scattered throughout the former Camp Beale and are included as another suspected munitions type in this area. Due to the complex historical usage of this site over many years and the overlapping network of historical ranges throughout, it is also likely that other munitions types beyond those listed above may be encountered.

4.4 SITE CONFIGURATION

The demonstration area totals approximately 10 acres divided into sub-areas for the MetalMapper, the portable systems, and a combined area where both collected data. The EM61 cart surveyed all three sub-areas at 100% coverage. The 50-acre demonstration site is shown in Figure 8 with the extent of the three sub-areas shown. Shape files delineating the final sub-area boundaries are available from the ESTCP Program Office.

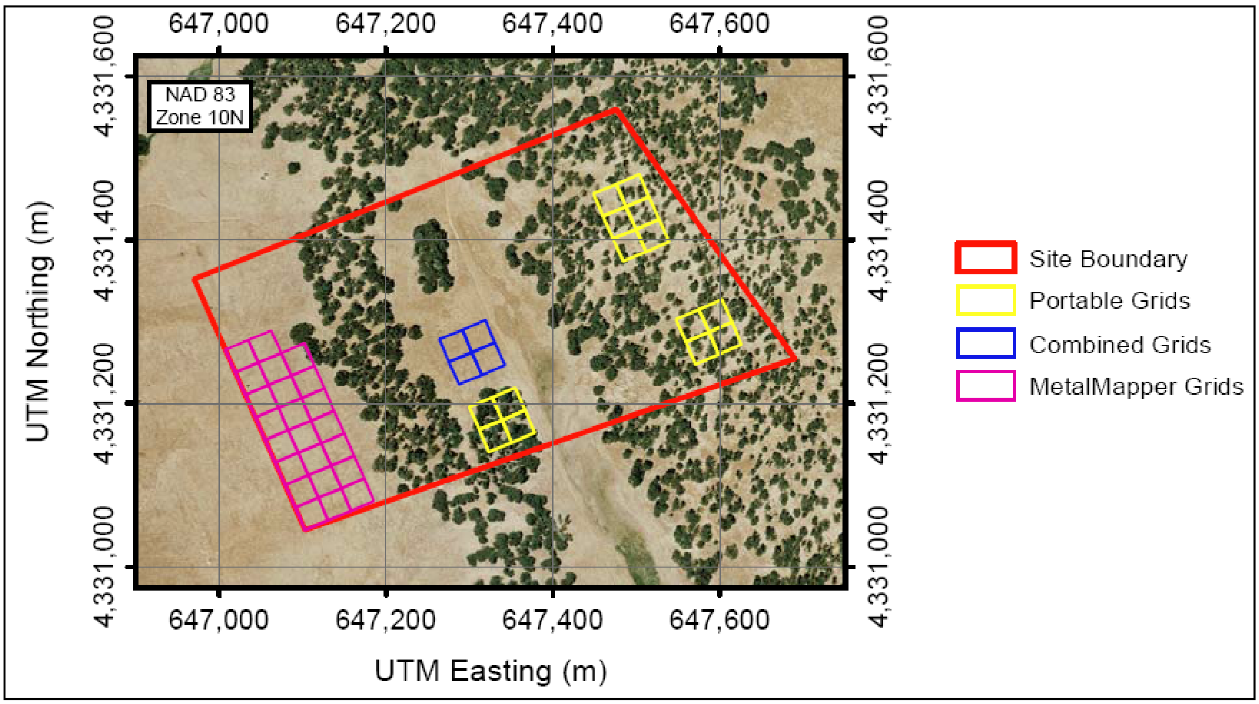

Figure 8: Fifty-acre site with the MetalMapper, portable system, and combined sub-areas delineated.

5.0 TEST DESIGN

The goal of the study is to demonstrate and characterize detection and discrimination with the MPV. Sensor discrimination performance is characterized as a function of the size and depth of the buried targets and the presence and effect of aggravating factors (nearby object, magnetic soil and complex terrain). This section describes data collection and analysis.

5.1 CONCEPTUAL EXPERIMENTAL DESIGN

Field data collection at Camp Beale was divided into calibration activities and discrimination surveys. Calibration had two components. On the first day, May 31, 2011 we measured the MPV response over a series of known targets placed in different orientations inside a training pit. The dataset was analyzed to verify the stability of the recovered target parameters and develop a library of known target features. Calibration was also performed on a daily basis by surveying over an Instrument Verification Strip (IVS), where 5 known targets are buried, to verify data quality, stability of the target responses and accuracy of beacon positioning. Details follow in Section 5.4. The IVS was also used after any repair and the data were immediately inverted before proceeding further.

Discrimination survey activities started on June 1, 2011 and spread over 14.5 field days, including 1.5 days of rain, 1.5 days of repairs and 1 rest day. The survey area was split in 4 areas. For each area a survey list was created such as to minimize the overall travel distance to visit every anomaly. After the daily IVS survey field operators walked to the next anomaly on the list and proceeded with cued interrogation surveys.

The entire field deployment was scheduled to extend over three weeks, planning for contingencies. Half a day was used at either end to unpack, assemble the sensor, set up the survey and base station and the converse tasks. Calibration measurements on a training pit and the first IVS survey took half a day. Some data pre-processing and quality control was performed during the deployment, on and off site, so that any required action could immediately be enacted. For instance, having noticed a significant soil response in the demonstration area and weak response in the calibration area, we took a series of background measurements at different height above ground to quantify the sensor response and verify its predictability (Section 5.4.3). The final pre-processing stage of preparing the data for distribution was completed within two weeks of survey termination.

The advanced tasks of feature extraction by geophysical inversion and target classification were accomplished over the summer of 2011. Some inversions were initiated while at Camp Beale to verify that meaningful parameters could be extracted; however, refined strategies for compensating or defeating soil background effects were done after the survey. Retrospective analysis and reporting were scheduled for the fall and winter.

The following Gantt chart shows the schedule for each phase of testing and how the various phases are related.

Table 1: Demonstration steps

	Preparation Calibration			Open Field		Post survey analysis		
Tasks and demonstration stages	**1.1**	**1.2**	**1.3**	**2.1**	**2.2**	**3.1**	**3.2**	**3.3**
Mobilization – Demobilization	X				X			
CALIBRATION ACTIVITIES: training pit		X						
CALIBRATION ACTIVITIES: training data inversion and parameters stability analysis		X						
CALIBRATION ACTIVITIES: twice-daily test strip			X	X				
If poor performance, change acquisition parameters and resurvey		X	X					
OPEN FIELD SURVEY: cued interrogation				X				
OPEN FIELD SURVEY: data pre-processing				X		X		
DATA ANALYSIS: feature extraction/inversion							X	
DATA ANALYSIS: classification and ranked list							X	
RETROSPECTIVE ANALYSIS								X
REPORTING								X

5.2 SITE PREPARATION

Site preparation was organized by ESTCP Program Office.

5.3 SYSTEM SPECIFICATION

Data were acquired in cued interrogation mode. The system was set for 25 milliseconds (ms) excitation and 25 ms recording of EMI transients. This was accomplished by using 0.9 seconds (s) data blocks with 9 repeats (100 ms per cycle). Stacking time was set to 6.3 s by using 7 stacks (effectively 9 x 7 = 63 cycles). Digital receivers use a 4 microsecond sampling rate. The data were recorded with 133 logarithm-spaced time gates (0.05% gate width) from 0-25 ms.

Local positioning was achieved with the beacon system. An Applied Physics 543 orientation sensor was mounted at the far end of the MPV handle to measure azimuth. The three-axis sensor data were also used for verifying the pitch and roll inferred from the beacon measurements. Practically, the beacon boom was laid on the ground within 2 meters of the survey flag. Boom orientation was recorded by placing the MPV head at the boom center and lining up the MPV's main direction (Y-axis) with the boom's direction. To facilitate quality checks, the boom was generally oriented in the North-South direction, and because the terrain was sloped, the boom

was placed uphill from the flag. After data processing, beacon-derived positions were located relative to the local flag and the geographic North, and subsequently globally-referenced using the supplied GPS coordinates of each flag. A Novatel real-time kinematic (RTK) GPS was also mounted on the MPV handle. It was used to locate pre-programmed flag locations and verify beacon accuracy whenever enough satellites were visible, in particular at the IVS and in the open-field "combined area", where we started the demonstration. The GPS operated at 20 Hertz; its base station was located at the NE marked monument, which position was convenient to service the entire site.

The original sounding pattern consisted in placing the MPV head at the four corners and center of an imaginary square centered on the anomaly. Having noticed that the flag location did not always coincide with the MPV peak anomaly, we modified the survey pattern to a 9-point grid. This approach had several benefits: first, setting a Standard Operating Procedure (SOP) relieved the operator from having to constantly monitor the sensor display to guess the target location; second, this reduced operator-dependency on data quality; finally, additional soundings can be useful to assess and mitigate background effects. In addition to the survey pattern, one sounding was acquired by tilting the head back by 45 degrees above the center or the detected anomaly peak. If the operator found that peripheral soundings showed significant signal above background, then additional soundings were collected as an attempt to capture the full spatial decay of the flagged target.

5.4 CALIBRATION ACTIVITIES

Calibration is necessary for verifying proper sensor operation and calibrating sensor response over known targets.

5.4.1 Training pit

Classification is easier when the typical response of expected targets is known – these responses can be aggregated into a library for comparison. The demonstration site was expected to host 37, 60 and 81 mm mortars and 105 mm projectiles, 4"-long steel cylinder (ISO) and potentially other types of UXO. A sample of these known targets was supplied by ESTCP to measure their response in a test pit. The target set was augmented with metallic fragments.

Figure 9: Calibration targets used in training pit.
The top row includes, starting from the left, 60 mm mortar body (no nose and fins), 37 mm, ISO cylinder, empty 57 mm casing, folded scrap and 81 mm. The center piece is a fragment of a 72 mm caliber projectile, and the bottom item is a 105 mm.

Each sample was successively placed inside a clutter-free training pit and surveyed in cued interrogation mode. Measurements were taken with the target oriented at a vertical and oblique angle, nose up and down, and in horizontal position. Depth and orientation were recorded (Figure 10). The data were subsequently inverted to verify that stable, target-specific features could be obtained. These features were included into the target library for classification.

Figure 10: Cued interrogation training at test pit.
A: Cued interrogation on a flat surface, following standard survey procedure. The pit remained hollow, no dirt was put back in to fill it in; therefore a sheet of plywood was placed to cover the hole.
B: Depth measurement of a 60 mm mortar body.

5.4.2 IVS

Control on sensor drift was performed through daily survey over the IVS, where known targets were buried in a clutter-free environment. The targets were an ISO, 37 mm, 60 mm and 81 mm mortars and 105 mm projectile. Each target location was marked with a flag; no detection survey was required. A cued interrogation survey was performed for each target, following a 9-point grid plus tilt. Data were generally inverted soon after the survey to verify data quality, stability of the recovered parameters and accuracy of the beacon positioning system. The IVS calibration survey generally took 20 minutes.

5.4.3 Background measurements

Soil had a distinct red tint in the demonstration area that suggested presence of iron oxides. These oxides are known to have an effect on EMI sensors (Pasion et al., 2008; Lhomme et al., 2008). Because oxidation depends on soil iron content and degree of weathering, there can be significant spatial variations at a site with varied topography. To document these potential variations and control response due to magnetically active soil, we collected a background shot for each target or cluster of targets. The measurements were made by placing the sensor head on the ground, at least 2 m away from the nearest flag, and quantitatively verifying the typical amplitude and decay response of magnetic soils (Figure 11).

Background responses at the IVS and in the field are shown in Figure 12 along with a schematic that illustrates the expected magnetic soil response for the MPV. The IVS shows a weak background response. In contrast, field soundings showed the characteristic viscous remanent magnetization that affects specific receivers (vertical and radial) with log-linear time decay (soil decays in *1/t*). Observation of this rule was quantitatively verified during the pre-

processing stage to confirm validity of the clean soil background measurements. In-air measurements away from any other potential noise sources were also periodically acquired. Use of these background measurements and noise compensation methodologies are discussed in a later section.

Figure 11: Background measurement in open field area, where red soil indicates presence of iron oxides. The sensor head is placed on the ground, away from the surrounding flags. The operator examines the recorded response to confirm the absence of metal objects in the sensor's field of view.

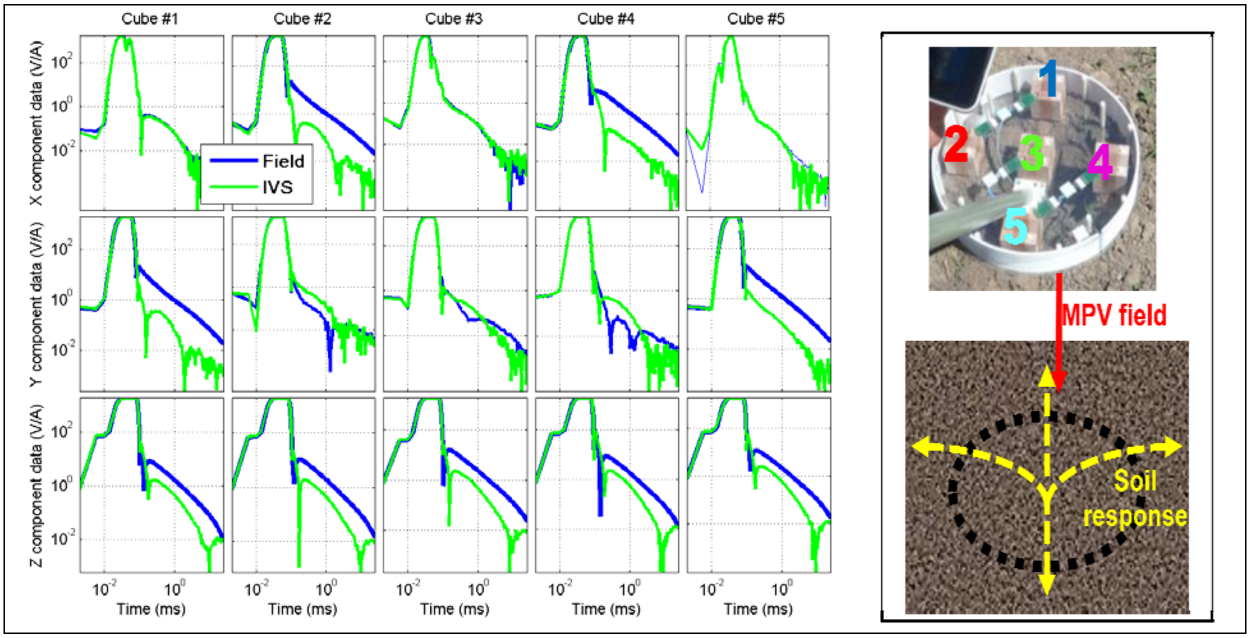

Figure 12: Effect of magnetic soil on the MPV sensor.
<u>Left</u>: Background measurements at IVS and in field with MPV sensor head placed on ground away from flag.
<u>Right</u>: Schematic of magnetically active soil response. The response mirrors primary field emitted by MPV circular transmitter. Therefore it affects X-component (East-West) data measured on cubes 2 and 4, Y-component (North-South) data of cubes 1 and 5, and Z-component (vertical) data for all cubes, as shown in left panel.

5.5 DATA COLLECTION

5.5.1 Scale

Data were collected over 912 targets spread in 4 different areas. Their spatial distribution is shown in Figure 13. The GPS base station and IVS were located in the central valley; the survey areas were distributed on the side slopes. Representative pictures of each survey area are shown in Figure 14.

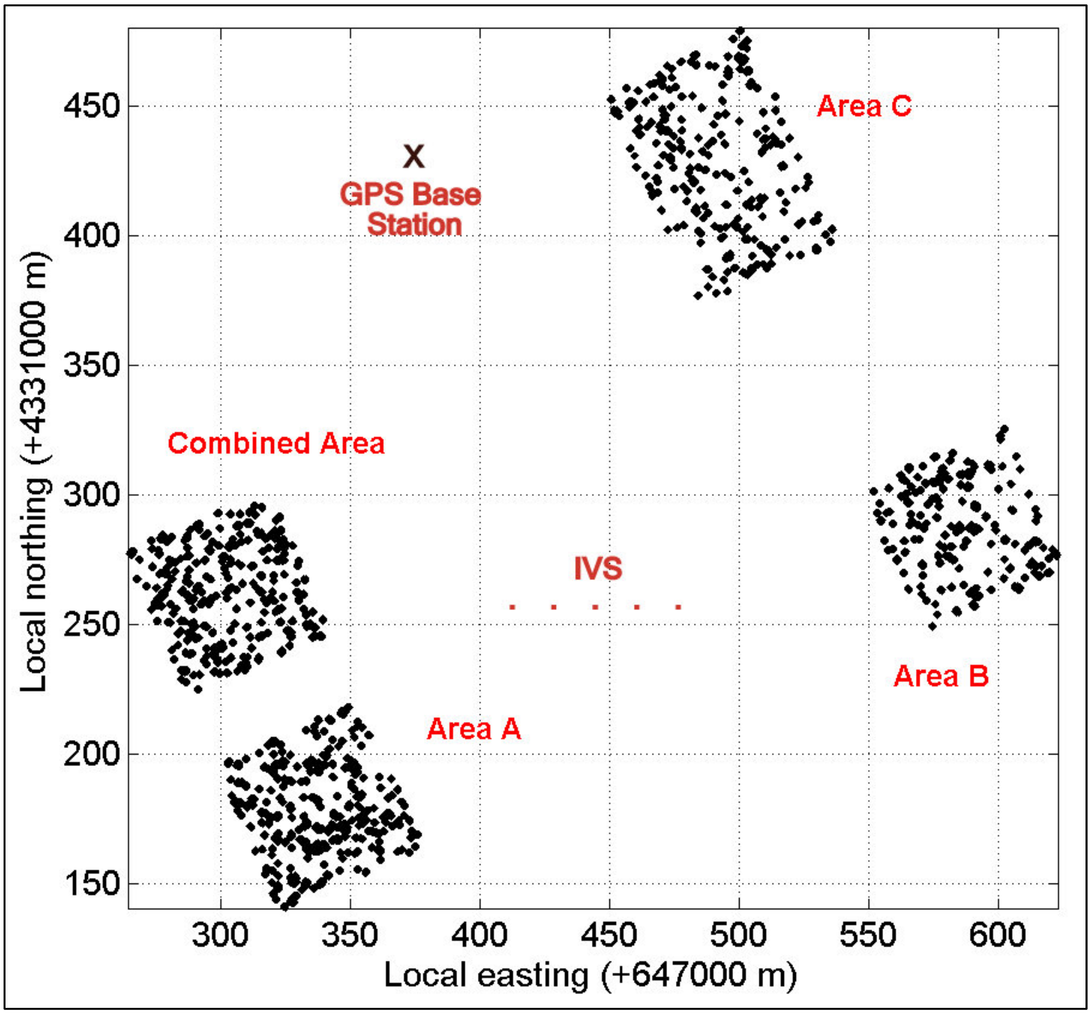

Figure 13: Sounding locations in Camp Beale demonstration.
The training pit was located next to the IVS, on the central valley floor.

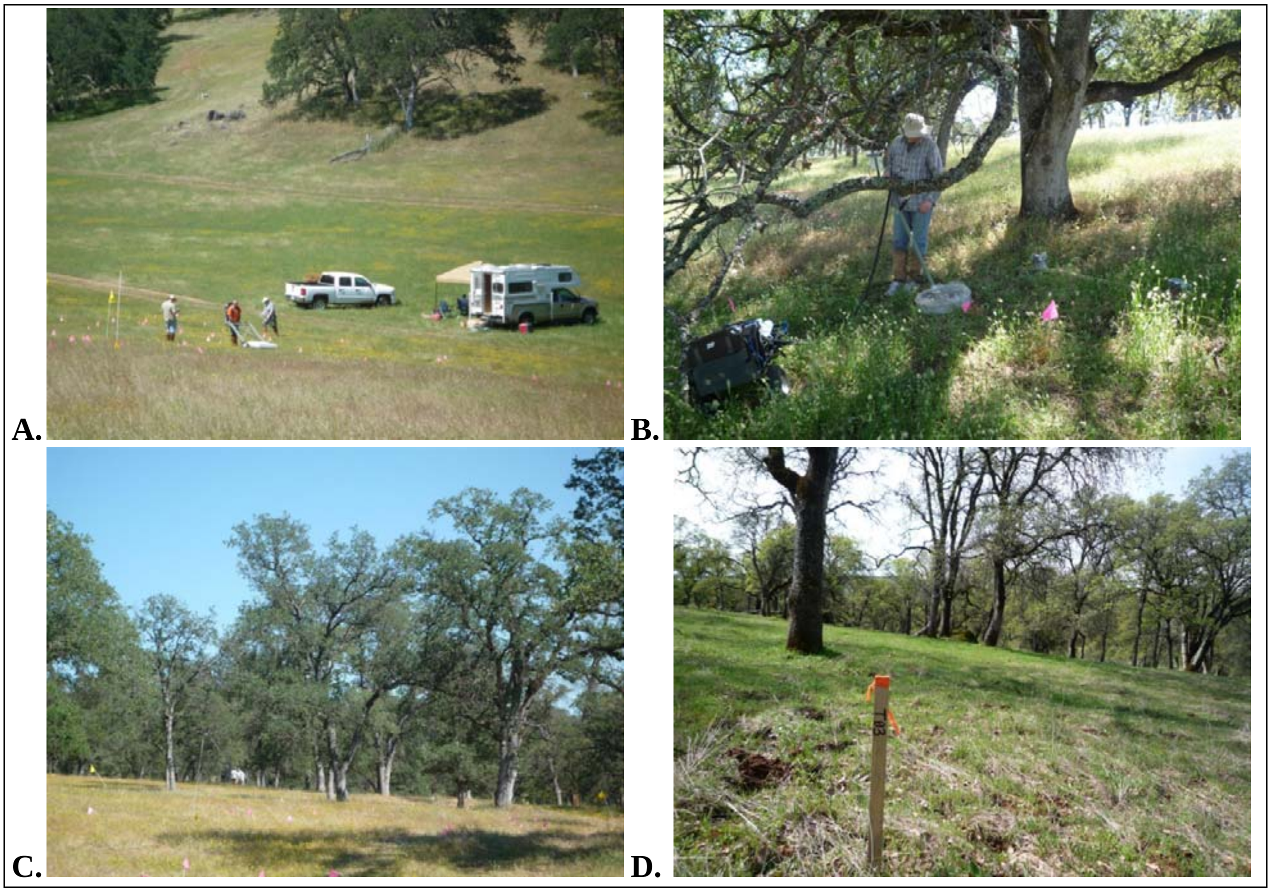

Figure 14: Photographs of the four survey areas (chronologically ordered).
A: Open field, sloped, combined area; the base camp was installed on the valley floor; the GPS base station is located above a rocky outcrop near a tire track in the top left corner of the picture. B: The steep, densely treed area A. C: The gently rolling, sparsely treed area C. D: The rolling and treed area B.

5.5.2 Survey pattern and sample density

Cued interrogation soundings were collected around the marked target location (ground paint and flag). The first sounding was acquired at the marker. The subsequent soundings were generally acquired in a virtual 3 x 3 points grid pattern as in Figure 15. Recorded data were displayed immediately after each sounding acquisition to help the operator estimate the anomaly location and assess spatial coverage. This was accomplished by examining recorded decay curves (Figure 16) and verifying that the furthest receivers were measuring weak signals (background). If residual target signal was detected on peripheral receivers then additional soundings were collected to improve spatial coverage. For instance, if the MPV front receivers showed above-background signal when the MPV was placed in position 2 (Figure 15, left panel), then a sounding would be collected 30 cm to the right of position 2. If a nearby, non-flagged interfering target was detected, then supplementary soundings were acquired to help separate the two sources. Finally, the MPV sensor head was placed above the anomaly peak at 45 degree pitch to stimulate a different excitation direction with high signal while remaining as close as possible to the target. Only one tilt test was performed because it was practically difficult to keep the sensor steady on its side.

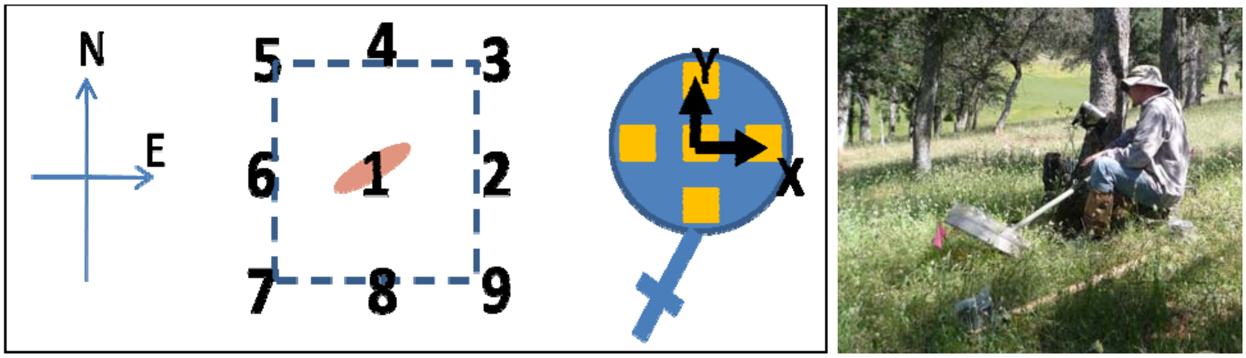

Figure 15: Soundings pattern for cued interrogation with MPV.
Left: Nine-point survey pattern is centered on target. Right: Sensor head is tilted with 45 degree pitch for transverse excitation at short standoff.

We had originally planned to adopt a 5-point square-like pattern with the possibility for the operator to acquire additional data points if the recorded signal indicated a large footprint. This process would have required intense focus from the operator, who would be expected to interpret decay curves for each receiver to locate the target and verify that signal had vanished on the peripheral soundings. Practically, this process put too high a demand on the field operator, especially when considering that 1000 soundings were collected on a daily basis. The method was also devised on the assumption that the first sounding was located at the signal peak. However, we found on the first surveyed targets that the flag location generally did not coincide with the target location, as suggested by the MPV receiver cubes (Figure 17). For these anomalies the peak signal suggested that the target could be located 15-30 cm off to the side. To relieve pressure on the operator and maximize our chances of obtaining full anomaly coverage, the standard operating procedure was modified to a 9-point grid pattern with 40-50 cm spacing. Given that receiver cubes were rigidly mounted with 18.5 cm separation, the maximum signal sampling space was approximately 20 cm.

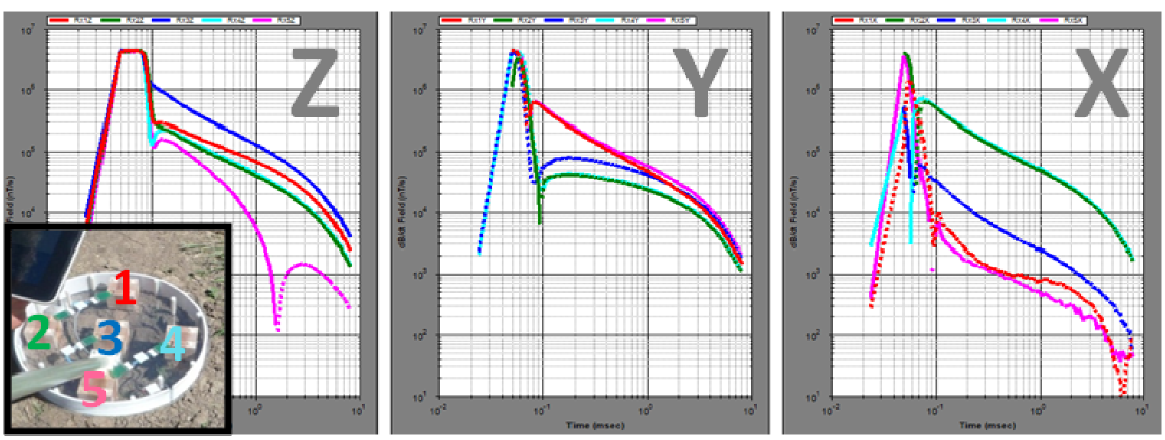

Figure 16: Typical target response above a buried metallic target.
The Z-component data show that the target is closest to center cube (#3) and equally distant from lateral cubes 2 and 4, while signal in 5 seems to be due to background. The Y data confirm that target is buried between front and back cubes (1, 5) and X data confirm that target is located between side cubes 2 and 4.

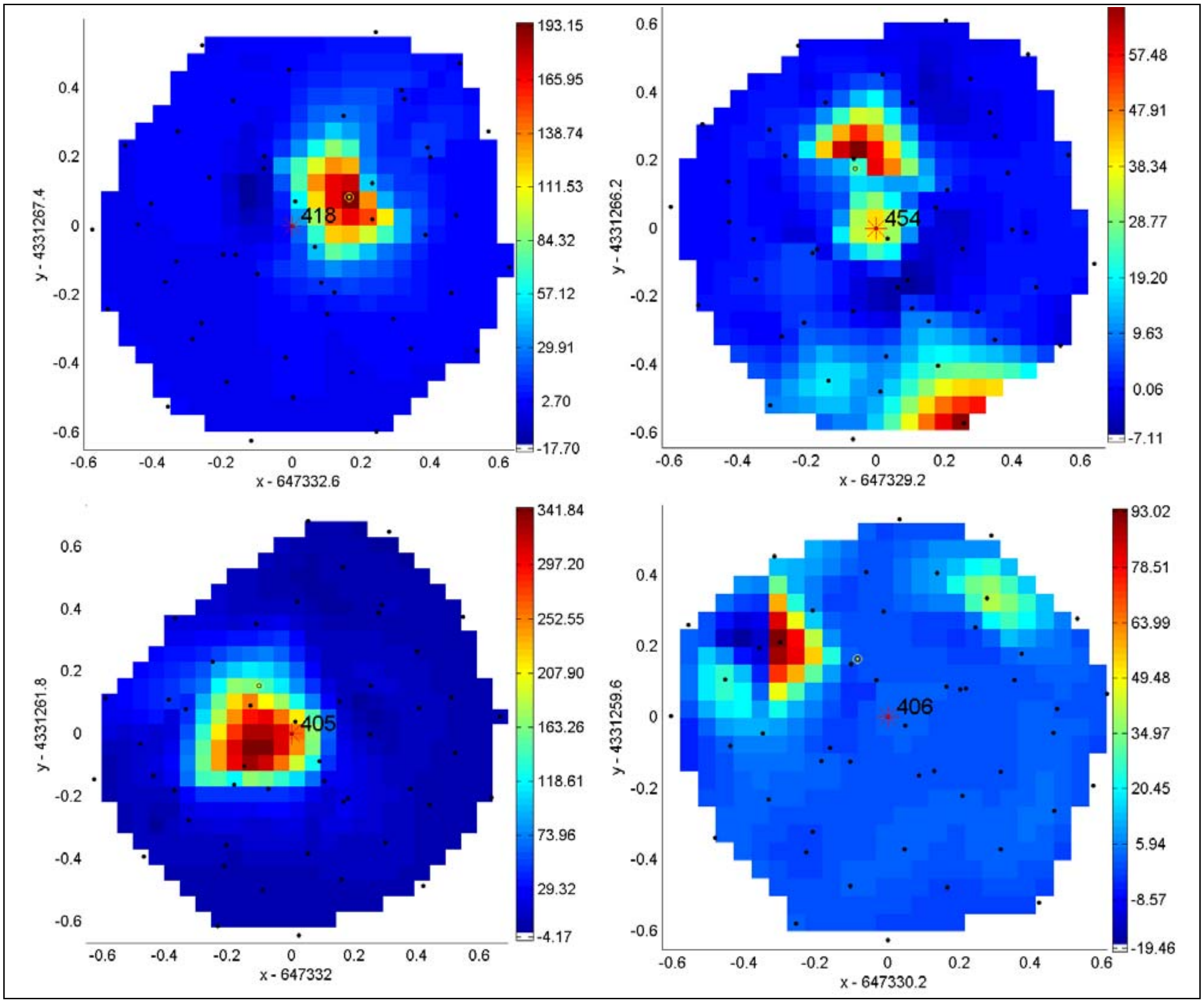

Figure 17: Gridded image of the vertical component receiver data for the first four targets collected at Beale. The flag location, indicated with the red star at coordinates (0, 0), is generally offset from the signal peak. This observation motivated use of a conservative 3x3-point-grid survey pattern.

5.5.3 Quality checks

Data quality checks were performed during and after the survey. As noted above each sounding was immediately examined to verify spatial coverage and to ensure that all receivers were properly operating. Any acknowledged abnormal sounding was re-acquired and tagged in the field notes to differentiate it from acceptable soundings. If a receiver failed then the survey was interrupted to verify that the failure was persistent and consider solutions. David George, who built the sensor, was invited to participate in the survey and was present on site for parts of the study with tools and spares for repair. Data quality was also controlled by daily visual data review. Any problem would be investigated and the affected anomalies would be resurveyed. For instance, we found that for 10 out of 912 targets the spatial coverage was insufficient. This was due either to a large target offset (up to 50 cm, e.g., Figure 18), or a shrunk survey imprint (operator distraction), or absence of a target at a flag (target 841, which flag was displaced by 3

m – we returned and found paint on the ground at the reported GPS location, brought the flag back and resurveyed).

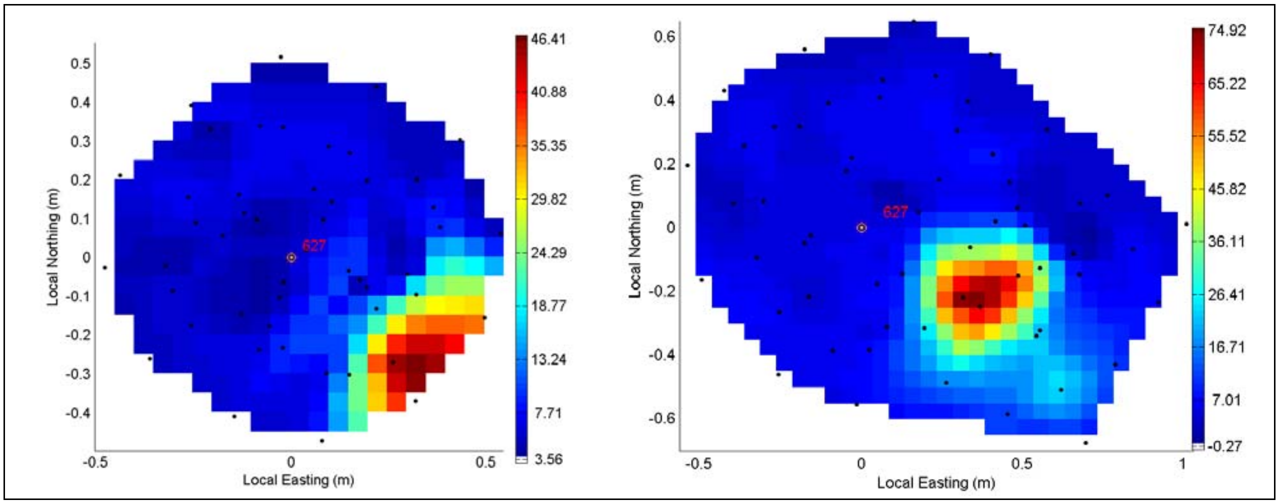

Figure 18: Example of target with large spatial offset requiring resurvey to obtain sufficient spatial coverage. The original data is showed on the left panel and the recollect on the right. The original data were roughly inverted and indicated a large, deep target with low confidence. Instead of potentially recommending the target for excavation, data were recollected; analysis indicated a small piece of metallic clutter.

Beacon-positioning was controlled through different steps. Firstly, field operators took care of placing the beacon boom approximately 1.5-2 m away from the target flag, and keep the data acquisition system (DAQ) and power unit at least 2 m away from the beacon boom cubes to avoid distorting the local EM field. Secondly, beacon signal were monitored on the sensor display on graphs similar to those of Figure 16 along with the other receivers. Weak beacon amplitude could be detected by the operator. Finally, data were pre-processed and visualized onsite, when possible, to infer beacon locations, compare with GPS and verify accuracy (Figure 19).

We also ensured that all anomalies were visited by pre-programming their GPS coordinates and displaying their location on the sensor display map (Figure 3). This tool was useful for approaching new flags. Each visited target was automatically crossed on the map to confirm survey. Given that the tree canopy was not completely opaque, the GPS was always functioning, though sometimes at low accuracy, so that we could obtain a rough estimate of our current location relative to flagged targets.

5.5.4 Data handling

Data were stored as .tem files on the DAQ and converted to .csv files before every battery change. A copy of all .tem and .csv files was kept on the DAQ, on a portable hard-disk drive and on the field laptops that were used for reviewing the data. Field notes recorded the association of target identities and file numbers, in addition to any relevant comment for non-standard events. Notes were digitized every day by taking pictures of the notes and filling out a spreadsheet to be used for pre-processing.

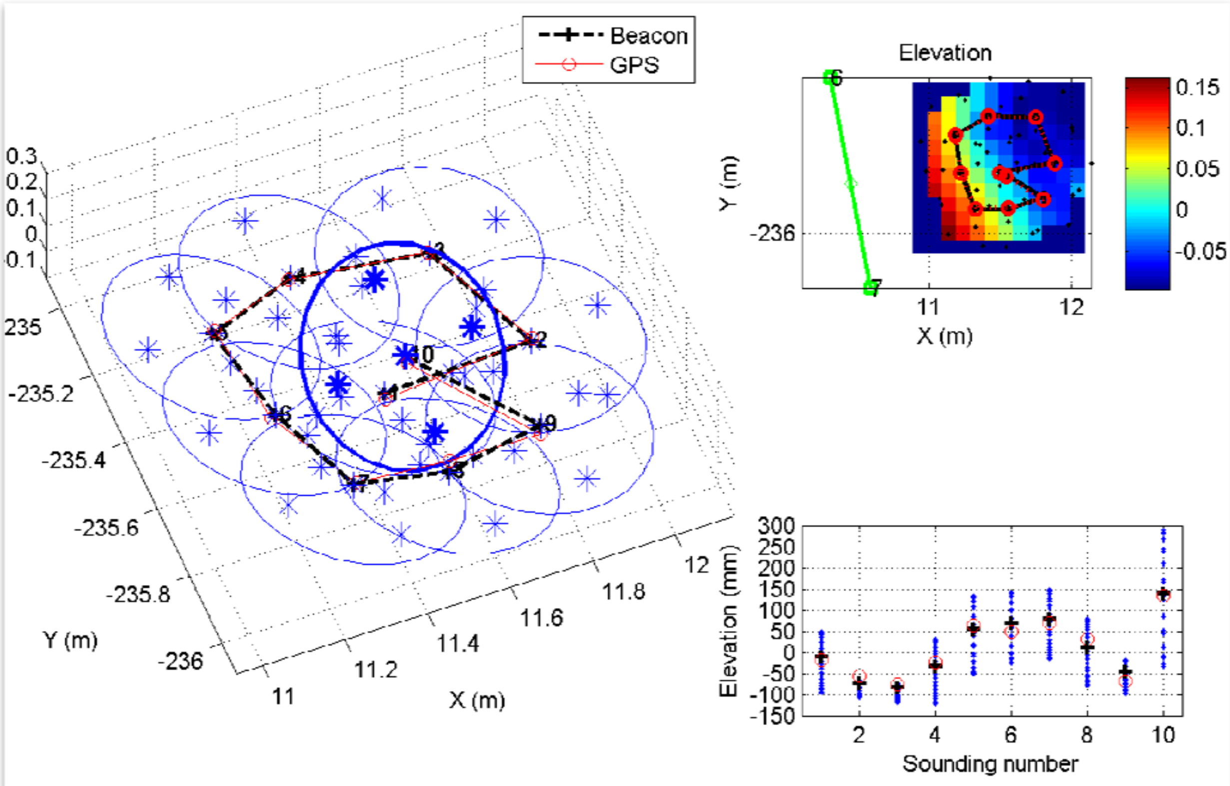

Figure 19: Sounding locations for a cued interrogation.

This type of figures was used for quality control over beacon accuracy and spatial coverage. The survey pattern followed a 3x3 points grid. The left panel shows a 3-dimensional representation of the target locations, as independently predicted by the beacon and the GPS – locations coincide within better than 2 cm. Stars mark receiver-cube locations and illustrate the spatial sampling. Large circles outline the MPV transmitter. The 10^th^ sounding is the tilted test, highlighted with thicker lines. The top right panel shows the sounding locations relative to the beacon boom (green line with cubes number 6 and 7) and a gridded image of the relative elevation of each receiver cube – terrain is gently sloping away from the beacon boom. The bottom right shows the predicted elevation for the GPS (red) and beacon (black cross for center cube, blue dots for side cubes); given that the beacon is a local prediction, we can compare the relative accuracy of the beacon and GPS by solving for the rotation and translation that matches their locations (least-squares minimization).

5.5.5 Data summary

The raw data reside with SKY and G&G Sciences and include one configuration file and one EM data file for each sounding. There are approximately 10,000 files for the entire demonstration. Files were merged and pre-processed as described in Section 6.1.

5.6 VALIDATION

Target validation was organized by ESTCP Program Office.

6.0 DATA ANALYSIS AND PRODUCTS

6.1 PREPROCESSING

6.1.1 Field data

The MPV DAQ computer records data streams from the sensor head, beacon receivers, attitude sensor and GPS with the GPS time stamp. The DAQ saves the data into a .tem binary file. Each sounding data is converted to a .csv file without any data alteration. Several pre-processing stages are performed before delivery to the analysts.

6.1.2 Positioning data

The beacon receiver data, the MPV transmitter current and the digital compass reading are combined to infer the MPV head location. The method is similar to a dipole inversion (Lhomme et al., 2011) and generally yields better than 2 cm accuracy. When the GPS has maximum accuracy (Q factor is equal to 4), its reading and the attitude sensor data can be utilized to predict the sensor head location for comparison with the beacon prediction. In case of aberration with a beacon location, GPS readings and field notes can provide information to diagnose the issue. Otherwise the sounding may be discarded. In practice there was no detected issue with the beacon at Beale.

6.1.3 Delivered data

The pre-processed data were delivered in individual files, each containing all the data associated with one target: EMI data, beacon-inferred sensor-head location, GPS-derived head location and nearby background sounding. The file name indicated the target label. Data files for the field data collection were supplied to ESTCP Program office for distribution, whereas calibration files from the IVS were directly sent to parties involved with the MPV analysis.

The data were delivered in two formats. The first dataset was fully pre-processed. The data were normalized by the transmitter current to remove EMI data dependency on battery power, which can vary by up to 20%. In-air background was subtracted from the EMI data to remove the transmitter ringing that can still be detected at early time (0.1-0.3 ms). The data were reduced to 32 time gates by logarithmic integration (through the same process that had reduced the 4 microsecond signal to the recorded 133 time gates). A nearby background soil signal, clean of any metallic clutter, was associated to each target for the analyst to devise his own soil correction. The second dataset was raw. Transmitter current, related in-air measurement, nearby soil-background measurement and all 133 time-gated data were supplied to the analyst.

One complicating factor was the occurrence of close targets. There were many targets with less than one meter spacing, sometimes 30 cm. Under such circumstances the soundings collected between the two neighboring targets may receive responses from both targets. Characterization of each target may therefore be subjected to the capability to separate the overlapping target responses. Doing so requires accurate relative positioning of the data tiles obtained for each target so that the joint dataset can be analyzed. Similarly, we observed cases where a detected anomaly would be located between two flags (Figure 20). There too the two tiles have to be stitched together for analysis, which requires accurate positioning between tiles.

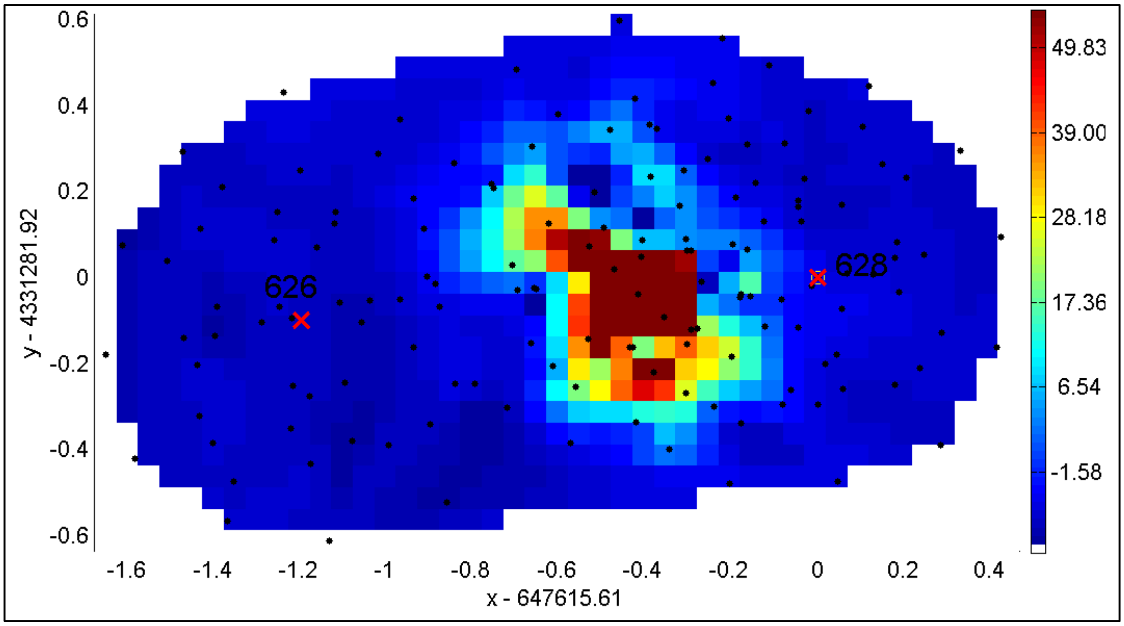

Figure 20: Ambiguous target identity located between two survey flags. Gridded image of the vertical component EM data.

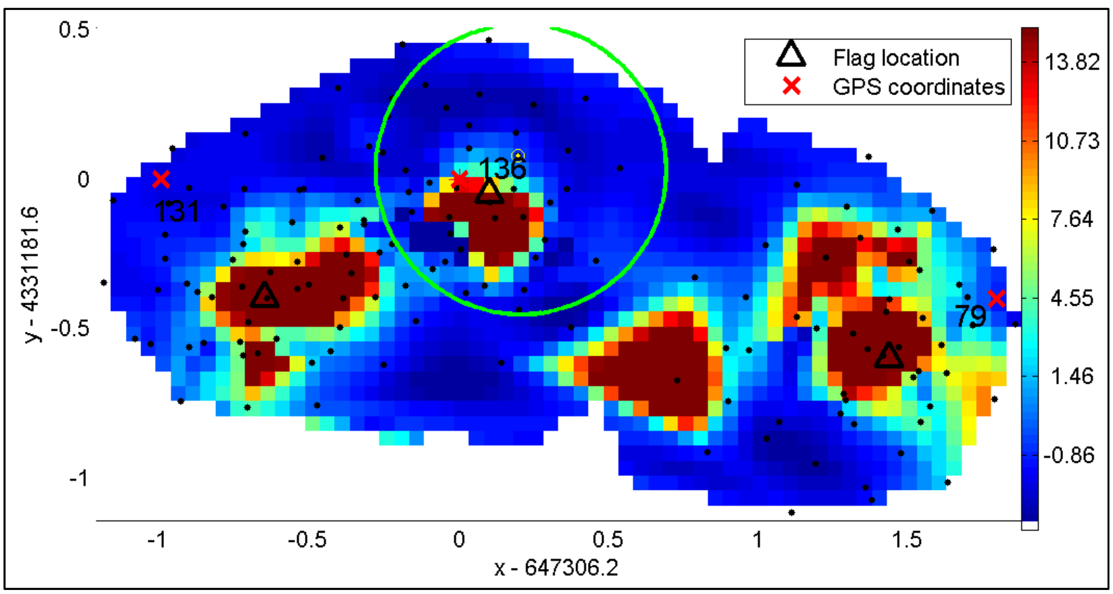

Figure 21: Survey of multiple targets with same beacon station and flag-GPS positional ambiguity. Field flag locations where well placed relative to the buried targets, though their placement significantly differed with reported GPS coordinates. Analysis was further complicated with presence of secondary targets. Targets proximity required masking for inversion of individual anomalies (green circle).

The survey protocol was devised with these constraints in mind. Whenever a cluster of flags was encountered, all targets were surveyed using the same reference beacon boom station so that targets could be accurately located relative to one another. This was particularly important in the woods, where GPS accuracy could deteriorate and lead to misleading interpretation of the distance between flags (Figure 21). Relying on the reported GPS locations to assemble independently-collected neighboring tiles could lead to gross errors. In total we surveyed 352

flags in a multi-target setting, in which several targets were deemed to be close enough to be covered with the same beacon station so that time could be saved by not having to relocate the beacon station, and overlapping signatures could be addressed if warranted. Out of these 352, there were 62 triplets and 8 quadruplets.

The delivered data were organized so that the analyst could recognize and handle the occurrence of multiple close targets. For each target, the provided file started with the data block pertaining to that target, followed with data blocks for its neighboring targets if their field-flag location was located less than 1 m away. We assumed that further targets would not interfere.

6.2 TARGET SELECTION FOR DETECTION

The detection survey was based on Geonics EM-61 data. Targets were selected by Parsons and ESTCP. Target names and locations were supplied for the cued interrogations presented in this study.

6.3 PARAMETER ESTIMATION

The pre-processed data presented in Section 6.1 were imported in the MatLab-based UXOLab software jointly developed by Sky Research and the University of British Columbia and used in numerous ESTCP and SERDP projects. Each anomaly was treated separately. In general there were approximately 10 soundings per anomaly.

The data were inverted using a three-dipole instantaneous polarization model. Inversion setup parameters such as noise estimation were decided upon examination of the training pit data and field background measurements. Solutions with one or multiple targets were investigated for every selected target. Decisions regarding the number of targets at a given location were left to be made through statistical classification by prioritizing munitions-like models. Inversion results were reviewed by an experienced geophysicist to identify any potential issues with the inversion setup or the sensor data.

6.3.1 Feature extraction with dipole model

In the EMI method, a time varying field illuminates a buried, conductive target. This illuminating – or primary – field induces currents in the target that subsequently decay, generating a decaying secondary field that is measured at the surface. These data are then used to estimate the position, orientation, and parameters related to the target’s material properties and shape. In the UXO community, it is commonly assumed that the secondary field can be accurately approximated as a point dipole (e.g., Bell et al. 2001, Pasion and Oldenburg 2001, Gasperikova et al. 2009). The process of estimating the parameters of the dipole forward model from the data is called data inversion.

The dipole model assumes that the time-varying secondary magnetic field **B**(t), is due to a point dipole **m**(t) located at **r**:

$$\mathbf{B}(t) = \frac{\mu_O}{4\pi r^3}\mathbf{m}(t)\cdot\left(3\hat{\mathbf{r}}\hat{\mathbf{r}} - \bar{\bar{\mathbf{I}}}\right), \tag{1}$$

where $\hat{\mathbf{r}} = \mathbf{r}/|\mathbf{r}|$ is the unit-vector pointing from the dipole to the observation point, **I** is the 3 x 3 identity matrix, $\mu_o = 4\pi \times 10^{-7}$ H/m is the permittivity of free space and $r = |\mathbf{r}|$ is the distance

between the center of the object and the observation point. The dipole induced by the interaction of the primary field $\mathbf{B}_o$ and the buried target is given by:

$$\mathbf{m}(t) = \frac{1}{\mu_o} \overline{\overline{\mathbf{M}}}(t) \cdot \mathbf{B}_O \,, \tag{2}$$

where $\mathbf{M}(t)$ is the target's polarizability tensor. The tensor reflects the characteristics of the buried target in terms of its shape, size, and material properties. It is written as:

$$\overline{\overline{\mathbf{M}}}(t) = \begin{bmatrix} L_1(t) & 0 & 0 \\ 0 & L_2(t) & 0 \\ 0 & 0 & L_3(t) \end{bmatrix} \tag{3}$$

The magnitude and decay of the polarizability tensor elements is a function of the size and electromagnetic properties of the target. The relative sizes of the tensor elements are indicative of the target shape. If ordering tensor elements such that $L_1 > L_2 > L_3$, then a steel body-of-revolution (BOR) would have $L_2 = L_3$ for a rod-like object and $L_1 = L_2$ for a plate-like object.

The target parameters of the dipole model (i.e. location, orientation, and polarizability tensor elements) are estimated in the process of data inversion. The objective of data inversion is to determine the set of parameters that most accurately predict the observed data. Numerical optimization methods are used to determine the parameters that minimize a data misfit objective function:

$$\textit{minimize} \quad \phi(\mathbf{m}) = \frac{1}{2} \| V_d^{-1/2} (d^{obs} - F(\mathbf{m}_{target})) \| \quad \textit{subject to} \quad m^{\inf} \le \mathbf{m}_{target} \le m^{\sup} \,, \tag{4}$$

where V_d is the data covariance matrix, which includes a user-defined noise estimate, d^{obs} is the observed data, F is the forward modelling operator, $\mathbf{m}_{\text{target}}$ is the recovered vector of target parameters, and m^{inf} and m^{sup} are the inferior and superior bounds on model parameters. The noise estimate corresponds to not explicitly modelled phenomena that can affect the data, such as sensor noise, geologic effects and positional error. We assume that noise is composed of a base level plus a factor that is proportional to the signal amplitude. In UXOLab noise parameters are set by the user before an inversion. The dipole model is an ideal candidate for inversion because (1) the forward model is physics based with parameters that are indicative of target characteristics, and (2) the forward model is fast to compute, which is important since numerical optimization implies an extensive search of parameter space that involves numerous calculations of the forward model.

6.3.2 Data quality

The main factors affecting data quality are instrument noise, environmental noise and positional error. The first two mostly depend on the sensor characteristics and on the EM interference with the background host, namely the magnetic soil found at Beale. The baseline noise was subtracted from sensor data before inversion; the variability of that noise was utilized to define the base-level noise estimate of the covariance matrix.

The most accessible mean for estimating instrument noise is to perform in-air measurements away from any interference source, assuming that there is negligible atmospheric EM disturbance (in practice, radio air-waves are eliminated owing to the fast 4 microsecond sampling rate and stacking). These measurements were performed several times a day to monitor any potential drift. The recorded signals were normalized by transmitter current intensity and

analyzed (Figure 22). The early time spikes correspond to ringing after the transmitter shuts off; receivers saturate as indicated by the truncated spikes. Each receiver has an individual response that depends on the degree of coupling with the vertical transmitter – vertical component receivers show the largest coupling with lasting effect until 0.3 ms – and on their location relative to one another and to the transmitter switch – the switch is located between cubes #4-5, which explains their particular X-Y-component responses. Signals were highly repeatable and rarely deviated from the median signal; the standard deviation at early time is one order of magnitude smaller than the median. The sensor was therefore remarkably stable. Stability of each receiver's response allowed subtraction of that signature from the target data. In practice we used the data in the 0.1-25 ms range. Residual sensor signature has limited repercussions for classification because it has fast decay – most of the signal has vanished by 0.3 ms. For comparison, target response for the deepest 37 mm and 81 mm ordnance at Beale exceeded 10 milli-Volt (mV) on all receivers and had a slow decay, thus dominating the sensor's signature past 0.1 ms. Soil background response is more significant and discussed in the next section.

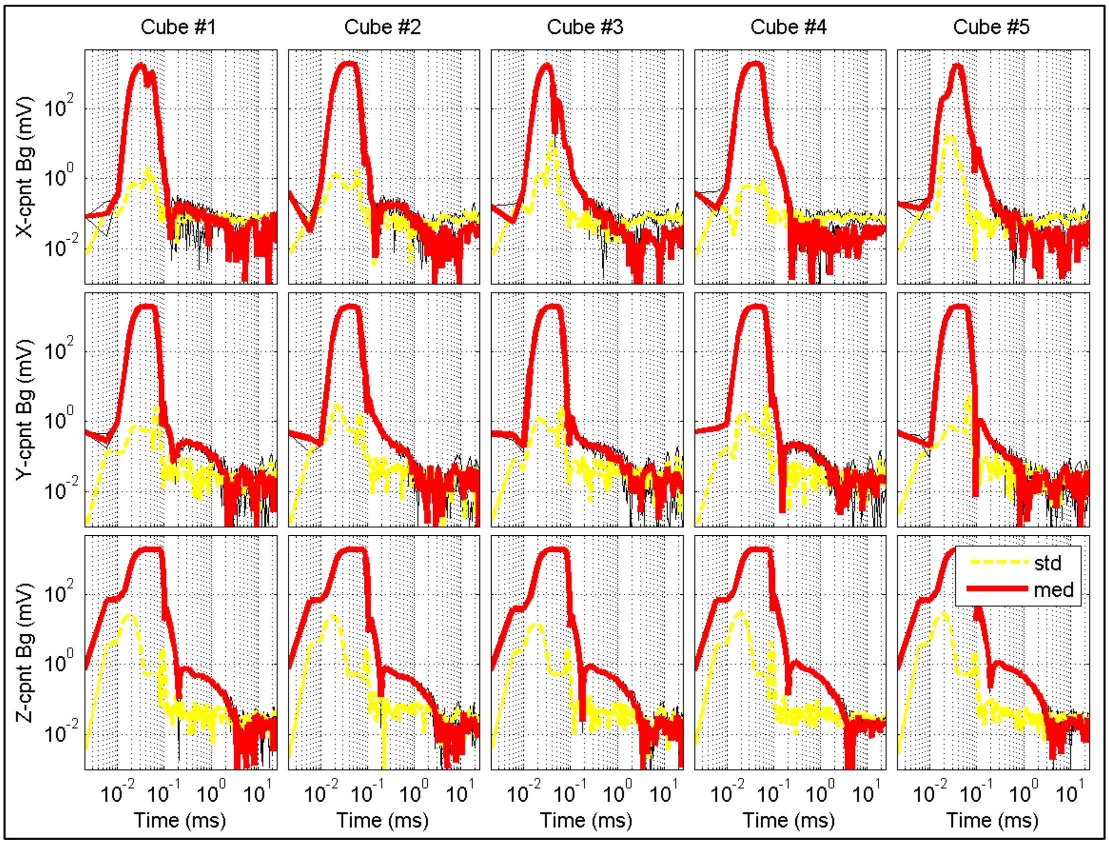

Figure 22: Stability of in-air background measurements for each MPV receiver.
The absolute value of the recorded signals in showed on a log-log graph. Downward spikes correspond to crossovers. Individual measurements are shown with black lines. Their median is indicated in red and the standard deviation in yellow – there is negligible variability in early time ring-down effects.

The Y-component of the central receiver cube had temporary problems. Given that there remained sufficient data for classification with 14 operational receivers and that the electrical engineer in charge of sensor maintenance was momentarily away from the site, we proceeded with the field data collection. This issue only concerned one day's worth of data collection and did not significantly affect classification results (a similar dysfunction had happened at the YPG

demonstration; we had verified stability of the recovered target parameters when omitting one central receiver). A cable connection issue was subsequently diagnosed and fixed.

Positional accuracy can also be considered as a data quality factor for a spatially varying signal. Positional errors are equivalent to measurement errors with the amplitude of the target response. Therefore we parameterized data errors as a floor value plus a percentage of the data amplitude to factor in positional errors. There is no direct way of verifying accuracy of the MPV positioning system in the field. We compared predicted sensor location with beacon and GPS, where applicable, and generally found 1-2 cm relative difference between the two (Figure 23).

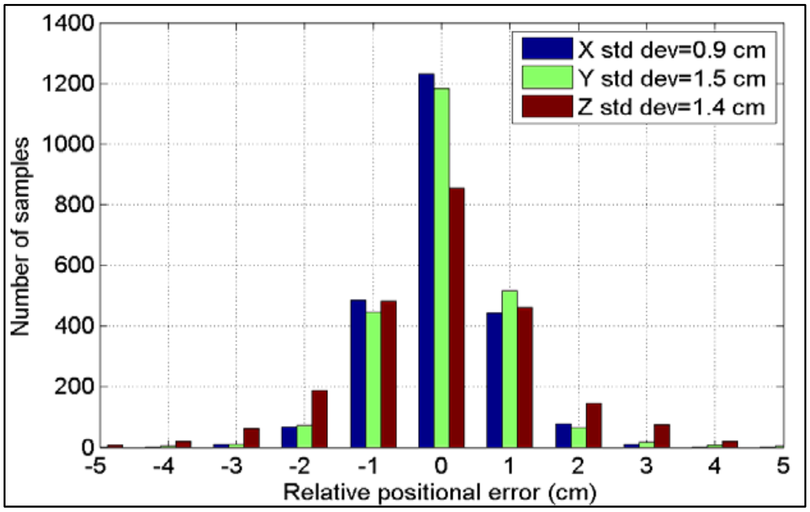

Figure 23: Relative accuracy of beacon positioning system compared with GPS.
The beacon method predicts the MPV transmitter location. The GPS and attitude sensor are mounted at the far end of the MPV handling boom and can also be used to predict the MPV transmitter/receiver head location with 2 cm accuracy in open field (1.5 m lever arm). Relative positional error was compared in open field in the combined area and at the IVS

6.3.3 Background noise from magnetic soil

As seen in a previous section, magnetically active soil has a typical signature with MPV data: vertical and radial component data have higher amplitude and log-linear decay. We devised a test to screen background soundings and verify that the response was clean of any metallic clutter and that the sensor head was flat on the ground. The test consisted of computing a linear fit to the decays, verifying the slope and residual error of that fit and verifying that the vertical component data had similar amplitude on the four lateral cubes. Background soundings that met these criteria were accepted as representative backgrounds for correcting the target data and support the following analyses.

Having noticed a distinct soil response during the field survey, we opted to collect a background sounding for every target to hedge against large variations. The soil response maps of Figure 24 show significant spatial variability in each survey area, which justifies our field strategy. The largest variability was observed in the densely treed area (panel #3). One distinct patch shows a 4-fold increase in background amplitude above baseline. Variability can also be observed in the amplitude and decay signal shown for each MPV receiver in Figure 25, where

typical soil responses are confirmed. The time-varying standard deviations for each receiver were derived from these curves and used for parameterizing data error expectations.

The densely treed area had a distinct surface cover: the top of the hill (left side) had long, thick grass and the lower part was bare. The former prevented the sensor to be in contact with the ground whereas the latter allowed the sensor to directly rest on dirt. Soil response approximately follows that spatial pattern. This could suggest that some of the variability might be due to ground clearance. In a later section (7.1) we present sensor height tests where we quantified that effect; our analysis shows that the sensor should be lifted by 15-20 cm to achieve such an effect, which is much greater than the grass cushion. The treed area clearly contained a sector with elevated magnetic soil content.

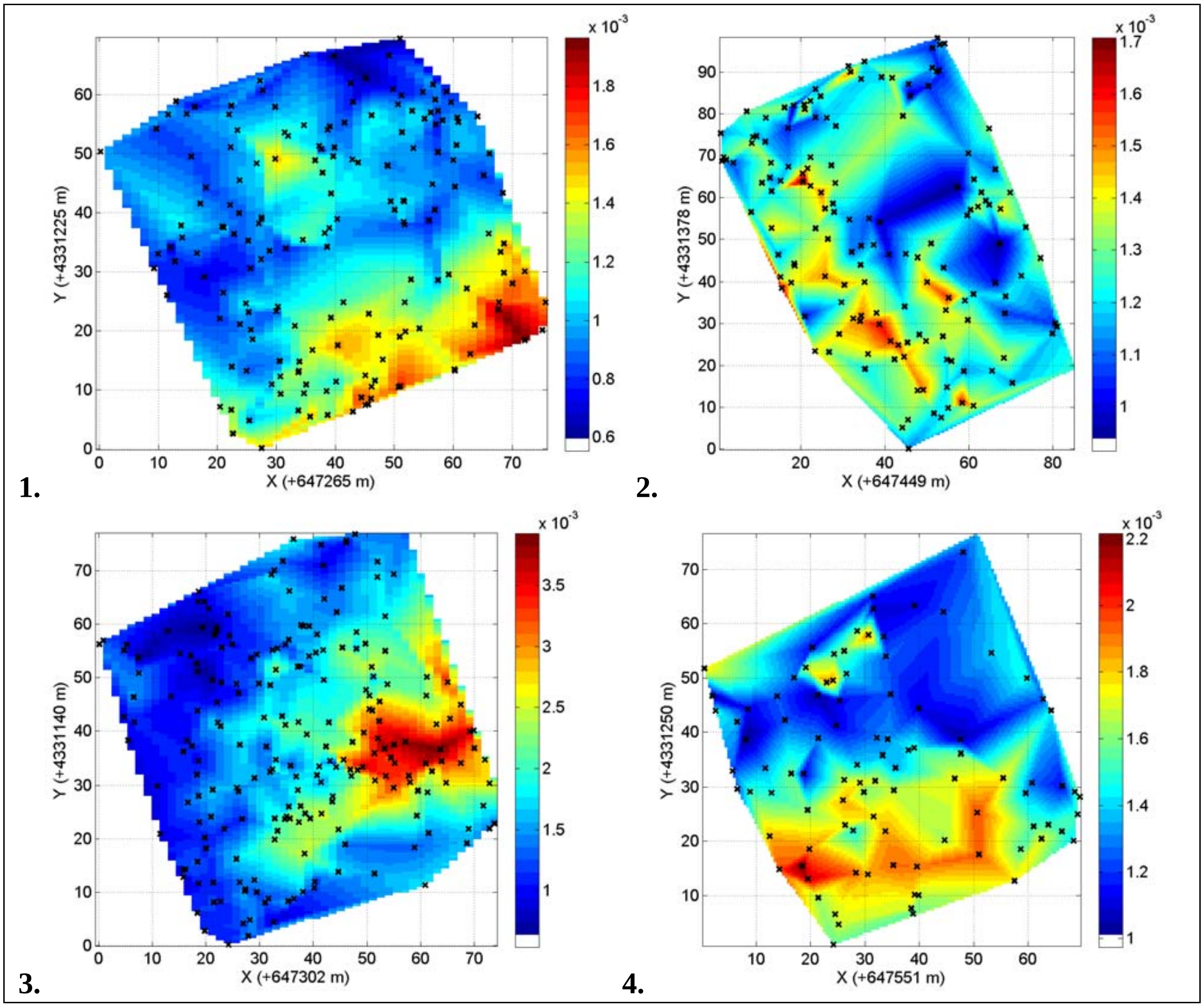

Figure 24: Spatial variability map for the magnetic soil background response.
Each panel corresponds to a survey area; panel position mimics geographical distribution (1=combined area, 3=densely treed, valley runs vertically between 1-3 and 2-4). The signal amplitude is the sum of all receivers and time gates between 0.2-0.57 ms. Black crosses indicate verified soil background sounding locations.

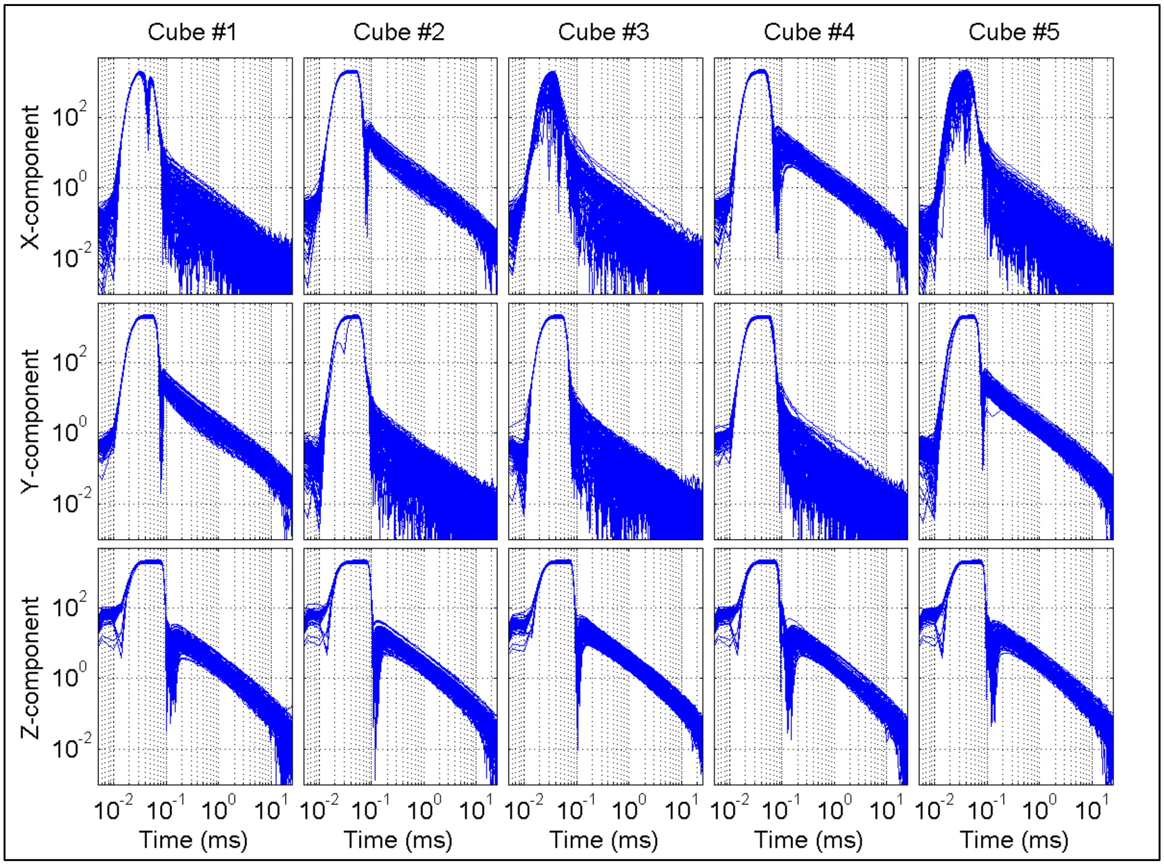

Figure 25: Soil background response in densely treed area. Typical magnetic soil responses are observed. Large amplitude signal in radial directions (X component of cubes 2 and 4 and Y component of cubes 1 and 5) and in vertical direction (Z component on all cubes), and log-linear decay after turnoff spike has vanished.

6.3.4 Strategies for defeating magnetic soil

Several methods were attempted to compensate for magnetic soil disturbance. The first method consisted of background subtraction. For each interrogated target, we took the ratio of the validated local background amplitude and that of the target sounding with the weakest response. If soil was uniform then the latter would have larger or equal amplitude and the ratio would be smaller than unity. To account for spatial variability we allowed a 50% tolerance on that ratio and used the resulting factor to define the amount of background to subtract to all target data. The corrected data were subsequently inverted for the presence of one or two dipole sources (method described in following section). In the case of two-dipole inversions applied to unique targets, the secondary dipole model would generally fit the residual soil signal that remained after the correction.

The second method was based on not correcting for background soil and letting the dipole model handle soil effects. This method consisted of a two stage approach. First we applied a single dipole inversion while using only the soil insensitive components. As seen in Figure 25, the X-component data of cubes 1, 3 and 5 and the Y-component data of cubes 2, 3 and 4 remained unaffected by soil when the sensor was parallel to the ground. Given 9 soundings per target, there could be sufficient informative soundings to solve for a single buried target. Then, at the second stage, we used that solution to constrain location of one target as part of a two-dipole

source inversion with all the sensor data, so that the second dipole might account for soil or other disturbances. A similar method was successfully applied by Pasion on highly magnetic Cambodian soil (SERDP MR-1573).

All validated models were then injected in the classifier. In general, both methods returned similar models because target signal was larger than soil disturbance. Retrospective analysis showed similar performance except for large composite targets that require two dipoles to model heterogeneity.

6.3.5 Overlapping signatures

At highly contaminated sites, anomalies often overlap due to the close proximity of multiple targets. Our data inversion strategy for overlapping targets was to decompose the inverse problem into several steps. Each step resolved a subset of model parameters. The first step was to solve for non-linear location parameters and subsequently solve for linear polarization parameters. With an optimal estimate of locations and dipolar polarizations, the orientations and polarizability decays of each object could be extracted from estimated magnetic polarizability tensors. Our multi-object inversion approach has been successfully tested as part of previous Discrimination Studies with ESTCP with Geonics EM63 data (Former Camp Sibert, Alabama), with static MetalMapper data (San Luis Obispo, California) and MPV (Yuma, Arizona).

We found many cases with close targets at Camp Beale (Figure 26). Approximately 40 flags had less than 0.5 m separation and 120 flags less than 1 m – this does not include cases where multiple anomalies could be attributed to the same flag. When two or more flags were found in close proximity, all targets were surveyed with the same beacon reference. All the data were imported together and the data were masked such as to keep only the data associated with the target of interest (Figure 21), for each target. In the case of overlapping signatures or when multiple anomalies seemed to be associated with a flag, we tested different masks as well as single and two-dipole source inversions until acceptable fits were achieved.

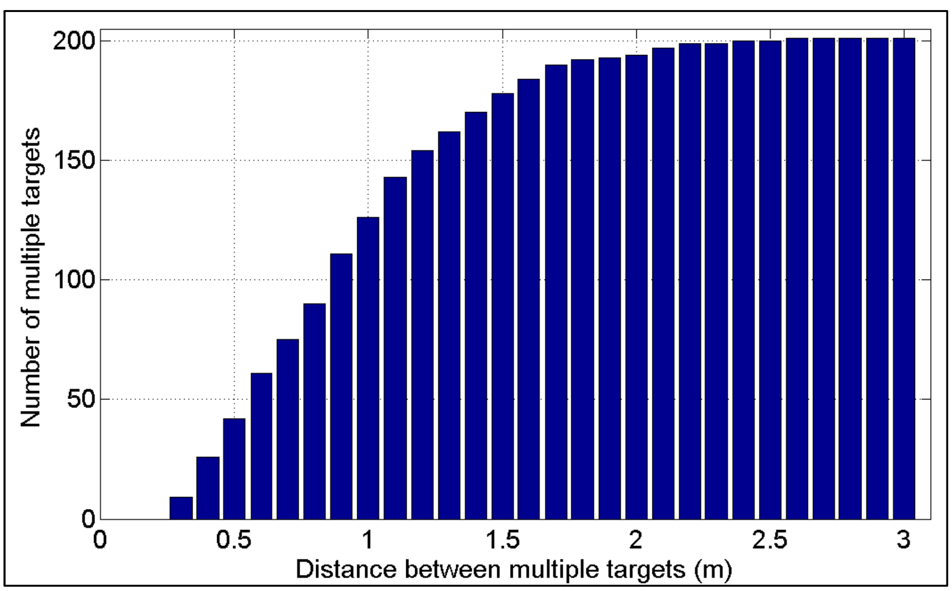

Figure 26: Histogram count of the number of multiple targets as a function of the target separation (measured with the beacon positioning system).

6.4 TRAINING DATA

The classification approach was based on the capability to recognize that a given target had similar features as a known object. The method therefore required a library of known target features that was utilized as training data for the classifier. The training data consisted of target polarizability features gleamed during previous MPV surveys and site-specific data.

A target library was built with the YPG calibration lanes, which offered a large sample set with approximately 100 anomalies, including 14 munitions-type of different size and shape and some clutter. The munitions had been buried at various depths and orientations, thus providing the opportunity to estimate feature vectors variance. This library was used for the initial steps of classification although its polarizabilities stopped at 8 ms as opposed to 25 ms at Beale. The data collected at Beale in the test pit and at the IVS were added to the library. The corresponding unprocessed data were made available to all analysts for them to develop their libraries.

Site-specific training data were obtained by requesting ground truth for distinctive targets. These were particularly useful to characterize unknown UXO-like objects or to understand complex target signatures and thus diminish the risk of misclassifying unexpected targets. The requested targets would appear at the front of the prioritized dig list; therefore it was in the analyst's best interest to wisely choose these training data such as to maximize their informative content while keeping their number low.

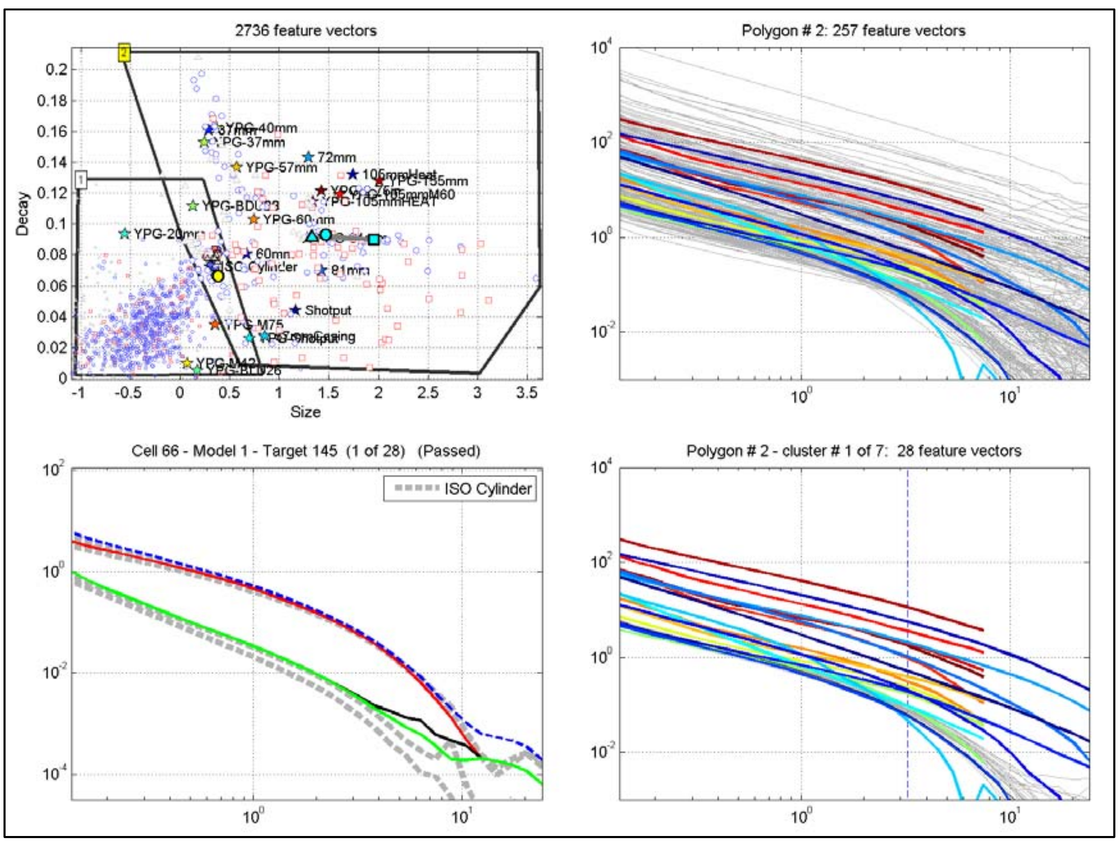

Figure 27: Clustering of recovered polarizability decays for training data analysis.
Top left panel shows feature space using simplified size-decay parameters. Training data from calibration and YPG are marked. Two polygons define regions where clustering was tested. Right panels show feature vectors – polarizability decays – from field (grey) and training data (colors; 8-ms-polarizabilities for YPG). Bottom left panel compares a field target (colors) to its most likely known target (grey, the ISO).

A clustering algorithm was applied to identify re-occurring models among the standard one and two dipole inversion models. The method was based on comparing all recovered polarizabilities with one another and group self-similar objects. A simplified size-decay description of classification model space is shown in Figure 27. Model space was divided in two regions: polygon #1 only enclosed small targets and polygon #2 included the large objects, where UXO are more likely. The clustering algorithm was independently applied to each region. There were 10 clusters in the small target region (Figure 28). The first two clusters have targets the size of a 20 mm projectile, though a faster decay. The third one has spherical shape and log-linear decay. The fourth cluster corresponds to the ISO cylinder; the remaining ones are smaller pieces of clutter. In the large-targets polygon #2 (Figure 29) the seven clusters correspond to items the size of the ISO, 81 mm, 37 mm and 60 mm targets; the last three clusters have plate-like characteristics and log-linear decay that are typical of magnetic soil models.

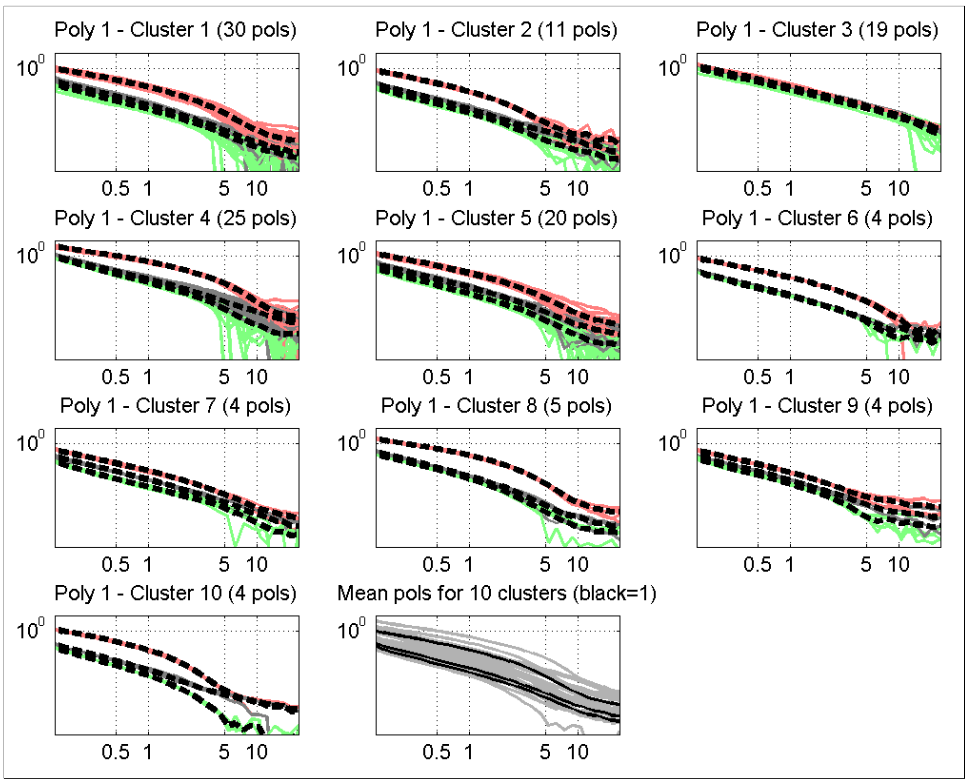

Figure 28: Clusters in the small target region. There were 10 clusters in polygon #1. The first 10 panels show the polarizabilities for each cluster and the mean polarizabilities (black dashed line, 1 for each of the 3 polarizabilities). Titles indicate the number of occurrences for each cluster in brackets. The first 5 clusters include many targets. We required at least 4 occurrences to constitute a cluster.

The requested training targets are listed in Table 2. Targets were chosen out of the clusters and corresponded to end-member models with the largest deviation from the cluster median. The returned ground truth indicated the presence of an expected TOI, a large fuze, which had three equal polarizabilities with log-linear decay and smaller amplitude than the ISO. Classification was devised to search for this target, which later was deemed to be harmless (non TOI).

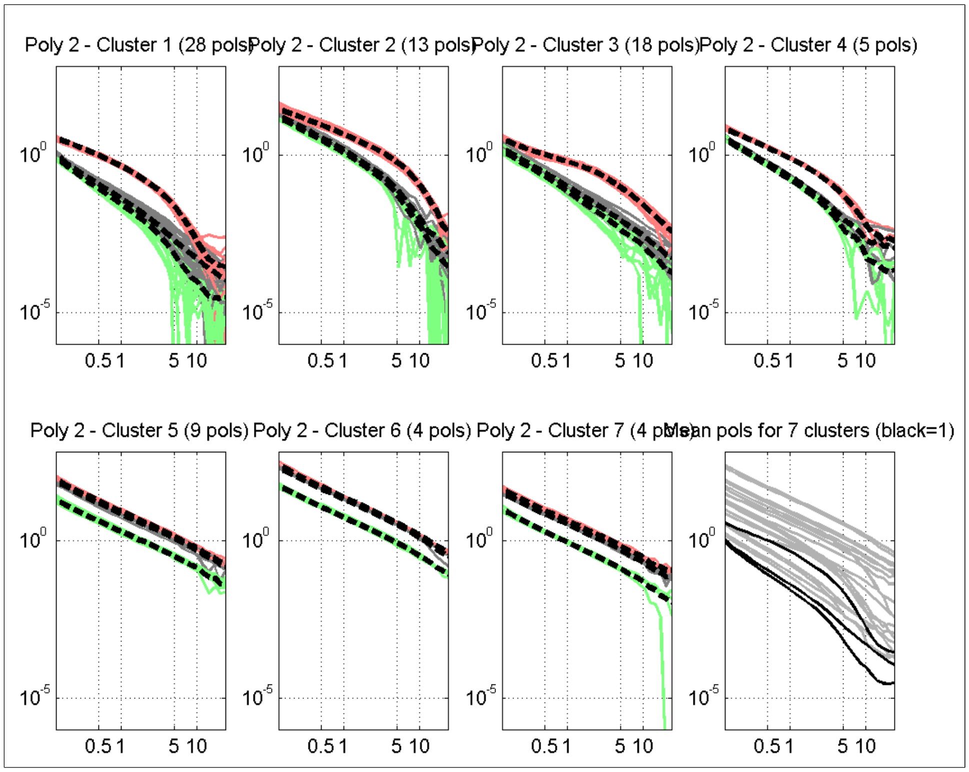

Figure 29: Large targets

Table 2: Training data requests

Target number	Cause	Ground truth
45	Poor fit, soil-like decay and total polarizability the size of 81 mm	Frag + soil
598	Poor fit, soil-like decay and total polarizability the size of 81 mm	No contact (soil)
631	UXO-like, smaller than ISO	Frag
553	UXO-like, smaller than ISO	Frag
200	Plate like scrap or soil	Frag
567	Sphere object	Large Fuze
511	Smaller ISO	Frag
528	Slightly different 81 mm	81 mm
357	Slow ISO	ISO
556	UXO-like, 20 mm size	Frag
836	Different 81 mm	81 mm
153	Smaller ISO	Frag

The classifier was trained by including these additional data to prepare the first prioritized dig list. Because we assumed that only targets within 30 cm of the flag would be validated – 30-cm-radius excavation hole – we excluded targets that were predicted to be located beyond 40 cm of the flag. Distant targets were labeled as “can’t decide” and placed after the stop-digging point. Target #4 was one such target, an 81 mm projectile that was predicted to be located 45 cm away from the flag. The target ID was released and included it in the training set.

6.5 CLASSIFICATION

The classification approach was chosen after examination of the training data while considering the site-specific magnetic soil disturbance. The following guiding principles were adopted:

- *Selection of models in classification:* We assumed that classification could be performed in an automatic and repeatable manner. Therefore user input was limited to verifying that acceptable fit to MPV data was achieved. Every model meeting that criterion was considered for classification without further user-dependent pre-screening. Given the effect of magnetic soil on the MPV, multi-target inversion tended to generate soil models that, depending on the predicted depth and amplitude, could be confused with 105 mm projectiles. Decisions were left to the classifier;
- *Selection of features:* By analysis of the training data, those features that contribute to separation of the different classes (comprising UXO types and clutter) were selected. This selection involved selecting combinations of the three polarizability decays and determining which time range offered the largest and most reliable class separation;
- *Choice of classification algorithm:* Through analysis of the training data the best performing classifier was selected. We focused on Support Vector Machine (SVM), which historically had yielded the best results. We also tried a rule-based method in which polarizability misfit with library items was measured;
- *Classification:* Anomalies were placed in a prioritized dig-list by using the classifier to compute probabilities of class membership for unlabeled feature vectors. The probability of membership of the clutter class was reported on the dig sheet;
- *Number of UXO-classes*: One or more UXO classes could be defined when seeking UXO of widely different sizes. When multiple UXO classes need to be used (assume there are M of them) then one can either train an (M+1)-class classifier, or train M two-class classifiers and combine the results.

Classification was generally based on a combination of a size and a time decay feature for the early ESTCP classification studies at San Luis Obispo, Camp Sibert and Fort McClellan. More recently, the ESTCP Camp Butner study (ESTCP-201004) and the MPV demonstration at YPG showed that new-generation sensors such as the Geometrics MetalMapper and the MPV could support richer feature vectors for classification owing to their extended time range and improved recovery of all three polarizability-component decays (Figure 5). Classification was improved by using a more complete description of target properties as opposed to the simpler size and decay pair. The main polarizability decay (L1) is an indicator of the object size at early time and of material properties at later time (wall thickness and metal types). Secondary (L2) and tertiary (L3) polarizability decays contain shape information along the target secondary and tertiary axes – their amplitude should be equal for a body of revolution such as typical ammunition. One of the challenges with using these rich features was to determine their stability, which depends on

data quality. L1 accounts for the first order data. It is therefore the most stable polarizability and can generally be used over its full time-decay range. L2 and L3 describe the second order data, which have lower amplitude, especially at late time. Only an early-time subset of L2 and L3 was kept for the classification features.

Polarizability decay features can be compared to library items through a misfit metric or a statistic classifier such as SVM, which can accommodate large feature vectors. The library misfit was not used as the primary classifier for the MPV data at Camp Beale. Although the method yielded remarkable results in ESTCP Pole Mountain survey based on MetalMapper data, we found the method to be less effective here because of the occurrence of magnetic soil models stemming from MPV data. Soil models usually show log-linear decays; their relative polarizability amplitudes are less systematically predictable, although it is expected that the first and second polarizabilities should be equal and greater than the third one if the sensor is parallel to an even ground surface. In practice there were numerous cases were the main polarizability has similar amplitude and decay to 81 mm or 105 mm projectile, thus resulting in low misfit numbers. Such false alarms cases could not be avoided using a simple misfit metric. Therefore we selected a non-linear classifier such as SVM and included in the clutter class a series of automatically selected soil models identified through their typical log-linear decay characteristics.

Determining the number of classes is a tradeoff: when using few classes the capability to separate targets is diminished because different types and sizes of munitions are lumped in the same class; when using as many classes as there are munitions, there is a risk of being too aggressive if misevaluating in-class variance – this can occur if signal-to-noise ratio (SNR) is too low for stable recovery of target polarizabilities, and if variance is underestimated because few instances of each munitions type are available for training. At Beale we grouped the targets of interest in four different classes according to size. We defined one class containing only 105 mm, one class for 81 and 60 mm, another class for ISO and 37 mm, and a final class for fuzes. We used the SVM algorithm from the MatLab-enabled Spyder toolbox, which was also the Sky Research classifier of choice for the Camp Butner and YPG studies.

The classification approach is illustrated in Figure 30. The SVM classifier was trained on each class to separate that class against the other classes and clutter. The four SVM classifiers were then applied to all field targets. For each class the SVM statistic indicated the likelihood that a target belonged to that class. The SVM statistic was greater than 1 for high-likelihood members of the class and below -1 for the least likely. Targets could be given priority for digging by sorting the SVM statistic by decreasing order. As shown in Figure 30, the sorted statistic has a L-shape that decays rapidly if there are few, distinct members of a class, and reaches a plateau for unlikely targets. The magenta curve, which aggregates all UXO into a single class, has the slowest decay and contains more targets at any given threshold than the sum of the other four classes at that same threshold. This suggests that classifying all UXO at once is less efficient than using multiple classes. We used the SVM classifier in multiple stages, starting with large targets and switching to the next smaller class below a given threshold. The training data were analyzed to determine the appropriate thresholds. Similar to an optimization problem, the L-shaped SVM statistic illustrates a trade-off between minimizing the uncertainty that there remain targets belonging to a class and minimizing the number of targets to dig out. In practice the SVM thresholds were automatically set.

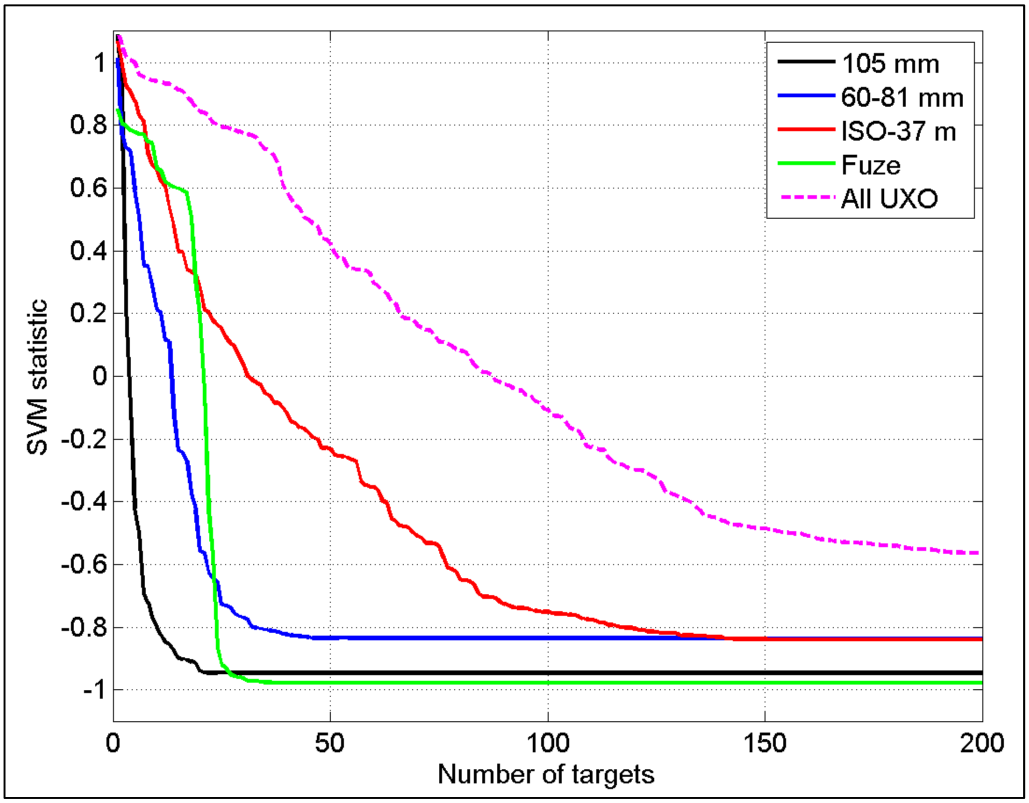

Figure 30: SVM classifier applied to multiple target classes.
For each class, the SVM classifier predicts the most likely class members. Each curve shows the sorted SVM statistic that a target belongs to a given class as a function of the number of targets. E.g., there are 10 targets with high likelihood of being 105 mm projectiles. The dashed magenta curve lumps all UXO in the same class.

This process was repeated for different feature sets to reflect reliability in parameter recovery. The first iteration included all 3 polarizabilities, then the first (main) and second, then the first and third, and finally the sum of all polarizability decays. As showed in Figure 31, the discriminating capability of each classifier degrades when reducing the number of polarizabilities. After each SVM stages and classes were exhausted, the remaining targets were sorted as a function of their misfit to known library items to produce a prioritized dig list.

The ranked classification anomaly list was formatted as shown in Figure 32. The first items on each anomaly list were the requested training targets. Next were to be those targets for which reliable parameters cannot be extracted and therefore had to be dug. In practice data quality was such that we considered that every anomaly could be analyzed; non-contact anomalies were found to yield soil models. The list continued with the “high confidence munitions” targets. Items were ranked according to decreasing confidence that the item was hazardous. Any items that were analyzed without reaching an unambiguous classification decision were placed next on the anomaly list. Finally, all items that were confidently classified as non-hazardous were ranked by their confidence.

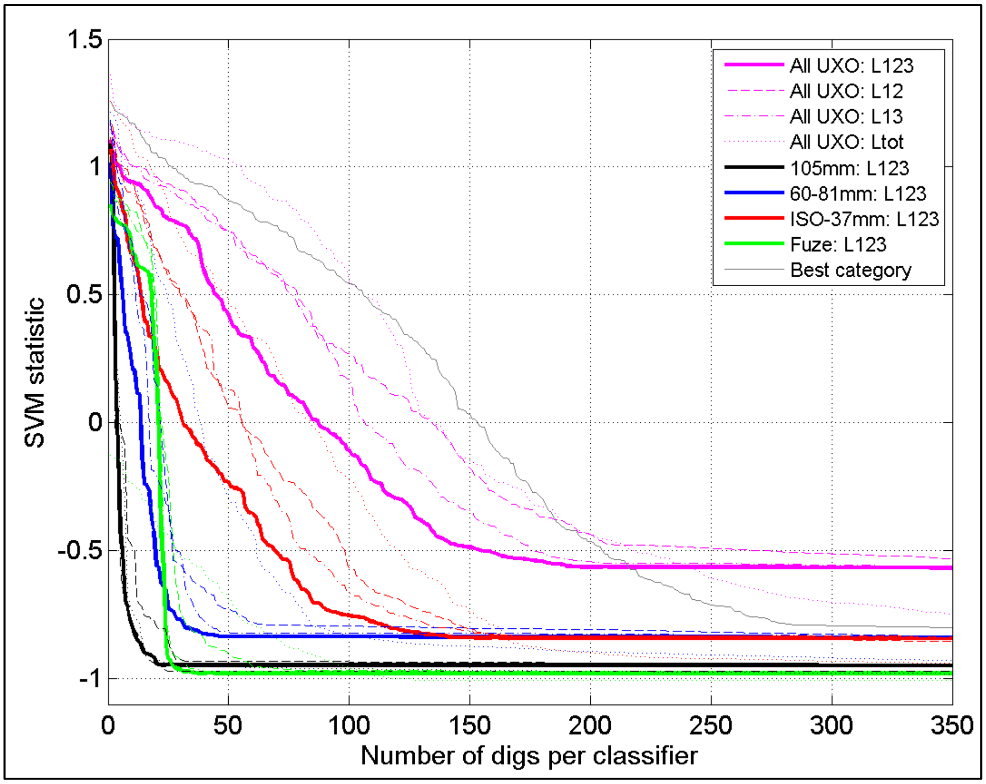

Figure 31: SVM classifiers applied to prioritizing the dig list. Similar to the previous figure, SVM statistics are computed for each class, using all polarizabilities (L123), subsets (L12 and L13) or the sum of all 3 (Ltot).

Rank	Anomaly ID	Decision Statistic	Category	Dig on First Pass	Comment
-9999	2498	-9999	0	1	Can't extract reliable features
1	247	.97	1	1	
2	1114	.96	1	1	High confidence munition
3	69	…	1	1	
…	…	…	2	1	
…	…		2	0	Can't make a decision
…	…		2	0	
…	…	…	3	0	
…	…	…	3	0	
…	…	…	3	0	
…	…	…	3	0	
…	…	…	3	0	High confidence non-munition
…	…	.03	3	0	
…	…	.03	3	0	
…	…	.02	3	0	
N	…	.01	3	0	

Threshold

Figure 32: Format of prioritized anomaly list to be submitted to ESTCP Program Office.

6.6 DATA PRODUCTS

The main data product was the prioritized dig lists. These were preceded with the initial training data request that included 12 targets (in practice the ground truth seemed to provide indications for 3 additional neighboring targets that were included in the training set). The lists are detailed below:

- Stage 1 (s1v1): The first lists had originally rejected all targets further than 0.4 m away (dig hole was set to 0.3 m radius). As a result we missed target BE-4, which was located 0.45 m away from its flag. Two dig lists were submitted: one automatic rule-based list and one edited version eliminating obvious non-UXO. The editing stage was due to the extremely conservative choice of feature vectors, which had excluded late time polarizabilities. The multi-stage classifier used SVM with L123, L12, then L1 and misfit on L123 afterwards.

- Stage 2, version 1 (s2v1): Dig list with 16 training items (12+3 and 1 from s1v1). Based on the released ground truth we realized that greater trust could be given to late-time data. In particular, the L1 classification stage was allowed to encompass the entire time range (we had originally excluded early and late time channels to avoid potential misclassification in cases of early-time signal saturation and late-time signal weaker than soil). We changed multi-stage classifier to L123, L12, L13, L1, misfit L1. We found that many obvious non-TOI picked in the automated s1v1 list spontaneously disappeared. The final dig list could have been more efficient with a less conservative first stage.

- Stage 2, version 2 (s2v2): Dig list reduced to 13 training items to be consistent with training data request.

- Stage 3 (s3v1): Final dig list, same as s2v2 and using later likely thresholds in cascading algorithm after the stop-digging point.

7.0 PERFORMANCE ASSESSMENT

7.1 SURVEY OVER MAGNETICALLY ACTIVE SOIL

This section examines the effect of magnetic soil on MPV data for classification to assess whether the adopted survey protocol with sensor on the ground was the most appropriate.

7.1.1 Effect of magnetic soil on MPV

The intensity of the magnetic soil effect on the MPV sensor was quantitatively studied with a sensor clearance test. After identifying a seemingly quiet location, we acquired background measurements at different heights: 0, 4, 11, 15, 22 and 33 cm. Cardboard boxes and foam pads were used to stabilize the sensor head at fixed heights. Recorded time decays in the 0.1-25 ms time range are presented in Figure 33. Colored curves show the soil response. Soil affected receivers exhibit the typical log-linear decay. The amplitude of the soil response decreases with sensor height, as indicated by the parallel curves, whereas the other receivers remain in the electric noise background regime. The grey and black curves illustrate the recorded signal for the central soundings that were collected above the deepest 37 mm and 81 mm targets for comparison with the magnitude of the soil effect. Target response is always larger than soil when the sensor is on the ground, which allows target detection. However, the relative difference is less than twofold on some receivers, which could affect inversion results if the background response was not adequately removed.

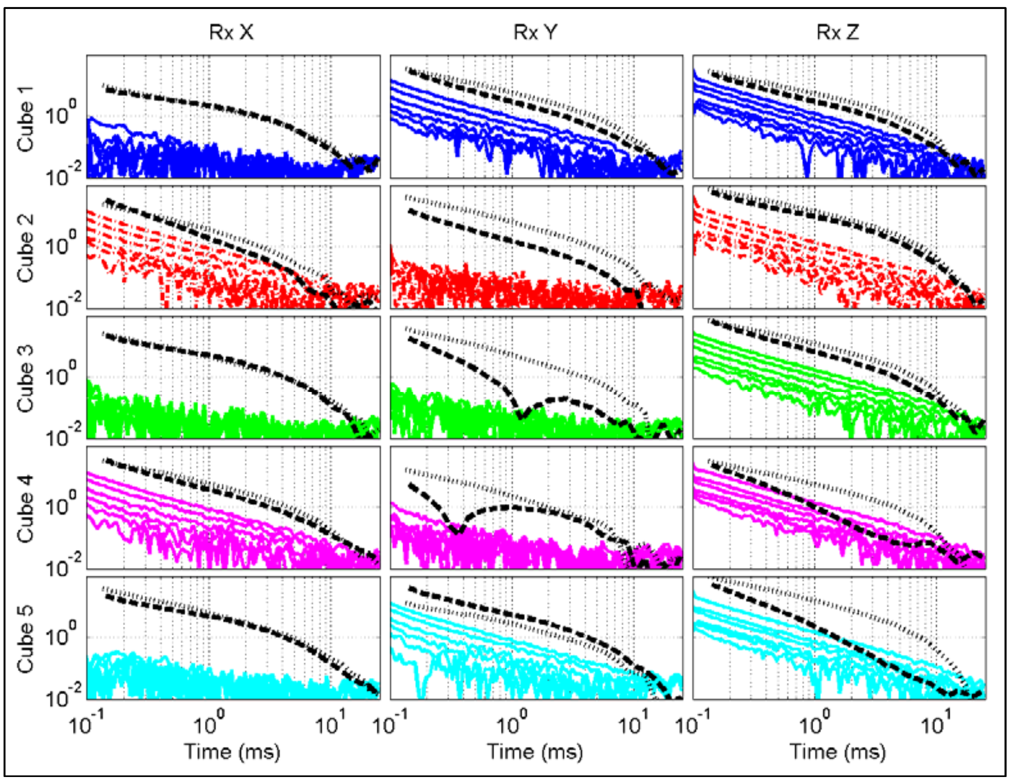

Figure 33: Recorded background response in sensor clearance test and comparison with target response. Colored curves show the recorded background response for different heights. The black and grey curves show, for comparison, the recorded signal for the central sounding above the deepest 81 mm and 37 mm, respectively. For clearance tests the sensor was placed at incremental heights above ground (4, 10, 15, 22 and 33 cm). Data were here background-corrected by subtracting the in-air instrument response.

As suggested in Figure 33, soil response amplitude depends on sensor height in a predictable manner. We found that this dependence could be empirically approximated for this test with a simple linear regression between the logarithm of signal amplitude and height. Slope factor was fairly consistent with an approximate value of -11.5 for horizontal components and -9 for vertical component receivers. The inferred rule was used to assess expected background response at different survey height.

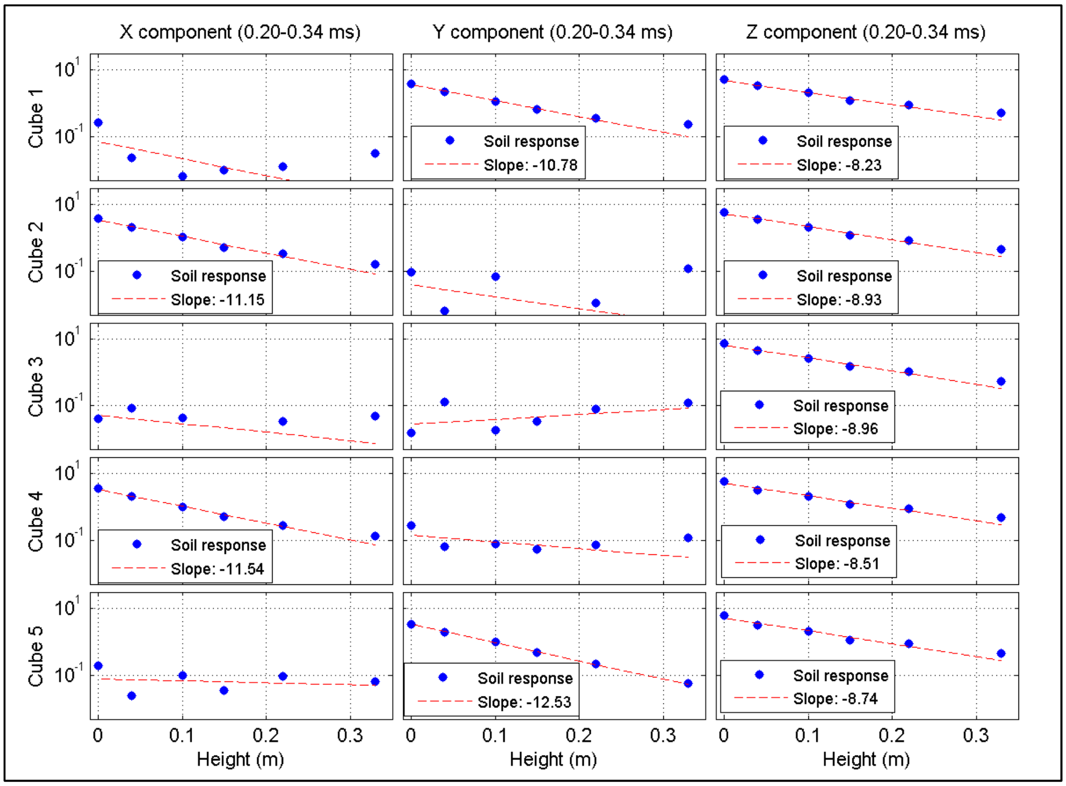

Figure 34: Amplitude of soil response as a function of height for each receiver.

7.1.2 Simulated ground clearance effect

The effect of sensor ground clearance was examined through Monte Carlo simulations. The effect was tested on UXO and clutter of various sizes to assess potential degradation in classification ability. Modeled items included a horseshoe, a small fuze, a common fuze (of the kind detected during training), and 37 mm and 81 mm caliber ordnance. The items were simulated to be buried at random orientation and depth below the ground surface within their expected depth range (e.g., 0.15-0.40 m for 37 mm; depth for fuzes was probably exaggerated). Target response was computed using the polarizabilities stored in the library. The background response for each sounding (9 grid soundings and one background sounding) was randomly drawn from a set of 200 validated soil background responses and attenuated for the appropriate sensor clearance (0, 0.05, 0.10 and 0.15 m) according to the rule derived in the previous section. Hence we obtained a data tile for each target, similar to the field data. Background response was similarly evaluated and compensated by comparing the weakest target sounding and the background sounding, computing the ratio (bound between 66% and 150%), multiplying that factor with the background sounding and removing its value for each target sounding. The process was applied to 1200 Monte Carlo realizations.

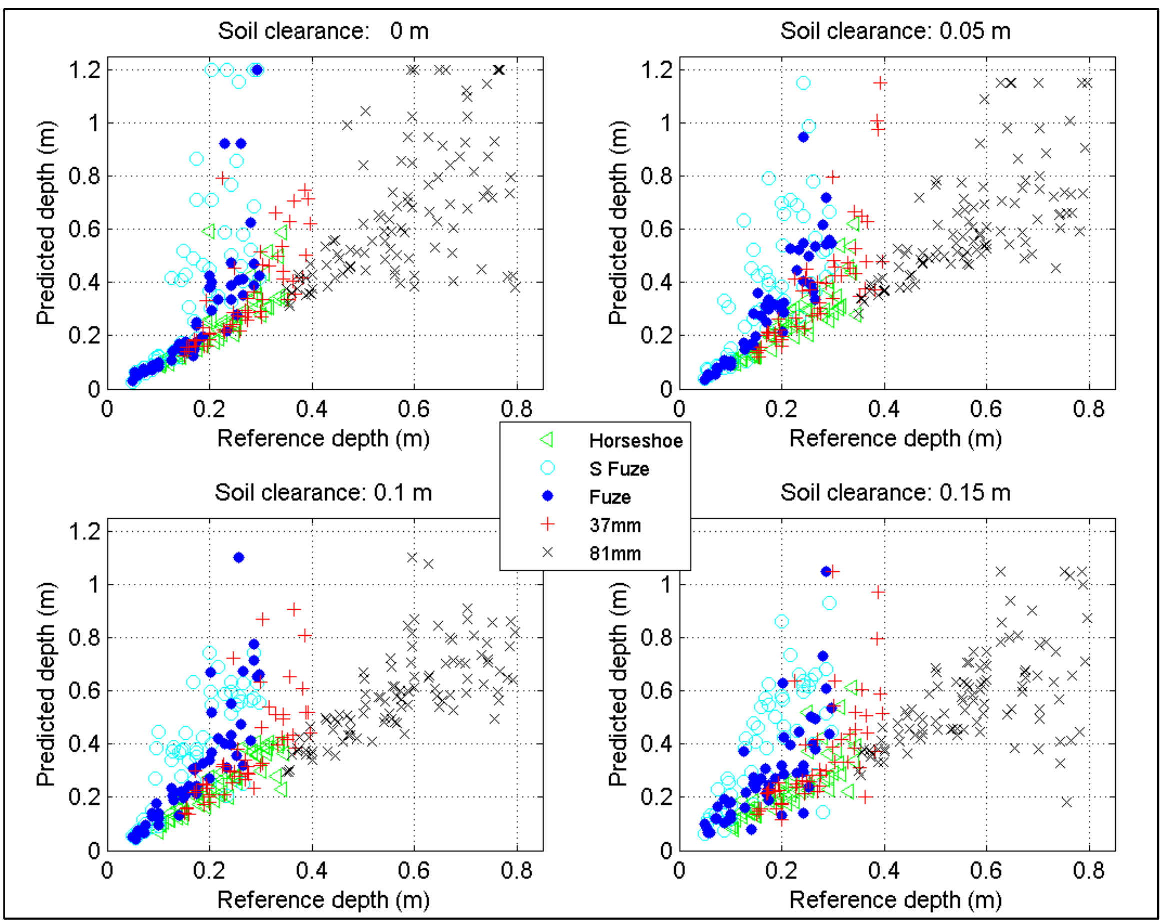

Figure 35: Comparison of predicted and prescribed depth in sensor clearance simulations.

Each realization was inverted like field data using standard one and two dipole models. Ability to recover depth generally is a reliable proxy for assessing inversion quality. The prescribed (reference) and predicted target depth are shown in Figure 35 for sensor clearance of

0, 0.05, 0.10 and 0.15 m. The best results are achieved when markers cluster along an imaginary 1:1 line. The upper left panel shows that depth was best recovered for small targets when the sensor was placed right on the ground. Deep 81 mm targets might be best recovered when the sensor is raised by 0.10 m – note that the deepest 81 mm at Camp Beale was buried at 0.45 m below the surface.

The results are also expressed in terms of misfit between the prescribed and the recovered polarizabilities in Figure 36. The best results correspond to the lowest misfits. The same trends are observed with the two metrics. These results can be explained with the fact that small targets have weak, fast decaying responses; therefore SNR matters through distance to sensor. In contrast, the response of large, deep 81 mm targets could be mixed with soil because of apparent log-linear decay at early time; therefore it might be best to raise the sensor to limit ground disturbance. In conclusion, given the targets and depths encountered at Camp Beale, this analysis suggests that there was no significant penalty in surveying close to the ground.

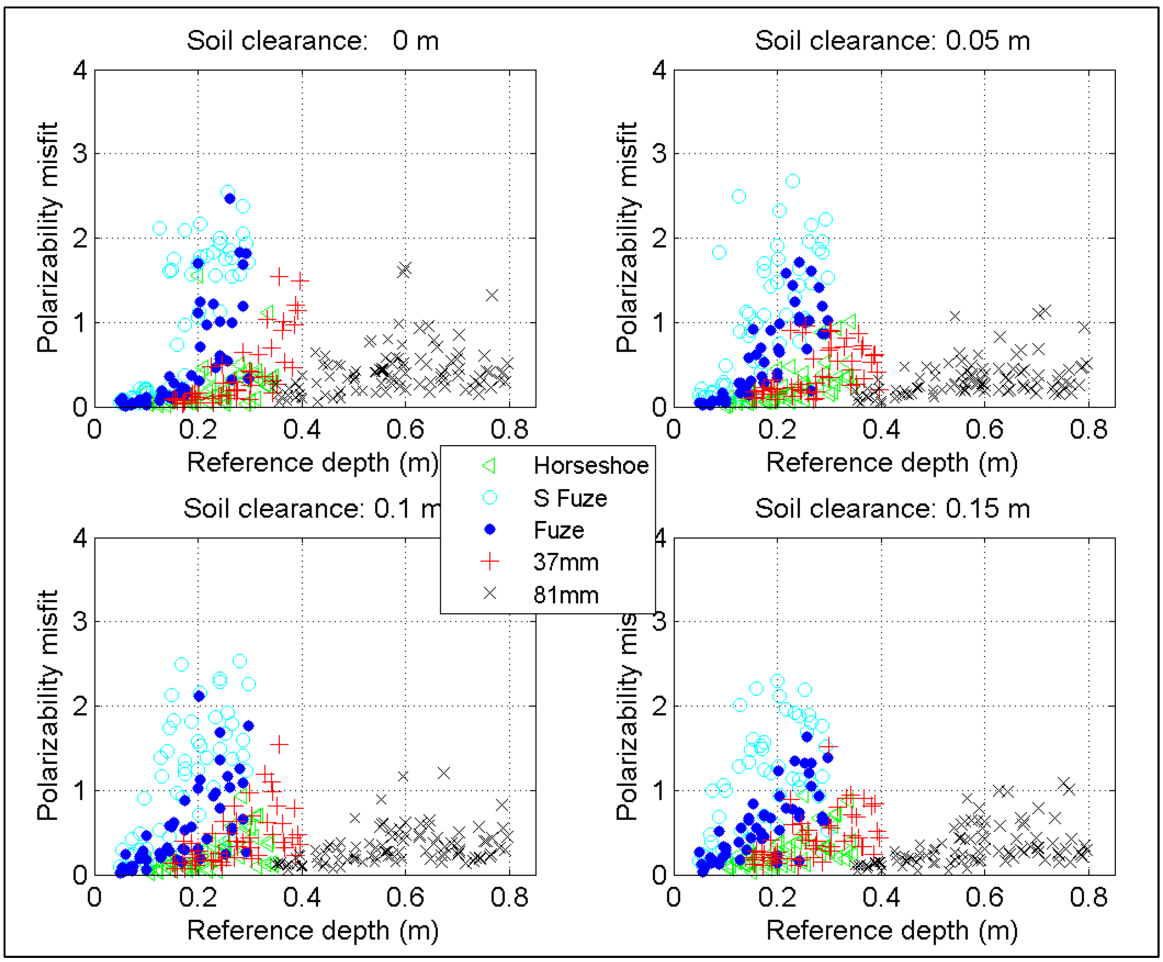

Figure 36: Simulated ability to discriminate targets measured as a function of polarizability misfit.

7.2 DETECTION OF MUNITIONS OF INTEREST

Detection requires that the recorded target response exceed the background response. Given that the MPV survey only included cued interrogation with static data, detect-ability was here measured by the presence of an anomaly in the cued data tile.

All targets were detected. The recorded target response primarily depends on the target size and depth. The response versus size relationship is shown in Figure 37, where object length is used as a proxy for size. The amplitude of target response and size co-varied and were modulated by burial depth. There were no large targets with weak responses in the Camp Beale survey because targets were buried at relatively shallow depths compared to their size. For instance the deepest 81 mm target was placed at 0.45 m depth. All TOI had SNR well above 100.

The portable areas at Camp Beale had 36 so called "no contact" flags, where no metallic debris was encountered. These generally coincided with weak instrument response lower than SNR=100. Reported "no contact" with larger SNR corresponded to nearby metallic debris that was detected by the MPV survey.

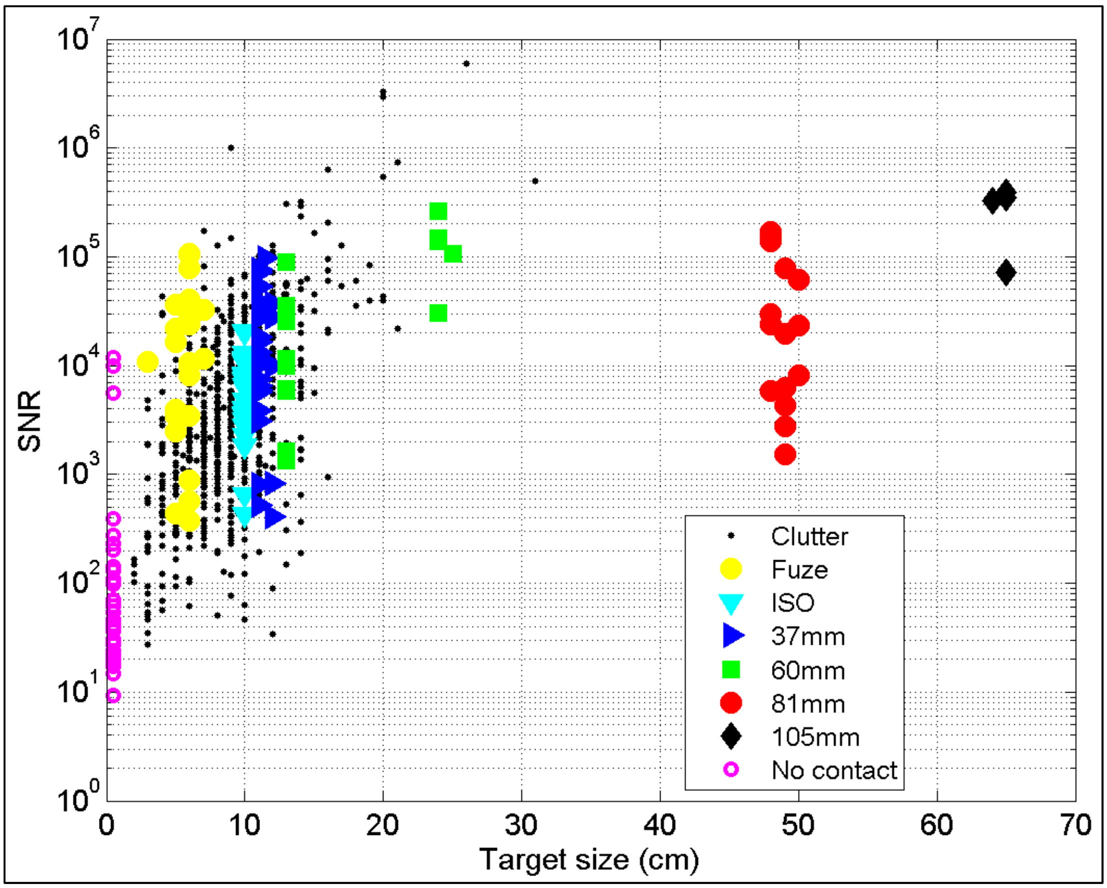

Figure 37: Signal to Noise Ratio as a function of target size. There are size variations in the TOI class – for instance 60 mm mortars are 13-24 cm long (body, or body with nose and fins); there are several fuze types and sizes.

7.3 CORRECT CLASSIFICATION OF MUNITIONS

The primary objective of the demonstration was to identify the presence of potential TOI against clutter. Given that the chosen classification approach relied on comparison with reference target signatures, success strongly relied on recognizing specific target types.

7.3.1 Stability of the recovered target parameters

The inferred polarizabilities for each TOI types at Beale are shown in Figure 38. The tight distributions of polarizability decay curves indicate that data quality was sufficiently high to recover at least two of three polarizabilities. Therefore predicted models were stable and could support relatively aggressive classification using all three polarizability decays for the most part, and at least two polarizabilities for all targets.

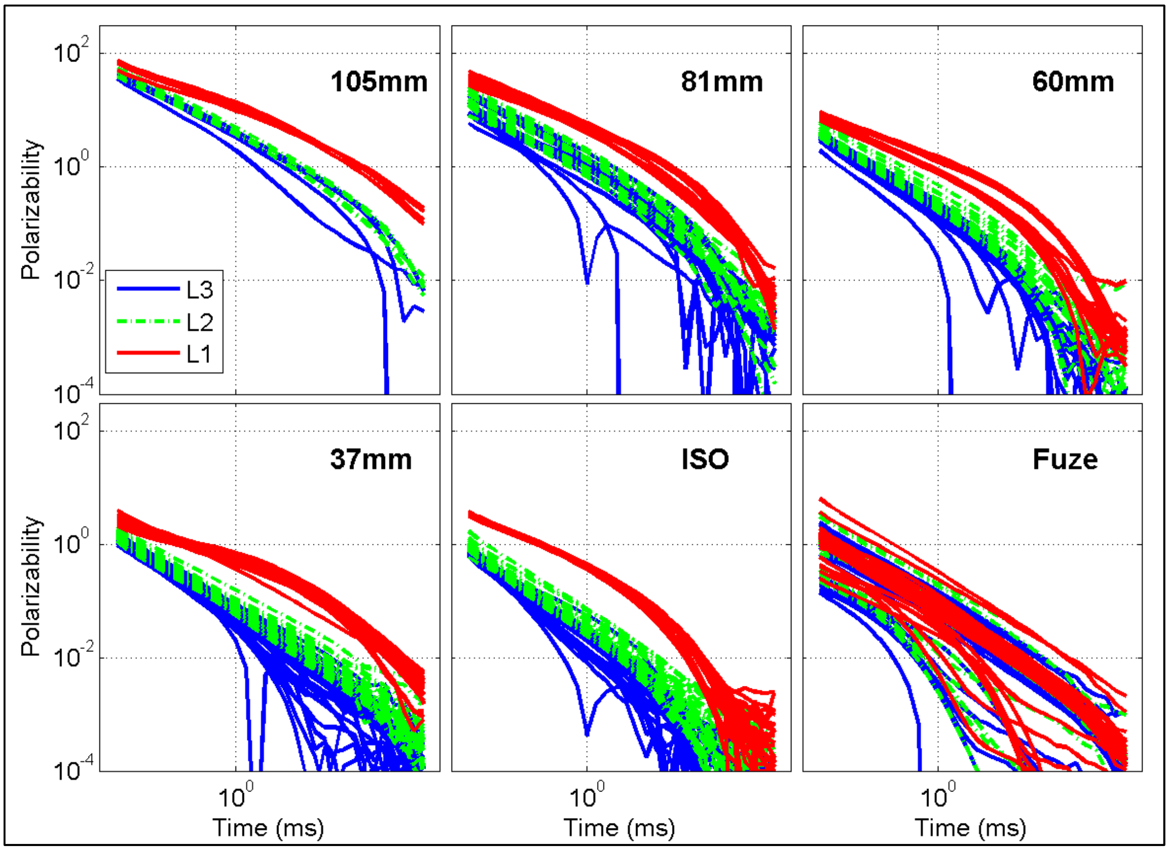

Figure 38: Recovered polarizabilities for Camp Beale field targets.
For each field TOI except the fuze, the closest model to the IVS reference item is shown.
Given that there are several fuze types, the standard single inversion model is shown.

There was some variability within each target class. For the 60 mm mortar, the main polarizability decays (red curves) suggest two distinct target types: the lower amplitude and faster decay correspond to the 60 mm steel body, whereas the larger amplitude and slower decay curve is the complete target with aluminum nose and tail (Figure 39). Retrieval of different decays suggests that the corresponding dipole models represent a heterogeneous target. In the past, two-dipole inversion of full 60 mm mortars had generally yielded one model for the body and one model for the tail. This might have not occurred here because the presence of magnetic soil might have had a greater contribution to the recorded signal that the isolated aluminum tail.

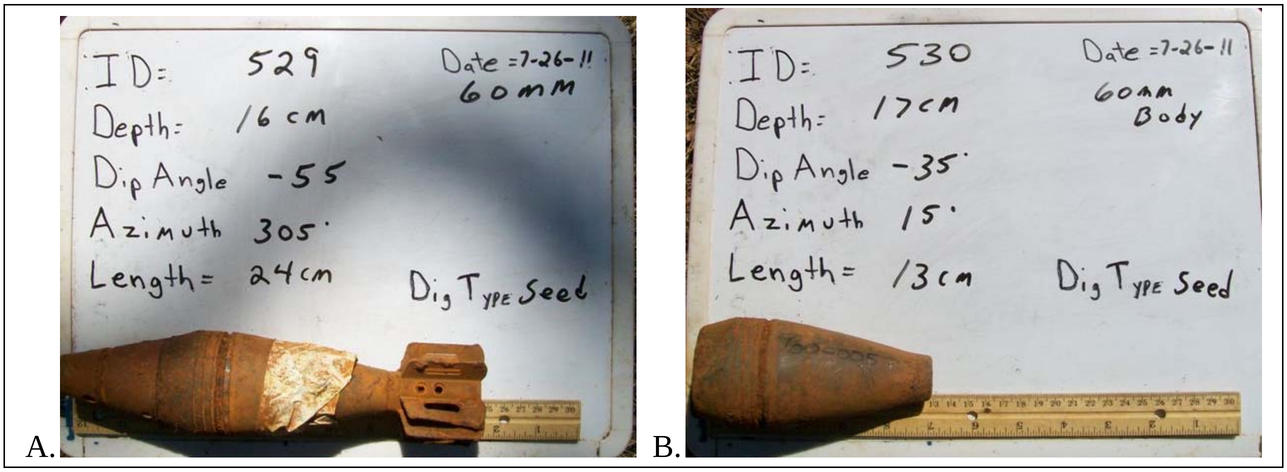

Figure 39: Pictures of intact and partial 60 mm mortars.

There was some variability in the 37 mm class too. The most notable outlier was target #754, which, as shown in Figure 40A, had a cracked copper band relative to standard 37 mm (panel B) and therefore decayed faster. Targets 363 and 908 had slightly faster late-time decay, which might be due to a characteristic pointy nose and absence of ring (Figure 40C-D).

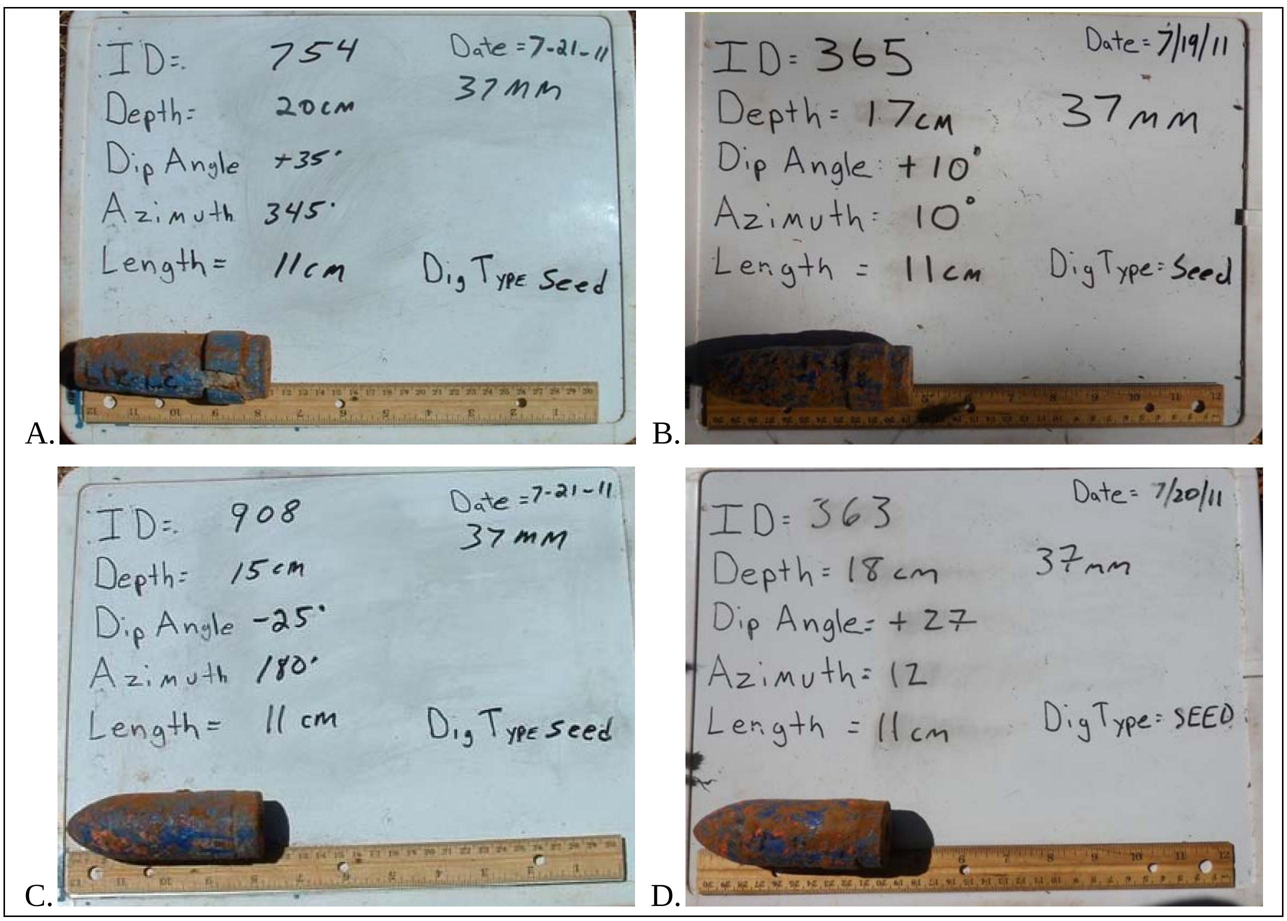

Figure 40: Picture of 37 mm outliers with faster decay.

7.3.2 Prioritized dig list

Performance of the ranked dig lists is presented in Figure 41 in the form of ROC curves. In these results fuzes were first considered as TOI by all analysts but scored as non TOI. Hence there remains 89 TOI. The top two curves are based on the same preprocessed data from this study. The top left originates from the classification presented here, using several soil strategies, 12 training labels and a cascading SVM classifier. All TOI are recovered after approximately 95 pieces of clutter had to be excavated – 87% clutter rejection rate. These results would be even more impressive in the absence of fuzes. We reran the classifier in a fully automated manner to train on TOI without fuzes and found that only 48 pieces of clutter would need to be excavated (Figure 42). Returning to Figure 41A, we chose a conservative stop-digging point because of the presence of fuzes. Note that the “can’t decide” category shown in yellow corresponds to targets that were predicted to be more than 0.5 m away from their associated flag.

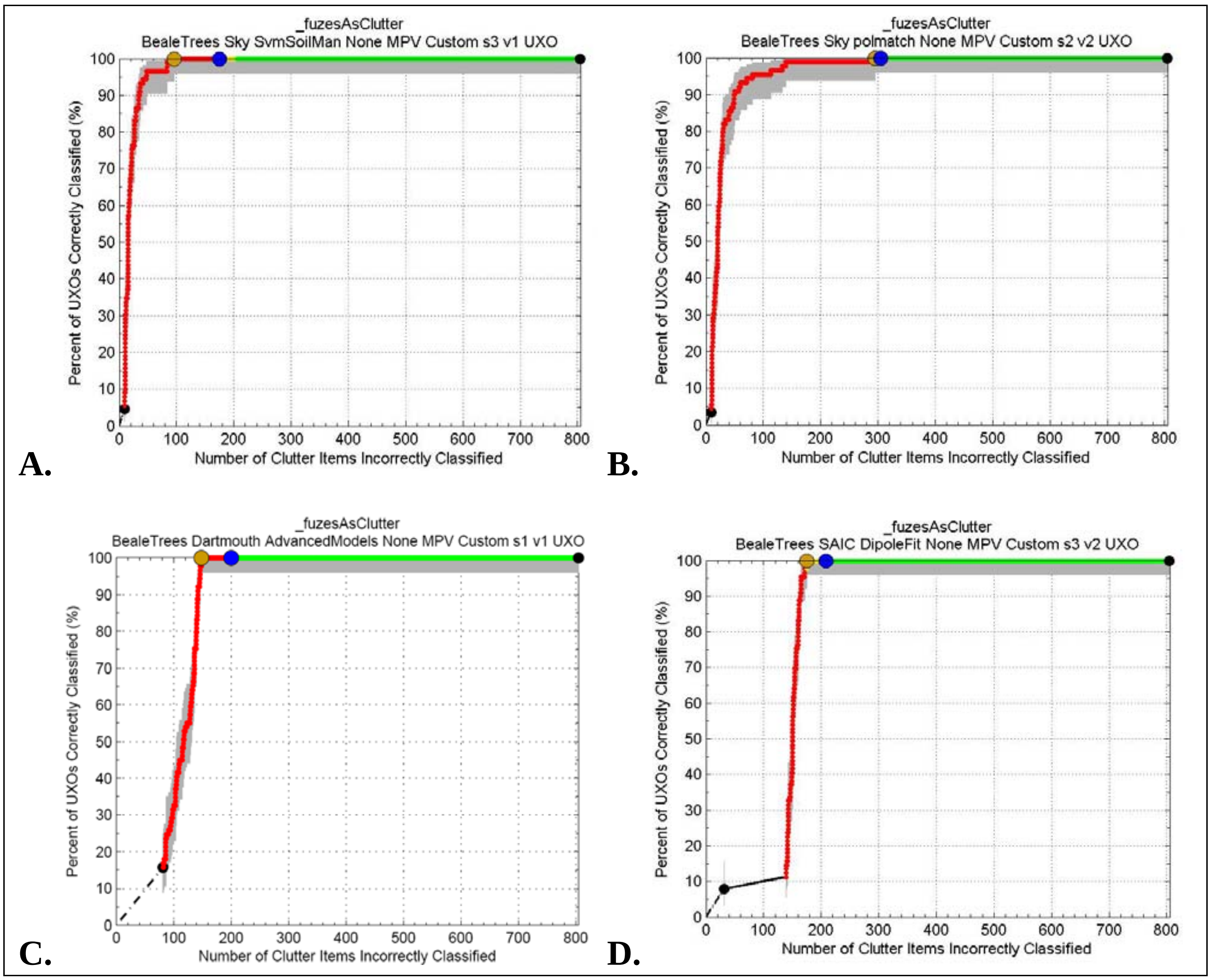

Figure 41: ROC curves for four different analysts with fuzes being considered to be clutter

Panel A corresponds to this study; B is another dig list by SKY based on standard single target inversions (using same background-compensated data); C comes from Dartmouth magnetic charge models; D is SAIC dipole-based analysis. Note: all analysts were looking for some kinds of fuzes when preparing their dig lists.

The dig list illustrated in Figure 41B corresponds to SKY standard processing techniques, using only the single-dipole inversion models, the same training items and polarizability matching (misfit to library items) for classification. Performance is excellent: all TOI are found and there are only 150 unnecessary digs – 80% of clutter rejection; the stop digging point was conservative to compensate for the lack of soil screening and multi-target inversion. These results are highly encouraging and suggest that relative simple data analysis methods can lead to solid classification.

The next two dig lists were created by researchers at Dartmouth College and SAIC. Both groups chose to request a large amount of training data, assumingly to compensate for their lack of familiarity with the sensor and different training philosophy. Both ROC curves show remarkable performance with near perfect dig list after training. Comparatively more clutter was excavated before the last TOI was found as a result of training. However, the stop-digging decision point came at a similar rank as ours, after approximately 300 digs (or 200 pieces of clutter). Together, these results suggest that excellent classification performance can be achieved with MPV data and that hands-on experience with the sensor is not necessary.

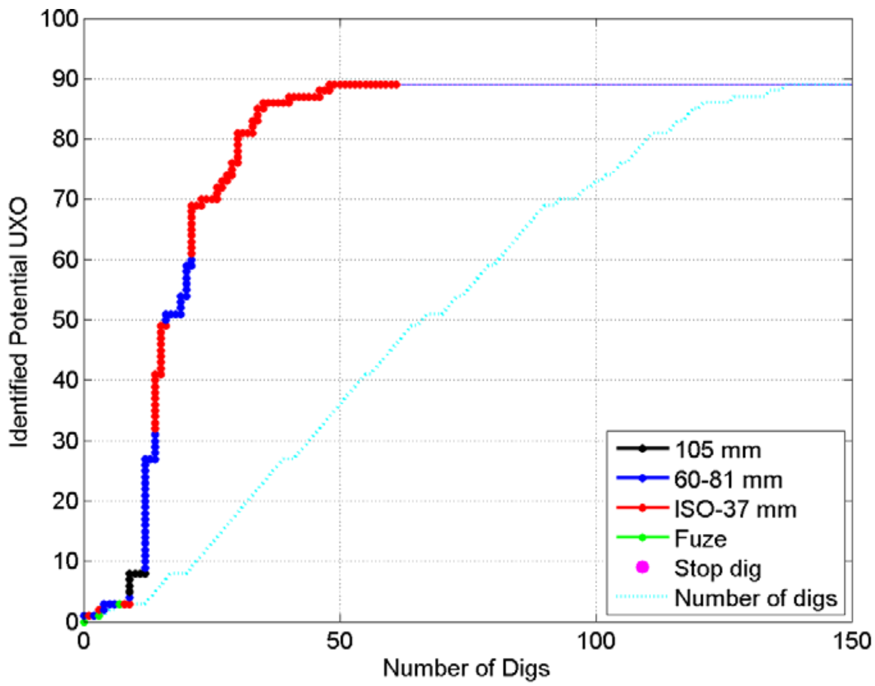

Figure 42: SKY ROC curve without fuzes as TOI: Results from fully automated classifier. The multi-stage, cascading clasisifer is illustrated with colored segments for each TOI class. The 89 TOI are recovered after 48 pieces of clutter had to be excavated (95% clutter rejection rate).

7.3.3 Ability to identify small fuzes

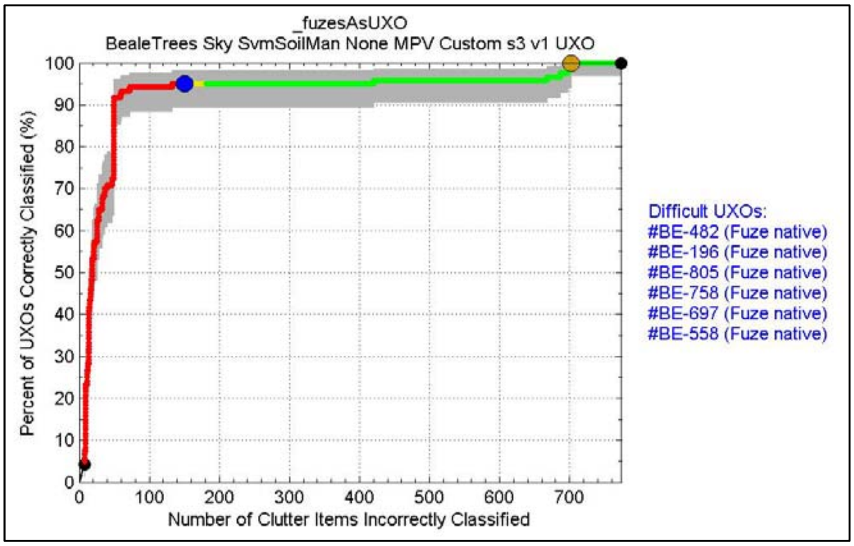

Figure 43: ROC curves with fuzes considered as TOI.

One of the challenges in classification at Camp Beale was the ambiguity on fuzes, which lead to unsatisfactory ROC such as the one shown in Figure 43. Some fuzes were originally found to contain a remaining explosive charge and labeled as potential TOI, while others did not. The difference between the two types is indistinguishable with an EMI system, which cannot detect powder content; therefore the technology is not suitable for separating the two kinds. Early ground truth suggested that some of these fuzes were TOI, which lead all analysts to try and find them. One complicating factor was the occurrence of multiple fuzes. Most fuzes showed a distinctive spherical-shape signature with three equal polarizabilities and log-linear decay. This re-occurring target features were noted by all analysts. We selected one of these targets for training and obtained the validation shown in Figure 44 for the 6 cm fuze.

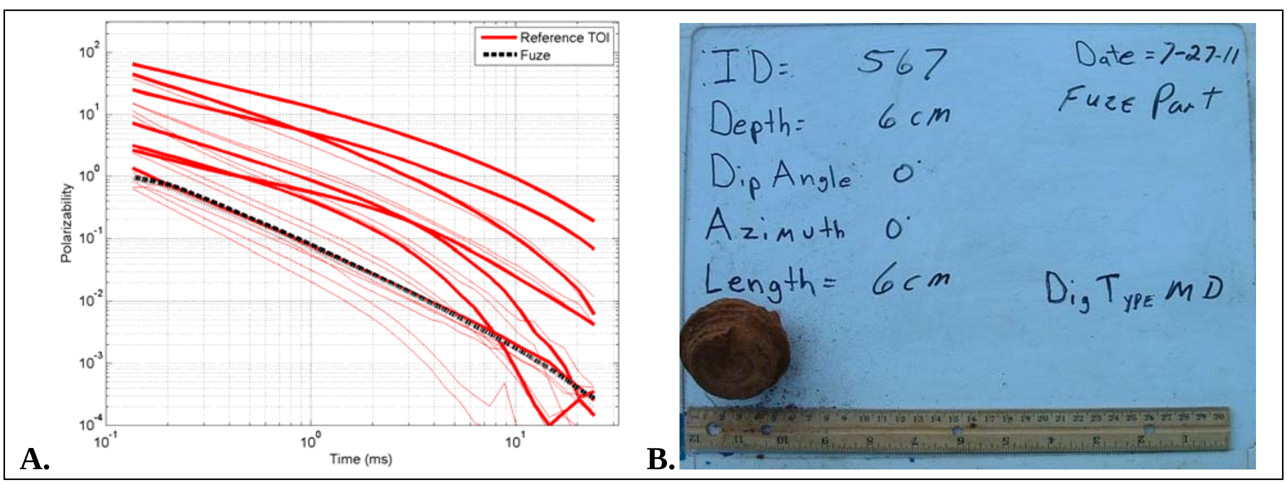

Figure 44: Fuze TOI selected for training.

A: Polarizability decay curves of fuze (black and grey) relative to all known TOI type (sorted by amplitude at early time: 105, 81, 72, 60, 37 mm and ISO from top to bottom).

B: Ground truth. Note: this target was first labeled as munitions debris (MD) and reported as TOI.

Other fuze types appeared after ground truth was released (Figure 45). There were seven occurrences of a 5-cm diameter type (A), two occurrences of a 4-cm type (B), and one unique 3-cm fuze that was found among other fragment pieces (C). The nature of our classification approach makes the latter two cases virtually impossible to find because our method relies on finding re-occurring targets. The first category could have been found, had we been looking for such small targets. Detailed examination of our Stage 2 dig list reveals that the 5-cm fuze in avertedly appeared on that list. The corresponding polarizabilities are shown in Figure 46. Multiple inversion methods raised several possible models, including one fitting the known 6-cm fuze, and one fitting an unknown type that turned out to be the un-encountered 5-cm fuze. Unfortunately we did not look at the recorded fuze size and remained unaware of this fuze type.

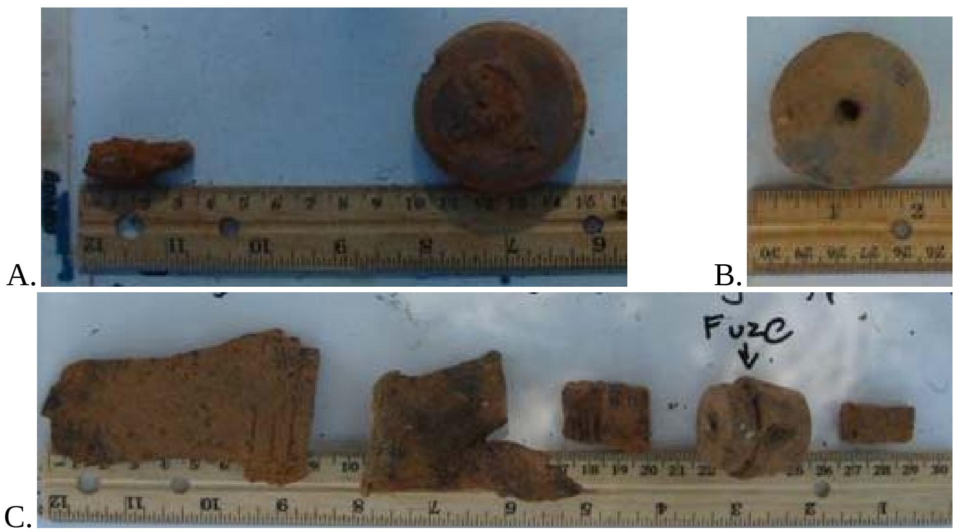

Figure 45: Pictures of small fuze types. A: 5-cm fuze; B: 4-cm fuze; C: 3-cm fuze.

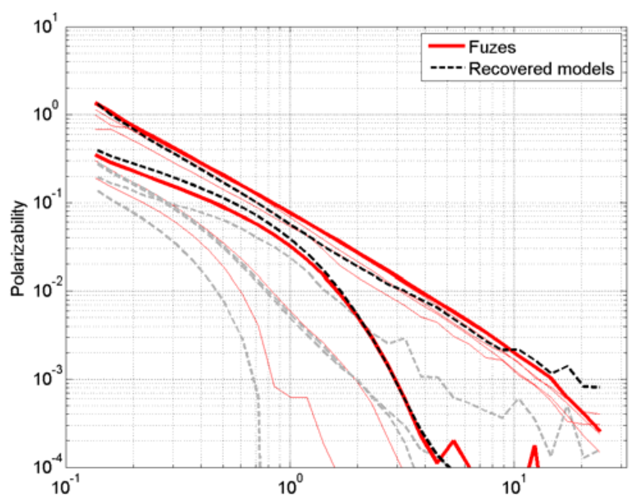

Figure 46: Recovered polarizability decays for one fuze. Several models were obtained using different inversion strategies. One model resembled the known 6-cm fuze type, and one model fit the 5-cm fuze type.

There were six missing fuzes in the ROC curve shown in Figure 43. Their corresponding polarizability decays are shown in Figure 47 and compared to the polarizability decays of the 5-cm fuze type. The yellow-colored panels indicate that three of these fuzes would have been

recoverable based on their polarizabilities, had we recognized the presence of the 5-cm fuze and trained accordingly. The remaining three correspond to the singular 4-cm (#196 and 697) and 3-cm (#758) fuzes of Figure 45. These could not be recovered through our classification approach. Note that Dartmouth researchers did find all fuzes through use of an extensive training set and close scrutiny of all polarizability decay curves to detect any target with symmetry features.

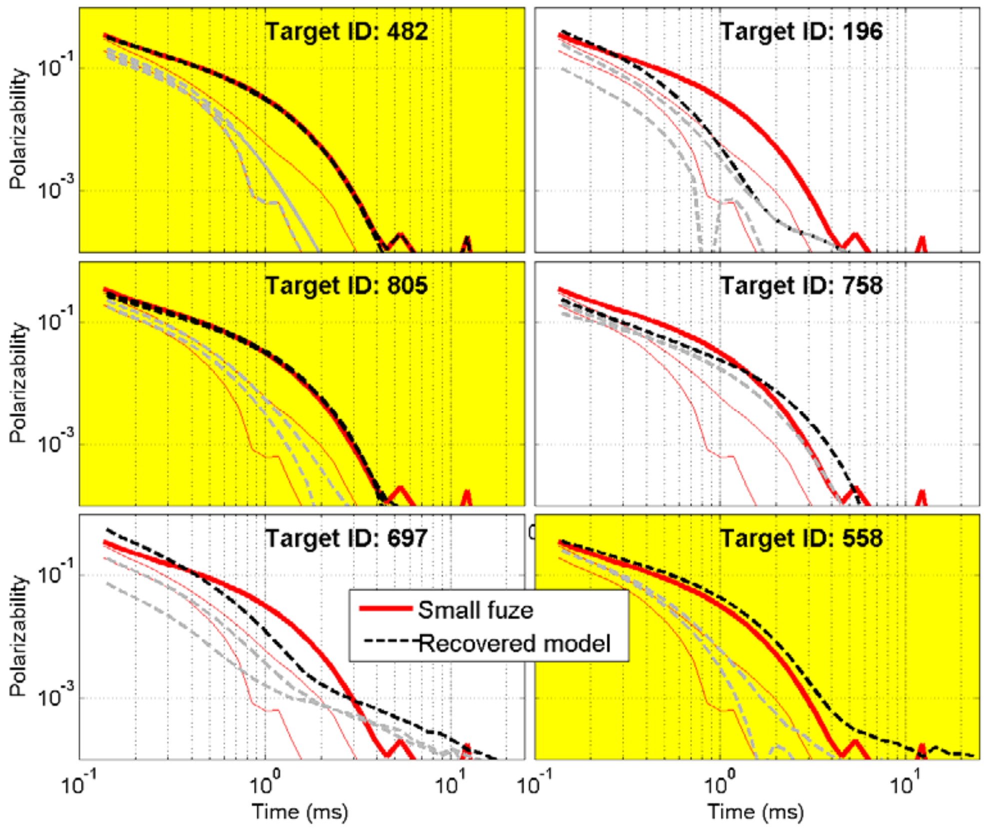

Figure 47: Polarizability decays for the 6 missing fuzes.
Yellow-colored panels indicate 5-cm fuzes that could have been identified through adequate training.

7.4 ANOMALIES THAT NEED RESURVEY

Ideally every target should be characterized after a single cued interrogation survey. Otherwise it might be cheaper to directly excavate that target. Field procedures were such that resurvey should never be necessary. These procedures included acquisition of a 3 x 3 grid of cued soundings that was centered on the target flag so that any target within 0.40 m of the flag could be detected with sufficient number of receivers to be reliably characterized. In addition, the field operator was asked to monitor the recorded data, if possible, to infer potential target offsets. In practice, over 1000 soundings were collected every day, making it extremely taxing for the operator to keep constant focus. As part of daily Quality Control the recorded data were also gridded to ensure adequate spatial coverage, by which an anomaly should appear on several soundings and the anomaly spatial extend should be delineated with data reaching the background level. Any target with poor coverage was marked for resurvey.

The nature of the terrain at Camp Beale, with side slopes and tree canopy, sometimes caused large offsets between the locations of survey flag and those of the picked anomalies from the

EM-61 survey map. One such case is shown in Figure 18. Although that target could be considered as No Contact for the absence of a nearby anomaly, we considered that the anomaly located in the SE quadrant could be further characterized. For verification, the data were inverted and suggested a large deep target. After resurvey the inverted data suggested a piece of clutter buried closer to the surface at a distance of 0.6 m from the flag. Frag was confirmed by excavation. The crew was sent to recollect 10 flags for which the anomaly was far from the flag or seemed to be undetected (no contact). The crew was asked to closely monitor the recorded data to locate the origin of potential anomalies and collect data to cover their spatial extent. None of these anomalies were associated with TOI.

7.5 LOCATION AND DEPTH ACCURACY

Outliers in predicted depth distribution (Figure 48, right) were due to deep soil-like models that occurred when the target was so small that soil was more likely, or when the data supported the presence of multiple dipole sources. Soil models were generally predicted at greater depth to account for a background response that affected all the data collected around a target.

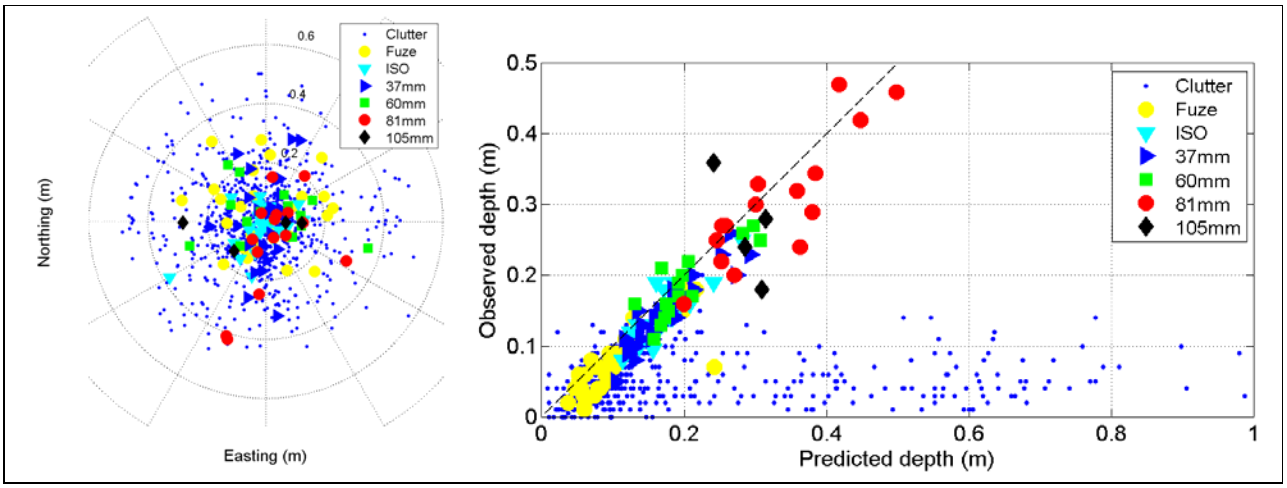

Figure 48: Comparison of the predicted and observed target location for targets of interest (TOI) and clutter. Left: Difference in easting and northing. Right: Difference in depth.

7.6 PRODUCTIVITY

Ultimately the time and cost associated with cued interrogation and classification should be smaller than that of a UXO-technician with a shovel – safety could also enter that equation. Survey time is determined by the number of cued interrogation soundings and any additional time-consuming field procedure. Classification time depends on the amount of non-automated user input that is required for data analysis.

7.6.1 Number of soundings per target

The number of soundings per cued interrogation was increased from 6 to 10 as a conservative measure to ensure adequate coverage through a simple SOP as soon as flag-anomaly offsets were detected. Fewer soundings are necessary for unambiguous target characterization. We found that as few as three high-fidelity soundings could be sufficient with the data collected at YPG.

We re-inverted the Camp Beale in retrospect using only 5 soundings for each target. The 5 soundings were selected by drawing every second point; the resulting pattern corresponds to the originally planned survey protocol with one center shot and the four corners of a square and omitted the tilt test. Data were inverted by applying standard single and double-dipole inversion methods without additional soil treatment. Inversion results were not quality-controlled and were directly sent into an automated classifier (cascading SVM without fuzes). Results are summarized in Figure 49 for all field targets and detailed in Figure 50 for TOI. Recovered target parameters remain stable. Predicted positions stay within 0.05 m of the reference 10 sounding models. Predicted main polarizability amplitude remains within 50% for most field anomalies and all TOI. Given that amplitude logarithmically scales with size, these variations are within the in-class variability of most TOI categories. The recovered polarizabilities remain stable for most TOI (Figure 50). The resulting classification performance, illustrated as a ROC curve (Figure 51), is marginally less efficient that the full blown approach. There was no QC and no particular soil-related-noise mitigation strategy; therefore performance could likely have been even better with optimal models. In conclusion, these results suggest that fewer soundings could be collected in future deployments while keeping similar classification performance.

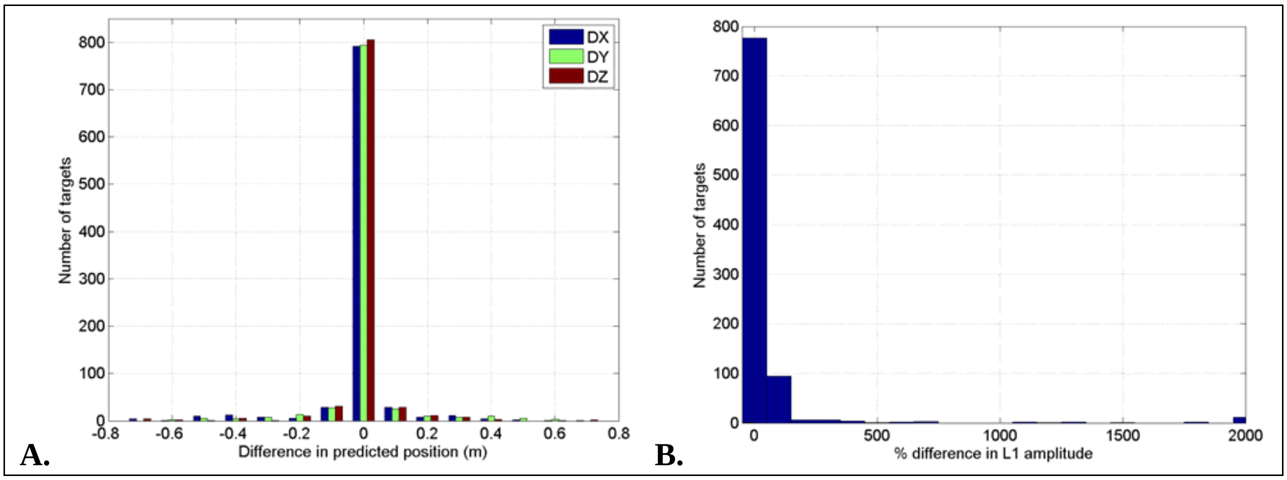

Figure 49: Recovered target parameters with 5 and 10 soundings.
A: Difference in predicted target locations between 5-10 soundings: predicted locations generally are stable.
B: Percent difference in amplitude of the main polarizability, which variations (on a logarithmic scale) are indicative of target size.

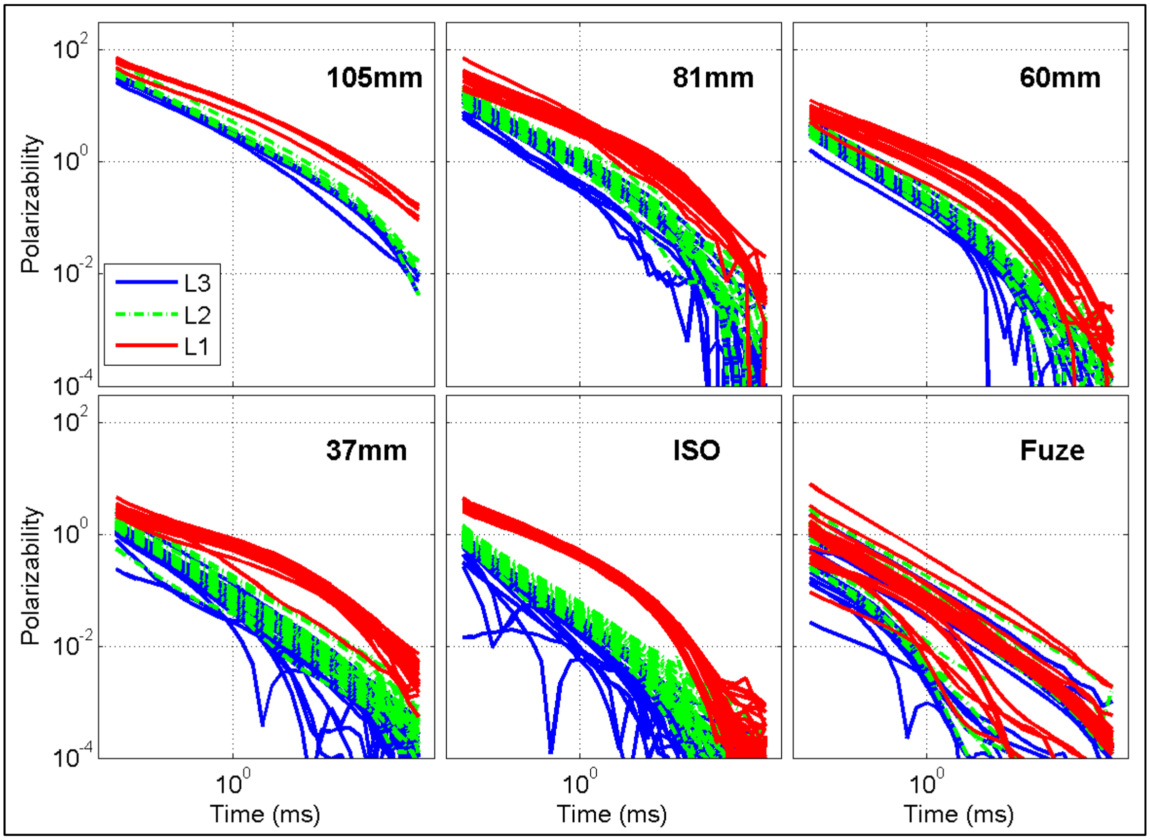

Figure 50: Recovered TOI polarizabilities with five-sounding surveys.

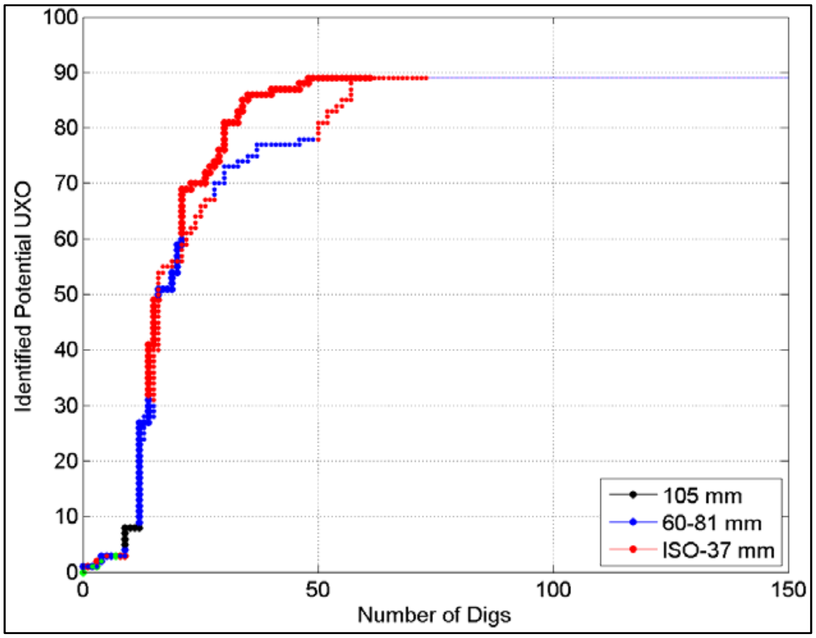

Figure 51: Comparison of ROC curves for 5 and 10 soundings without fuzes.
The thick line corresponds to the automated classifier used in this study, without the fuze class. The thin line applies the exact same approach based on 5-sounding inversion models without QC.

7.6.2 Time delays in the field

Most of the time in the field is spent on collecting data. On average it takes approximately 4 minutes per target. That time is spent between moving the equipment, positioning the beacon boom and acquiring one sounding on top of it to register azimuth (30 sec), collecting 10 soundings with 6.3-sec stacks, waiting 2-10 sec for the sensor display to register each sounding, and collecting and verifying a background sounding. There are several ways of increasing productivity.

Reducing the number of soundings from 10 to 5 would save approximately 1 minute per target, thus increasing productivity by 30%. We showed in the previous section that classification performance would not be significantly affected. Depending on environmental conditions, in particular the magnetic soil setting, fewer background soundings could be collected instead of taking one and verifying its validity for every single target, which costs 15-20 sec.

Productivity could be further increased through instrument upgrades. One obvious area of efficiency improvement is the display system. The MPV DAQ is controlled through a touch-screen control display that runs Remote Desktop Protocol (RDP) over a local Wi-Fi network. Each sounding requires the operator to tap on the touch-screen display and wait for a message indicating that stacking is complete. The system suffers from time lags that are due to the capacity of the touch-screen display to register the tap, the limited bandwidth of RDP and the stability of Wi-Fi. For instance, we found that a Panasonic Toughbook was better at registering taps that an Apple iPad. We anticipate that use of a dedicated touch-screen field monitor using a wired connection would save a significant amount of time by avoiding these three layers of complexity. We can also assume that a dedicated monitor could be more efficient at registering taps. A wired monitor would provide direct connection to the DAQ without communication lags. This could save at least 30 sec per target based on the original 10 soundings. An audible notification after stacks are completed would further speed acquisition by telling the operator to move on.

Beacon azimuth registration is time consuming because the MPV head has to be lined up with the beacon boom with great care. At least 20 sec could be saved and positional accuracy could be improved by installing a dedicated compass on the beacon boom. A standard digital compass with 1-degree accuracy would be more reliable than a careful operator. This would require minor modifications to the data format to accommodate this new data stream.

7.6.3 Data analysis time

At this project maturity stage, there remained many data processing steps for which manual user intervention were needed to ensure that quality and stability were preserved.

The first time consuming activity was the manual entry of recorded file numbers. Each sounding generated a separate file. File numbers were consolidated in a spreadsheet that registered the file numbers for the beacon azimuth shot, the cued survey and the background sounding. This implied over 1000 file numbers for a standard 90-target daily survey. Although some logic was implemented to automatically populate the spreadsheet, manual entries were necessary when multiple targets were surveyed with the same beacon station, or when the operator changed the number of cued interrogation soundings. The spreadsheet was subsequently

read to merge the data files and create a data tile that was visually checked. This process could be easier if a strict data collection was enforced so that file number sequence would be invariable.

The second stage was computation of beacon-inferred locations. These positions were compared to the GPS-predicted ones and displayed in a graphical report. Results were examined for each target to ensure that the right parameters had been used. The process is now stable and should require less manual QC in the future.

Given the noted effect of magnetic soil, time was invested in characterizing that effect. We estimated its amplitude, variability and spatial distribution. We tested different data processing strategies firstly to remove some of its effect on the data that would be inverted, and secondly by testing various inversion schemes using single or multiple dipoles, omitting soil sensitive receiver data and deriving model constraints. Specific programming codes had to be developed for these tasks.

Occurrence of close targets also caused additional work. Close targets were processed as part of the same data tile to allow for the capability to jointly invert these targets. This can be necessary if their signals overlap. There were also cases where the relative location of field flags and detected anomalies caused ambiguity on the expected target to be characterized. In all of these cases the analyst had to mask the data to be inverted, much like an EM-61 survey, and subsequently examine the inversion results to ensure that all detected anomalies had been fit with a model. This process was particularly time consuming when manual re-masking or changes to model constraints had to be done and data had to be re-inverted and QC-ed.

Classification was relatively straightforward, given that a multi-stage cascading method had already been implemented for the YPG demonstration, where 14 TOI had to be classified. The one complicating factor was the need for devising means of identifying and weaning off soil models in the automated SVM classification framework.

Overall, we expect that data processing would be faster for the upcoming demonstrations through use of the numerous algorithms and QC protocols that were implemented as part of this survey.

8.0 COST ASSESSMENT

The figures presented hereafter reflect the costs incurred to date for system maintenance, software modifications and upgrades, shakedown testing, and deployment and analysis of data collected during the Camp Beale demonstration. Deployment costs could be considered to be higher than expected production-type surveys as there remained some development tasks, sensor data characterization studies and some instrument issues that had to be addressed in the field, thus causing delays in completing the project.

8.1 COST MODEL

Time and resources were tracked to assess the cost of deploying the technology for future live sites. Note that some of the cost might decrease as the technology matures and survey procedures get formalized. In particular, most of the data QC tools and data processing methods would be well defined and not require additional development. The site had particular environmental conditions (active magnetic soil) that required in-depth background noise analysis and testing of alternative parameter extraction and classification strategies for defeating potential noise disturbance. Presence of close target was also a new feature of an MPV survey and required special care at the parameter extraction stage. A cost model is proposed in Table 3 based on the survey of 912 anomalies and 15 days in the field. Retrospective analysis and reporting are not included.

Table 3: Cost model for MPV demonstration at former Camp Beale.

Cost Element	Data Tracked During Demonstration	Estimated Costs
Instrument cost	Component costs and integration costs • Engineering estimates based on current development • Lifetime estimate • Consumables and repairs	 N/A N/A 1.5 days
Survey cost		**400 hours**
Mobilization and demobilization	Cost to mobilize to and demobilize from site • Travel to town base • Daily travel to site	 10 hours/ppl/stage 2 hours
Pre-survey activities	Before mobilization: Cost of one-time event • Sensor verification at G&G workshop On site: Cost of one-time preparation and testing • Programming of GPS • Preparation of target location list • Collection of training data (test pit with 3 ppl) Preparation of QC tools: Total cost • Hours per anomaly • Personnel required	 4 hours 2 hours 4 hours 3x4 hours 40 hours 1 geophysicist
Instrument setup costs	Unit: Cost to set up and calibrate (IVS) • Hours required • Personnel required • Frequency required	 0.33 hours/ppl 2 ppl Daily

Data collection costs	Unit: Cost of collecting & recording data per anomaly • Hours per anomaly • Personnel required	 1/15 hours 2 field ppl
Pre-processing costs	Unit: Cost per anomaly • Hours per anomaly • Personnel required	 1/15 hours 1 geophysicist
Discrimination data processing		**255 hours**
Data extraction	Unit: Cost per anomaly • Time required • Personnel required	 1/20 hour 1 geophysicist
Parameter extraction, including inversion and review	Data analysis of local background noise: Total cost • Time required • Personnel required Unit: Cost per anomaly • Time required • Personnel required	 60 hours 1 geophysicist 1/20 hour 1 geophysicist
Classifier training	Define strategy for defeating soil: Total cost • Time required • Personnel required Unit: Cost per anomaly • Time required • Personnel required	 40 hours 1 geophysicist 1/50 hour 1 geophysicist
Classification and production of multiple prioritized anomaly list	Unit: Cost per anomaly (includes multiple list stages) • Time required • Personnel required	 1/20 hour 1 geophysicist

8.2 COST DRIVERS

The MPV was developed to provide a moderate cost, reliable, portable sensor with advanced discrimination capabilities that can operate at sites with challenging surveying conditions. As a portable system, deployment logistics and costs for transport and operation are quite low relative to towed arrays or other vehicular-based systems. The primary costs are incurred for labor and travel for the operators, and the primary cost driver becomes the duration of deployment, directly related to the acreage to be surveyed as well as the difficulty of the terrain (steep, rocky, very uneven, and wooded terrain will take somewhat longer to survey than just because it is more difficult to hike across these areas).

8.3 COST BENEFITS

The primary driver for developing the MPV is to make discrimination feasible at a wide range of sites where field conditions prohibit the use of cart-based systems, and for small-scale deployment where a small area needs to be surveyed or where anomalies need to be resurveyed at a lower cost than a cart-based system.

9.0 IMPLEMENTATION ISSUES

A flow chart showing the managerial hierarchy and the relationship between the principal investigator (PI) and other personnel is shown in Figure 52.

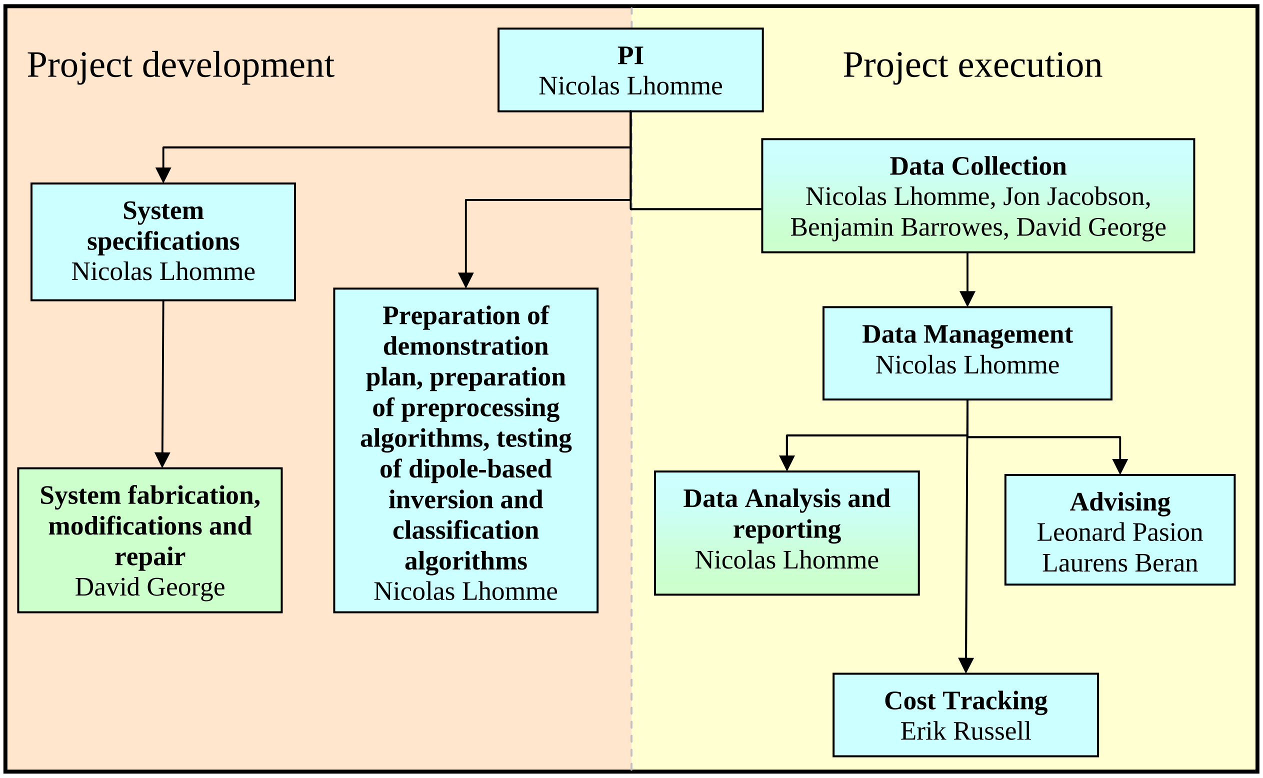

Figure 52: Project management hierarchy with Sky Research personnel (blue) and other personnel (green). The hierarchy is split between development and execution components.

The primary personnel for the demonstration were Nicolas Lhomme (PI, Sky Research), David George (Electronic/Electrical Engineer, G&G Sciences) and Benjamin Barrowes (Scientist, ERDC-CRREL). N. Lhomme was present at the site for the entire project duration (approx. two weeks). D. George was originally planned to be there for the whole time too, but had to leave for almost a week in the middle of the project. B. Barrowes came for the first three days to help with setting up the survey. Jon Jacobson participated in the last 10 days of field tests as a field geophysicist and main MPV operator. Leonard Pasion and Laurens Beran were consulted on data inversion and classification strategies; Erik Russell was the project manager responsible for cost tracking.

10.0 REFERENCES

Barrowes, B.E., Recent advances in Vector EMI Sensors. ESTCP SERDP/ESTCP Partners in Environmental Technology Symposium, Wash., DC, Dec. 2007a.

Barrowes, B.E., O'Neill K, George, D.C., Snyder, S., Shubitidze, F. and Fernandez, J. P., Man-Portable Vector Time Domain EMI Sensor and Discrimination Processing. SERDP 1443 FY07 Annual Report, 2007b.

Bell, T. H., Barrow, B. J. and Miller, J**.** T., Subsurface discrimination using an electromagnetic induction sensor**.** IEEE Transactions on Geoscience and Remote Sensing, 39, 1286–1293, 2001.

Bell, T., Geo-location Requirements for UXO Discrimination. SERDP Geo-location Workshop, 2005.

Billings, S., Pasion, L**.,** Lhomme, N. and Oldenburg, D., Discrimination at Camp Sibert using Time-Domain EM. SERDP/ESTCP Partners in Environmental Technology Symposium, Wash., DC, Dec. 2007.

Fernandez, J. P., Barrowes, B. E., Bijamov, A., Grzegorczyk, T., Lhomme, N., O'Neill, K., Shamatava, I., and Shubitidze, F., MPV-II: an enhanced vector man-portable EMI sensor for UXO identification. Proceedings SPIE 8017, 2011.

Gasperikova, E., Smith, J. T., Morrison, H. F. and Becker, A., BUD results from the ESTCP Demonstration sites. SERDP/ESTCP Partners in Environmental Technology Symposium, Wash., DC, Dec. 2007

Gasperikova, E., Smith, J. T., Morrison, H. F., Becker, A., and Kappler, K., UXO detection and identification based on intrinsic target polarizabilities. Geophysics, 74, B1-B8, 2009.

Grzegorczyk, T. M., Barrowes, B. E., Shubitidze, F., Fernández, J. P., Shamatava, I. and ONeill, K. A.: Detection of multiple subsurface metallic targets using the man-portable vector EMI instrument. Proceedings of SPIE Defense+Security, Orlando, FL, April 2009.

Kingdon, K. A., Pasion, L. R. and Oldenburg, D. W., Investigating the Effects of Soils with Complex Magnetic Susceptibility on EMI Measurements Using Numerical Modelling of Maxwell's Equations. Proceedings of SPIE Defense+Security, Orlando, FL, April 2009.

Lhomme, N., Pasion, L., Billings, S. and Oldenburg, D., Inversion of frequency domain data collected in a magnetic setting for the detection of UXO. Proceedings of SPIE Defense+Security, Orlando, FL, March 2008.

Lhomme, N., Barrowes, B. E. and George, D. C., EMI sensor positioning using a beacon approach. Proceedings of SPIE Defense, Security+Sensing, Orlando, Florida, April 2011.

Pasion, L. & Oldenburg, D., A Discrimination Algorithm for UXO Using Time Domain Electromagnetics. Journal of Engineering and Environmental Geophysics, 28, 91-102, 2001.

Pasion, L., Billings, S. and Oldenburg, D., Improving Detection and Discrimination of Buried Metallic Objects in Magnetic Geologic Settings by Modeling the Background Soil Response. Proceedings of SPIE Defense+Security, Orlando, FL, March 2008.

Pasion, L., Kingdon, K. and Jacobson, J., Simultaneous Inversion of Electromagnetic Induction Data for Target and soil Parameters. Presentation at SPIE Defense, Security+Sensing, Orlando, Florida, April 2011.

Shubitidze, F., Barrowes, B. E., Shamatave, I. and O'Neill, K., Application of the NSMC model to the multi-axis time domain EMI data. SPIE Defense+Security, Orlando, FL, March 2008.

Smith, T.J. and Morrison, H.F., Optimizing receiver configurations for resolution of equivalent dipole polarizabilities in situ. IEEE Trans. on Geosci. and Rem. Sens., 43(7), 2005.

APPENDICES

Appendix A: Health and Safety Plan (HASP)

Health and safety procedures will be followed as indicated below, and will also comply with the ESTCP guidance for this demonstration.

- **Applicable local, state, and federal health and safety laws and regulations**

Sky Research, Inc. staff on-site at the Beale test site will comply with health and safety requirements in accordance with Code of Federal Regulations (CFR), Part 29, Section 1910.120 and any site-specific requirements as noted during site orientation or other direction provided by ESTCP and Department of fish and Game representatives. Although 29 CFR 1910.120 pertains to personnel conducting activities at known or suspected hazardous waste sites and may not be directly applicable to the planned activities, the code provides a reasonable framework safe work practices.

- **Potential for worker exposure to hazardous materials and/or other hazards**: None or minimal. Any site-specific hazards also will be briefed during orientation.
- **Physical requirements are expected of workers:** Basic fitness, heat resilience.
- **Number of people required to operate the technology:** Two
- **Technology's history of breakdowns or accidents:** No issues to date.
- **Potential effects from the transporting of equipment, samples, wastes, or other materials associated with the technology:** All components of the technology are inert, to the exception of Li-ion batteries that must be shipped by ground according to federal regulation.
- **Impact of technology on surrounding environment:** None. Technology is non destructive and man portable.
- **Closest medical facility**

Rideout Memorial Hospital
726 4th Street
Marysville, CA 95901
(530) 749-4300

Directions: The hospital is located 28 miles or 45 minutes away.

Waldo Rd

1. Head **north** on **Waldo Rd** toward **Smartville Rd**

1.7 mi

2. Slight right at **Smartville Rd**

4.6 mi

3. Turn right to stay on **Smartville Rd**

1.0 mi

4. Turn left at **CA-20 W**

19.7 mi

5. Turn left at **CA-20 W/CA-70 S/B St** (signs for **Yuba City/Sacramento**)

0.2 mi

6. Take the 1st right onto **9th St** (signs for **CA-70/CA-20/Yuba City/Sacramento**)

0.3 mi

7. Turn left at **E St**

0.3 mi

8. Turn right at **5th St**

0.2 mi

9. Turn left at **H St**

420 ft

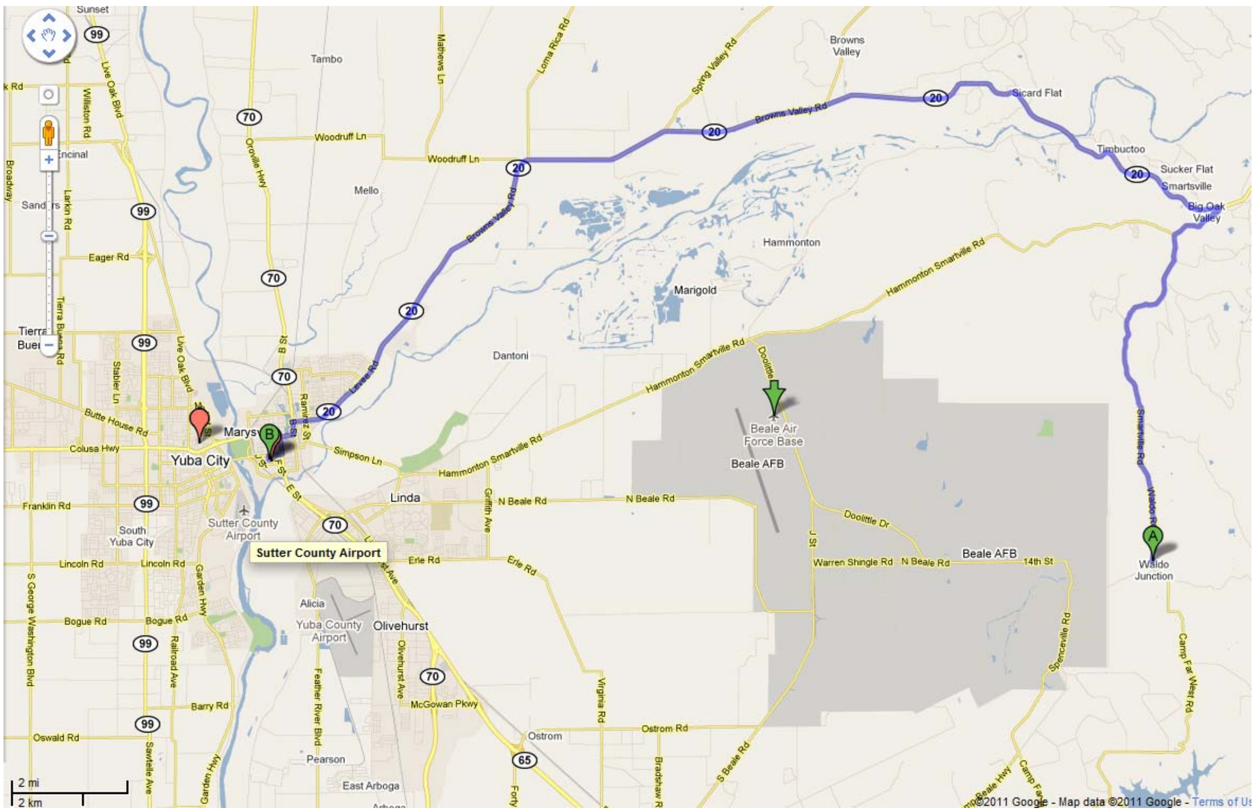

Figure 53: Directions to Rideout Memorial Hospital Facility

Appendix B: Points of Contact

Points of contact (POCs) involved in the demonstration and their contact information are presented in Table 4.

Table 4: Points of Contact for the MPV Demonstration.

POINT OF CONTACT Name	ORGANIZATION Name Address	Phone Fax E-mail	Role in Project
Dr. Nicolas Lhomme	Sky Research Inc. 112 A, 2386 East Mall, Vancouver, BC V6T 1Z3, Canada	Tel: 541-552-5180 Fax: 604-221-1055 Nicolas.lhomme@skyresearch.com	PI
Erik Russell	Sky Research Inc. 445 Dead Indian Memorial Road, Ashland, OR, 97520, USA	Tel: 541-552-5197 Fax: 541-488-5606 Erik.Russell@skyresearch.com	Project coordination
David George	G&G Sciences, Inc. 873 23 Rd Grand Junction, CO 81505	Tel: (970) 263-9714 Fax: (970) 263-9714 dgeorge@ggsciences.com	Sub-contractor
Dr. Benjamin Barrowes	72 Lyme Road, Hanover, NH 03755-1290	Tel:(603)646-4822 Fax:(978)702-0448 benjamin.e.barrowes@usace.army.mil	Co-investigator
Dr. Herb Nelson	ESTCP Program Office ESTCP Office 901 North Stuart Street, Suite 303 Arlington, VA 22203-1821	Tel: 703-696-8726 Herbert.Nelson@osd.mil	ESTCP Munitions Management Program Manager